



Acknowledgements

The work presented in this master thesis was carried out in the Molecular Microbiology group of Professor Leiv Sigve Håvarstein, Department of Chemistry, Biotechnology and Food Sciences at the Norwegian University of Life Sciences from January 2014 to May 2014.

First of all, I want to thank Professor Leiv Sigve Håvarstein for giving me the opportunity to write my thesis in collaboration with the Molecular Microbiology group. It has truly been a pleasure and incredibly educational.

Big thanks to my supervisor Dr. Daniel Straume for excellent supervision and scientific guidance. I am indebted to you for all your contributions during this period, for always taking the time and for having faith in me. I highly appreciate all the help you have given me during the writing process and I have certainly learned a lot from you.

Thanks to Dr. Kari Helene Berg and PhD-student Gro Anita Stamsås for including me in your group, for countless advice and amusing moments. I am going to miss your “passion for baking” and our brief, but wonderful time together. I also need to thank Zhian Salehian for always being available and gladly helping with lab technical issues. Thanks to PhD-student Cyril Alexander Frantzen for proofreading and valuable advice of the thesis.

Last but not least, thanks to my friends, family and loved ones for all your support, encouragement and care throughout the process. A special thanks to Foreningen Hunkatten for providing me with social activities and a memorable time as a student at NMBU.

Silje-Marie Wærn van Hoek

Ås, May 2014

Abstract

The bacterial cell wall with its peptidoglycan layer is essential for cells to maintain their shape and for protection against osmotic pressure. The cross-linked polymer peptidoglycan forms the scaffold of the cell wall. In addition, cell wall components are required for a numerous physiological processes including cell growth and division.

Streptococcus pneumoniae has a typical Gram-positive cell wall with an ovoid shape and are typically arranged in pairs (diplococci) or chains. Peptidoglycan synthesis in *S. pneumoniae* is believed to occur in a combination of peripheral and septal synthesis in the mid-cell regions of dividing cells. The murein hydrolase PcsB is, amongst other, thought to play a key role in splitting of the cross wall peptidoglycan between daughter cells. PcsB is highly conserved among group B streptococci and the deletion of the *pcsB* gene results in misplacement of the division septum, reduced growth rate and abnormal cell shape. Consequently, studies have shown that PcsB is essential for proper cell division and proliferation in *S. pneumoniae*.

In the present study, PcsB was purified to produce PcsB-specific antibodies, which will be a valuable tool for studying PcsB in *S. pneumoniae*. It was shown that the PcsB-specific antibody has high specificity towards PcsB. Growth studies performed to determine the correlation between amounts of cell-associated PcsB and secreted PcsB showed that PcsB is a relatively abundant protein in *S. pneumoniae*. Quantitative studies showed that PcsB accumulates outside the pneumococcal cells as they grow and divide, which is in agreements with recent studies suggesting how the mechanisms of PcsB work. Furthermore, the ComRS depletion system was used to determine whether the amounts of cell-associated PcsB and secreted PcsB remained stable or were degraded. Growth and morphological studies confirmed that the depletion of PcsB had a negative effect on the cells viability. Cells showed abnormal shape, clumping and the formation of longer chains demonstrating PcsB's importance in cell division. These results contribute to strengthen the theories of PcsB's involvement in cleaving peptidoglycan in the septal cross wall to separate the two daughter cells during cell division.

Sammendrag

Den bakterielle celleveggen består blant annet av et peptidoglykan-lag som har en essensiell rolle ved å opprettholde morfologien og beskytte cellen mot osmotisk trykk. Det er kryssbundet peptidoglykan som danner skjelettet i celleveggen. Celledeling og celleveggsyntese hos bakterier er nøye regulert og koordinerte prosesser hvor mange komponenter inngår.

Streptococcus pneumoniae har en typisk Gram-positiv cellevegg med ovoid morfologi og danner ofte par (diplokokker) eller kjeder. Celleveggsyntesen i *S. pneumoniae* skjer i en kombinasjon av perifer og septal syntese og foregår i midten av celle regionen. PcsB er peptidoglykan hydrolase som virker å ha en viktig rolle i splittingen av det septale peptidoglycanlaget når datterceller skal skilles. PcsB er svært konservert blant klasse B streptokokker og studier har vist at PcsB er avgjørende for riktig celledeling og spredning i *S. pneumoniae*. Delesjon av *pcsB* genet fører til feilaktig celledeling, redusert vekst og unormal celle morfologi.

I dette arbeidet ble PcsB rensert for å produsere PcsB-spesifikke antistoff, noe som vil være et viktig verktøy for å studere PcsB i *S. pneumoniae*. PcsB-spesifikke antistoffer viste seg å ha tilfredsstillende spesifisitet og sensitivitet. For å bestemme sammenhengen mellom celle-assosiert PcsB og sekretert PcsB, ble det utført vekstforsøk. Det ble vist at PcsB finnes i rikelige mengder i *S. pneumoniae*. Beregninger viste at PcsB akumulerte utenfor cellene ettersom bakteriene deler seg, noe som er i tråd med nylig forskning om hvordan man tror PcsB sin mekanisme fungerer. Videre har ComRS-depletionsystemet blitt brukt til å fastslå om mengde celle-assosiert PcsB og sekretert PcsB opprettholdes eller degraderes. Vekst- og morfologistudier indikerte at depleksjon av PcsB hadde en negativ effekt på cellenes levedyktighet. Cellene viste unormal morfologi, klumpdannelse og dannet lengre kjeder noe som viser PcsB sin betydning i celledeling. Dette viser viktigheten av PcsB i celledeling hos pneumokokker. Disse resultatene bidrar med å styrke teorier om PcsBs rolle i peptidoglykan kløyving i den septale "cross wall" for å skille de to dattercellene under celledeling.

Table of contents

1. Introduction	1
1.1 <i>Streptococcus pneumoniae</i>	1
1.1.1 Phylogeny, morphology and metabolism	1
1.1.2 Epidemiology	3
1.1.3 Horizontal gene transfer	4
1.2 Natural genetic transformation	4
1.2.1 Competence induced cell lysis - fratricide	6
1.3 The bacterial cell wall	7
1.3.1 Peptidoglycan	8
1.3.2 Peptidoglycan synthesis	9
1.3.3 Daughter cell separation	9
1.4 Structure and biosynthesis of the pneumococcal cell wall	10
1.4.1 Penicillin binding proteins (PBPs)	11
1.4.2 Peptidoglycan biosynthesis and daughter cell separation in <i>S. pneumoniae</i>	12
1.5 The peptidoglycan hydrolase PcsB	13
1.6 Thesis objectives	16
2.0 Materials	17
2.1 Bacterial strains and plasmids	17
2.2 Peptides	17
2.3 Primers	18
2.4 Standards, enzymes and nucleotides	19
2.5 Antibiotics	19
2.6 Kits	19
2.7 Antibodies and substrates	20
2.8 Computer software	20
2.9 Chemicals	21
2.10 Technical equipment	22
2.11 Recipes – growth media, buffers and solutions	24
2.11.1 Growth media	24
2.11.2 Solutions for C-medium	25
2.11.3 Buffers and solutions for protein purification	27
2.11.4 Buffers and solutions for Agarose gel electrophoresis	28
2.11.5 Buffers and solutions for SDS-PAGE	28

2.11.6 Recipes for separation gel and stacking gel used for SDS-PAGE	29
2.11.7 Solutions for Coomassie staining og gels	29
2.11.8 Solutions for Western Blot.....	30
2.11.9 Solutions for Immunofluorescence microscopy	30
3.0 Methods	32
3.1 Cultivation and storage of bacteria	32
3.1.1 Cultivation of <i>Escherichia coli</i>	32
3.1.2 Anaerobic cultivation and transformation of <i>S. pneumoniae</i>	32
3.1.3 Depletion of gene expression in <i>S. pneumoniae</i>	33
3.1.4 Storage of bacteria	34
3.2 Protein purification of mature PcsB.....	34
3.2.1 Bacterial strains and growth conditions	34
3.2.2 DEAE-Cellulose affinity chromatography.....	35
3.2.2.1 Protocol DEAE-Cellulose affinity chromatography.....	35
3.2.3 Dialysis and TEV protease digestion	36
3.2.3.1 Protocol dialysis.....	36
3.2.4 Immobilized Metal Affinity Chromatography	36
3.2.4.1 Protocol IMAC.....	37
3.2.5 Ion Exchange Chromatography	37
3.2.5.1 Protocol IEC.....	38
3.3 Polymerase Chain Reaction	38
3.3.1 Primer desgin	38
3.3.2 Phusion® High-Fidelity DNA Polymerase	39
3.3.2.1 Protocol for using Phusion® High-Fidelity DNA Polymerase.....	39
3.3.3 Taq DNA Polymerase	40
3.3.3.1 Protocol for using Taq DNA Polymerase.....	40
3.3.4 PCR-screening	41
3.3.5 Overlap-Extension PCR.....	41
3.4 DNA sequencing	42
3.5 Agarose gel electrophoresis	43
3.5.1 Protocol for agarose gel electrophoresis	44
3.6 DNA-extraction from agarose gel	44
3.7 Sodium dodecylsulfate polyacrylamide gelelectrophoresis (SDS-PAGE).....	45
3.7.1 Protocol for casting SDS-polyacrylamide gels	46
3.7.2 Coomassie blue staining of SDS-polyacrylamide gels	46
3.7.2.1 Protocol for Coomassie blue staining	47

3.8 Western Blot	47
3.8.1 Electroblothing.....	47
3.8.1.1 Protocol for electroblotting.....	48
3.8.2 Membrane blocking	48
3.8.2.1 Protocol for blocking.....	48
3.8.3 Immunodetection of PcsB.....	49
3.8.3.1 Protocol for immunodetection.....	49
3.9 Microscopy	50
3.9.1 Immunofluorescence microscopy of FLAG-tagged PcsB	50
3.9.2 Differential interference contrast (DIC) microscopy	51
3.9.2.1 Protocol for DIC.....	51
4.0 Results.....	52
4.1 Expression and Purification of PcsB	52
4.1.1 Removal of the CHiC-tag.....	53
4.1.2 Ion exchange chromatography of PcsB.....	54
4.1.3 Calculating the amount of purified PcsB	55
4.2 Immunodetection of recombinant PcsB	56
4.3 Immunodetection of native PcsB compared to 3xFlag-tagged PcsB	57
4.4 PcsB is an abundant protein accumulating outside the cells.....	58
4.4.1 PcsB is fairly abundant in <i>S. pneumoniae</i>	61
4.5 Depletion of PcsB results in reduced growth and morphological abnormalities	62
4.5.1 Low levels of PcsB results in morphological abnormalities.....	65
5.0 Discussion	69
5.1 Anti-PcsB shows satisfactory specificity.....	69
5.2 PcsB accumulates outside the cells.....	70
5.3 Depletion of PcsB.....	72
5.4 Depletion of PcsB influences cell shape and chain formation	73
5.4.1 Immunofluorescence microscopy	73
6.0 Concluding remarks and future work.....	75
7.0 References	77
Appendix	I
Appendix A	I

Appendix B..... II
Appendix C1 IV
Appendix C2 V

1. Introduction

1.1 *Streptococcus pneumoniae*

Streptococcus pneumoniae is a major human pathogen and plays an important role in microbiology and molecular biology. The bacterium is found in the nasopharynx of human hosts and was first isolated, independently and simultaneously, in 1880 by Georg Stenberg and Louis Pasteur. Consequently, within a decade after the isolation of *S. pneumoniae*, several of the infections caused by *S. pneumoniae* were identified. Research on *pneumococci* has been vital to the understanding of immunology and for the development of vaccines (Austrian 1981). It was in 1928 that Frederick Griffith, during his pioneering work on pneumococcal vaccines, discovered natural genetic transformation in *S. pneumoniae*. Griffith found that mice injected with living but avirulent (lacking a capsule) *R-pneumococci* together with heat-killed virulent (with capsule) *S-pneumococci* ensued in pneumonia and death. Introduced separately, the bacteria did not cause disease or death. This discovery indicated the possibility of transforming phenotypes from dead organisms to living organisms (Griffith 1928). The significance of this experience was not acknowledged until Oswald T. Avery, Colin MacLeod and Maclyn McCarty demonstrated that DNA was the fundamental unit of the “transforming principle” of pneumococcus, thus the evidence that the genetic material is DNA, not protein (Avery *et al.* 1944).

1.1.1 Phylogeny, morphology and metabolism

S. pneumoniae is, according to Bergey’s Manual of Systematic Bacteriology (cf. Garrity *et al.* 2004), classified amongst the low G+C (36-46%) Gram-positive bacteria belonging to the phylum Firmicutes (Schleifer and Ludwig 1995). Table 1.1 shows a complete overview of the taxonomy of *Streptococcus*.

Table 1.1 Taxonomic overview of the genus *Streptococcus* (Garrity *et al.* 2004)

Taxon	Name
Domain	<i>Bacteria</i>
Phylum	<i>Firmicutes</i>
Class	<i>Bacilli</i>
Order	<i>Lactobacillales</i>
Family	<i>Streptococcaeae</i>
Genus	<i>Streptococcus</i>

The genus *Streptococcus* includes over 50 species that are divided into six major clusters based on phylogenetic analyses of 16S rRNA-sequences (Kawamura *et al.* 1995; Kilian *et al.* 2008). Figure 1.1 shows the phylogenetic distance between 34 *streptococcus* species divided into the six subgroups. *S. pneumoniae* is by this classification included in the Mitis group together with 11 other species that are prototype commensals of the upper respiratory tract. Most members of the Mitis group, including pneumococci, are naturally competent for genetic transformation (Kilian *et al.* 2008).

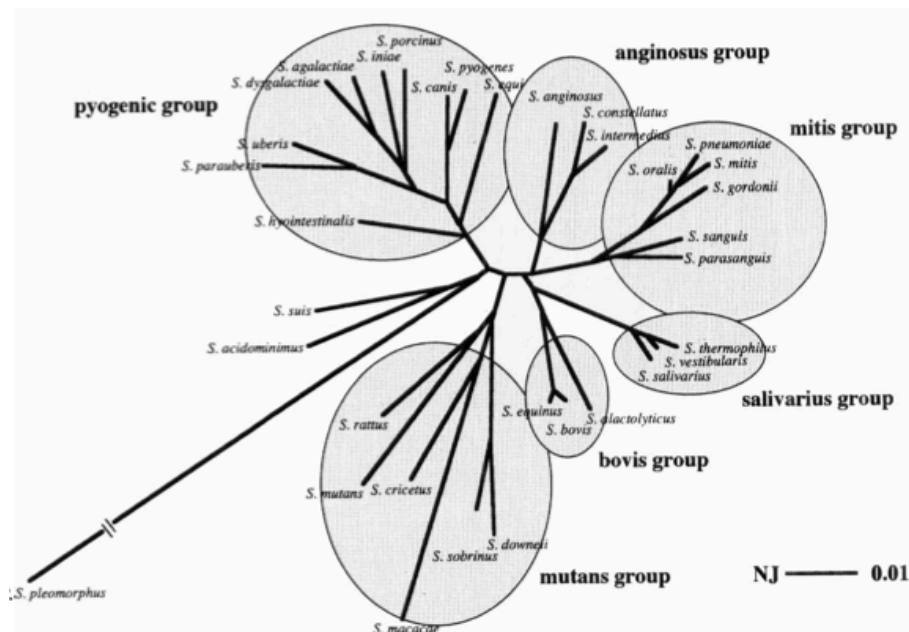


Figure 1.1 Overview of the phylogenetic relationships among 34 *Streptococcus* species based on 16S rRNA analyses. The genus *Streptococcus* is here divided into six major clusters. The distance is calculated based on the principles of neighbor-joining (NJ). *S. pneumoniae* belongs to the Mitis group, today comprising 12 species (Kilian *et al.* 2008). Figure from Kawamura *et al.* (1995).

S. pneumoniae, like other species of the genus *Streptococcus*, are spherical or ovoid cells, typically arranged in pairs or chains (see Figure 1.2). They are Gram-positive, facultative anaerobe, catalase negative, non-sporing, and non-motile. They are also characterized by being nutritionally fastidious requiring complex medium for growth. The bacterium obtains energy via fermentation of carbohydrates.

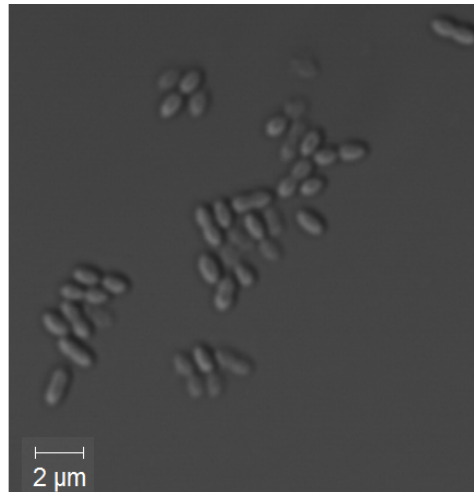


Figure 1.2 *Streptococcus pneumoniae*. Differential Interference contrast microscopy image of *S. pneumoniae* showing the typical diplococci structure common in these species. The image is taken from Professor L.S. Håvarstein's laboratory.

Pneumococci are usually enclosed by a polysaccharide capsule that is of significance regarding its virulence (Kilian 1998, Hardie *et al.* 1997). *S. pneumoniae* strain R6, used in this study, is an unencapsuled, avirulent mutant that is easier to transform and used worldwide as a standard laboratory strain (Hoskins *et al.* 2001; Hiller *et al.* 2007). The *S. pneumoniae* R6 genome contains none of the required genes that comprise the tricarboxylic acid (TCA) cycle. As a result, *S. pneumoniae* R6 is incapable of synthesizing aspartate (Hoskins *et al.* 2001). In addition to carbohydrates and amino acids, the bacterium requires supplements like peptides, purines, pyrimidines, salts, and vitamins for optimal growth (Kilian 1998). Due to these requirements, highly nutritious media are used for cultivation of *S. pneumoniae* (Lacks & Hotchkiss 1960).

1.1.2 Epidemiology

Bacteria belonging to the genus *Streptococcus* live in association with human and animal hosts, as either commensal or pathogenic organisms. *S. pneumoniae* is an important, opportunistic human pathogen causing invasive diseases such as meningitis, septicaemia and pneumonia (Hoskins *et al.* 2001; Bogaert *et al.* 2004a; Hiller *et al.* 2007). The polysaccharide capsule (prevents phagocytosis by the host's immune system), pneumolysin (Ply), the major autolysin (LytA), choline binding protein A (CbpA) and a number of surface proteins are among some of the pneumococcal virulence factors contributing to its infections in the human host (Jedrzejewski 2001; Sham *et al.* 2012). The composition of the pneumococcal polysaccharide capsule can vary and is classified into different serotypes. Over 90 different

serotypes of *S. pneumoniae* are registered (Giefing *et al.* 2008; WHO 2013). The distribution of serotypes that cause diseases varies by several factors such as host age, disease syndrome and geographic region (WHO 2012). Pneumococci frequently colonize the nasopharynx of approximately 40% of the human population, and especially in children. Approximately, 1 million children under 5 years of age die of pneumococcal diseases annually worldwide (Bogaert *et al.* 2004b, WHO 2013). In developing countries and countries that have a high prevalence of HIV-1 infections, the numbers are even higher (Kadioglu *et al.* 2008). There are several vaccines available to prevent pneumococcal diseases, and all target the pneumococcal polysaccharide capsule. Both 23-valent (covers 23 serotypes) vaccine for adults and the 7-valent vaccine for children have proven to be efficient. However, horizontal gene transfer among *Streptococci* leads to capsular switching and increasing penicillin resistance in *S. pneumoniae*. The consequence of this is pneumococcal strains evading the immune system of vaccinated hosts and inefficient antibiotic treatments (Bogaert *et al.* 2004b; Giefing *et al.* 2008; Sham *et al.* 2012).

1.1.3 Horizontal gene transfer

Horizontal gene transfer (HGT) refers to the transfer of genes between organisms in another way than traditional reproduction (parasexual). HGT comprises of three known mechanisms: Natural genetic transformation, transduction and conjugation (Håvarstein 2010; Johnsborg & Håvarstein 2009). Stable maintenance of the DNA in the recipient microorganism is a prerequisite for successful gene transfer and can be obtained through different processes: 1) homologous recombination, 2) persistence as an episome (plasmid), 3) integration mediated by bacteriophage integrases; and 4) illegitimate incorporation. Through these mechanisms, virtually any sequence can be transferred to and between bacteria (Ochman *et al.* 2000). HGT is a primary reason for the spread of bacterial antibiotic resistance, and has an important role in the evolution of bacteria (Johnsborg & Håvarstein 2009; Lorenz & Wackernagel 1994).

1.2 Natural genetic transformation in *S. pneumoniae*

Natural genetic transformation of bacteria is a mechanism of HGT and depends on the function of several genes located on the bacterial chromosome (Claverys *et al.* 2009). Natural transformation is defined as the ability of a cell to take up and heritably integrate extracellular DNA from the environment (Johnsborg *et al.* 2007). Bacteria that are competent for natural genetic transformation, e.g. *S. pneumoniae*, take up and incorporate exogenous DNA into

their genome by homologous recombination (Johnsborg *et al.* 2008). Because they take up extracellular DNA, regardless of its source, it means that competent *streptococci* do not discriminate between homologous and foreign DNA.

S. pneumoniae becomes competent during the exponential growth phase. Competence is a transient state in the pneumococcus and is initiated by the specific production of the alternative sigma factor ComX, which induces a transcriptional reprogramming of cells (Johnsborg *et al.* 2008; Fontaine *et al.* 2013). Induction of competence is regulated by an auto-inducing regulatory system comprising the secreted competence stimulating peptide (CSP) encoded by *comC*, and a two-component system comprising a membrane embedded histidine kinase receptor (ComD), and its cognate response regulator (ComE) (Håvarstein *et al.* 1995; Johnsborg *et al.* 2007). The two-component system ComDE monitors and responds to the extracellular concentration of CSP (Håvarstein *et al.* 1995; Johnsborg & Håvarstein 2009). During growth, CSP slowly accumulates in the surroundings where it binds to ComD of the CSP-producing cell or cells in close proximity. Interaction with CSP leads to autophosphorylation of ComD. The phosphoryl group is then transferred to the response regulator ComE which then becomes active. ComE in its phosphorylated state, activates transcription of *com*-genes like *comCDE* and *comX* in addition to approximately 20 other early *com*-genes (Håvarstein *et al.* 2006; Johnsborg *et al.* 2007; Johnsborg & Håvarstein 2009). When the CSP-concentration gradually increases outside the cells during growth, the number of phosphorylated ComE increases accordingly leading to elevated expression of ComCDE. The higher level of ComCDE eventually triggers the self-inducing autocatalytic loop, which enhances the expression of competence genes. This will then trigger competence development simultaneously throughout the culture (Claverys *et al.* 2009; Martin *et al.* 2010; Martin *et al.* 2013).

ComX controls the transcription of approximately 80 late competence genes, some of which encode for proteins involved in the DNA uptake and recombination machinery (Johnsborg & Håvarstein 2009; Johnsborg *et al.* 2007). A schematic overview over the regulation of competence is shown in figure 1.3.

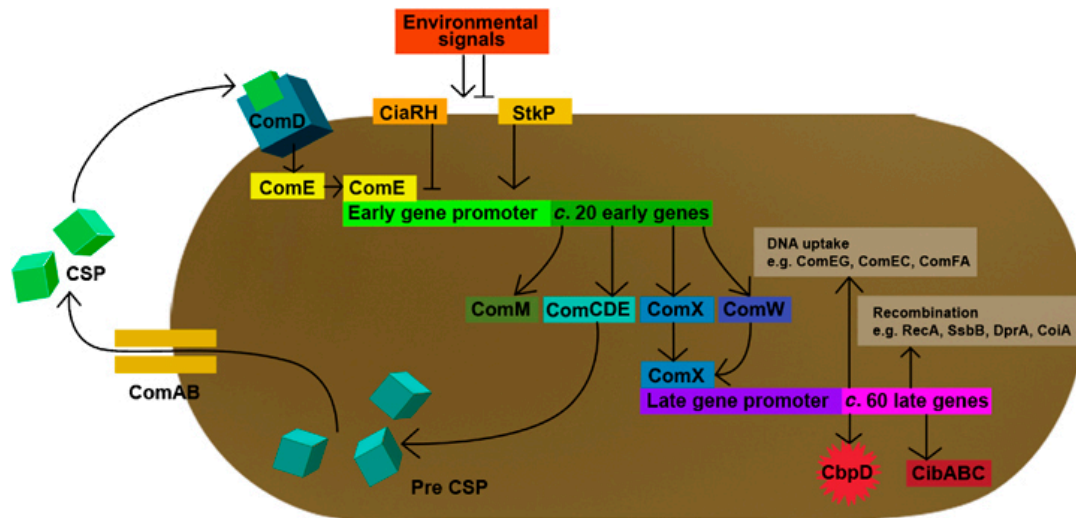


Figure 1.3 Competence regulation in *Streptococcus pneumoniae*: The CSP precursor (encoded by *comC* gene) is processed and secreted by ComAB transporter, which leads to extracellular accumulation of mature CSP. It is believed that the binding of CSP to its ComD receptor results in autophosphorylation of ComD and subsequent transfer of the phosphoryl group to the ComE response regulator. ComE binds and activates transcription. ComE binding results in increased transcription of the *comCDE* operon, which again leads to a bigger production of CSP, ComD and phosphorylated ComE. Figure from Johnsborg & Håvarstein 2009.

Because the competent state is transient, the autoregulatory ComCDE circuit must be switched off. Recently, *S. pneumoniae* has been observed to exit the competent state by the ComX regulated DprA protein. DprA (late *com*-gene) has a dual function during competence; it functions as a RecA loader on the transforming DNA and it interacts with P~ComE and inactivates its activity. By inactivating P~ComE, expression of ComX is turned off and competence is shut off (Mirouze *et al.* 2013).

1.2.1 Competence induced cell lysis – fratricide

In 2002, Steinmoen and coworkers reported that DNA is actively released from pneumococci during induction of the competent state by competence-induced lysis of a subfraction of the cells. They also showed that DNA release and uptake are induced by the same signal transduction pathway (ComCDE) in *S. pneumoniae*. This suggested that lysed cells might act as donors of transforming DNA to the surviving competent cells in the population (Steinmoen *et al.* 2002; Berg *et al.* 2012).

The competence induced murein hydrolase CbpD enables competent cells to kill and lyse non-competent but otherwise isogenic cells. The term fratricide (“killing of brothers”) was adopted to describe this mechanism. For fratricide to take place, both competent and non-

competent cells need to be present. The choline binding murein hydrolase CbpD, the autolysins LytA, and LytC constitute the lysis mechanism in *S. pneumoniae*, with CbpD being the key component and a triggering factor of the fratricide mechanism (Johnsborg & Håvarstein 2009; Berg *et al.* 2012). Studies showed that without CbpD present, competence-induced cell lysis was nonexistent. Furthermore, competent cells express immunity against their own lysins by expressing the immunity protein ComM (Håvarstein *et al.* 2006; Johnsborg *et al.* 2008; Johnsborg & Håvarstein 2009). It is believed the production of fratricins in streptococci is to increase their chances of taking up homologous DNA during the competence period (Berg *et al.* 2012).

1.3 The bacterial cell wall

For cells to maintain its shape and for protection against osmotic pressure, the bacterial cell wall with its peptidoglycan layer is essential. There are two general classes of bacterial cell walls: Gram-positive and Gram-negative. This classification has its origin from 1884 when the Danish bacteriologist Hans Christian Gram discovered a technique (Gram-staining) for distinguishing between two major classes of bacteria (Cabeen & Jacobs-Wagner 2005).

In both Gram-positive and Gram-negative bacteria, the cross-linked polymer peptidoglycan forms the scaffold of the cell wall. The structure of peptidoglycan is relatively similar in all bacteria differing only in amino acid composition of the stem peptides and the length of the glycan chains (Scheffers & Pinho 2005; Cabeen & Wagner 2005). The structure of peptidoglycan is explained in detail in section 1.3.1. For a schematic overview and detailed explanation over the differences between Gram-positive and Gram-negative cell walls, see Figure 1.4 below.

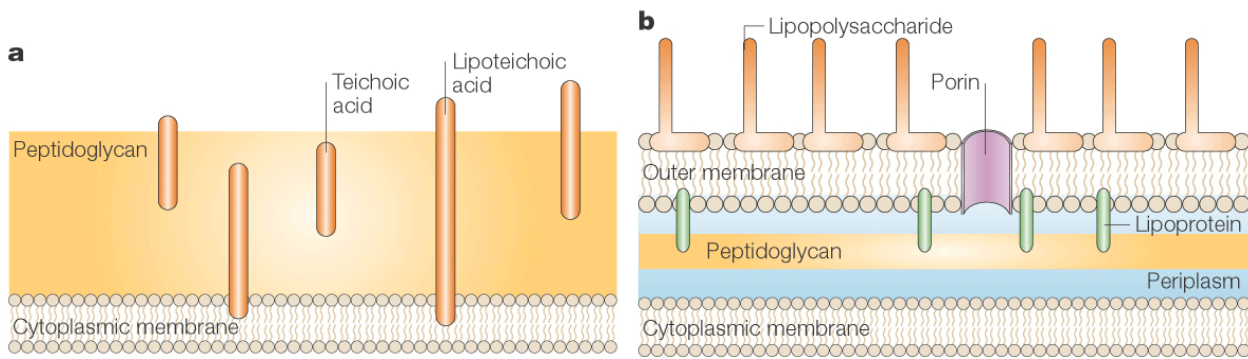


Figure 1.4: Gram-positive and Gram-negative cell walls. A) The Gram-positive cell wall is composed of a thick, multilayered peptidoglycan. Teichoic acids are linked and integrated in the peptidoglycan, while lipoteichoic acids are extended into the cytoplasmic membrane. B) The Gram-negative cell wall is composed of a thin peptidoglycan layer that is surrounded by the outer membrane. The outer membrane and peptidoglycan are linked to each other with lipoproteins and there is a periplasmic space between the inner and outer membrane. Porins allow for passage of small hydrophilic molecules across the outer membrane. Lipopolysaccharide molecules extend into extracellular space in Gram-negative bacteria, the outer membrane is important for shape generation and/or maintenance (Vollmer *et al.* 2008a; Cabeen & Jacobs-Wagner 2005; Scheffers & Pinho 2005). Figure is modified after Cabeen & Wagner 2005.

1.3.1 Peptidoglycan

Peptidoglycan (murein) is a polymer consisting of long glycan chains made of alternating N-acetylmuramic acid (MurNAc) and N-acetylglucosamine (GlcNAc) residues that are connected by short peptides (Vollmer *et al.* 2008b; Egan & Vollmer 2013). The glycan chains together with the cross-linked peptide bridges form a strong and elastic structure. This structure protects against lysis of the underlying protoplast due to high internal osmotic pressure (Scheffers & Pinho 2005). In addition, cell wall components are required for numerous physiological processes, including cell growth and division, uptake of substrates, signaling in quorum sensing, uptake of DNA during transformation, adsorption of phages, autolysis, binding to external macromolecules and adhesion to surfaces (Vollmer 2007; Vollmer *et al.* 2008b). The peptidoglycan in Gram-negative bacteria is 3-6 nm thick compared to the approximately 10-20 nm thick peptidoglycan in Gram-positive species. Central in Gram-positive peptidoglycan is that they have secondary cell wall polymers (wall teichoic acid (WTA) and capsular polysaccharides) covalently attached to it (Denapaite *et al.* 2012; Egan & Vollmer 2013). During growth and division, the combined activities of penicillin binding proteins (PBPs), which synthesize peptidoglycan, and autolysins, which hydrolyse peptidoglycan, maintain and remodel the structure of the cell wall (Pinho *et al.* 2013).

1.3.2 Peptidoglycan synthesis

Biosynthesis of peptidoglycan involves more than 20 enzymes and can be divided into three steps (Vollmer 2007; Pinho *et al.* 2013). Peptidoglycan biosynthesis starts in the cytoplasm where the nucleotide-activated precursors UDP-GlcNAc and UDP-MurNAc are synthesized. UDP-MurNAc is synthesized from UDP-GlcNAc by the enzymes MurA and MurB. It is shown in *E. coli* that the sequential ligation of L-Ala, D-Glu, m-Dap, and D-Ala-D-Ala is catalyzed by amino acid ligases (MurC, MurD, MurE and MurF) to UDP-MurNAc (Egan & Vollmer 2013). Following, precursor lipid intermediates are synthesized at the cytoplasmic membrane. UDP-MurNAc-pentapeptide is transferred to the membrane acceptor bactoprenol, forming lipid I. Then, the formation of lipid II occurs by adding GlcNAc residue (from UDP-GlcNAc) to lipid I (Egan & Vollmer 2013; Scheffers & Pinho 2005). Lipid II is transported to the outside of the cell membrane. Here the final stage of peptidoglycan biosynthesis is done when newly synthesized disaccharide-peptide units is incorporated into the growing peptidoglycan. This is achieved through two reactions that are catalyzed by penicillin binding proteins (PBPs). The first reaction is transglycosylation that is responsible for the formation of glycan bonds. The second reaction is transpeptidation, responsible for peptide bond formation. The reaction results in glycan chains cross-linked with pentapeptides (Scheffers & Pinho 2005; Cabeen & Jacobs-Wagner 2005). The different steps in peptidoglycan biosynthesis involve more enzymes and reactions than mentioned, but the details are not further described here.

1.3.3 Daughter cell separation

The mechanism and location of the machinery involved in the cell wall synthesis varies between bacteria with different morphology. Gram-negative bacteria synthesize and split the septum simultaneously, resulting in a constriction. By contrast, Gram-positive bacteria synthesize a complete septum cross wall before cell separation (Egan & Vollmer 2013). For rod shaped bacteria like *E. coli* and *B. subtilis*, cell wall synthesis occurs by alternating between septal and peripheral peptidoglycan synthesis. Spherical species obtain their shape only through septal peptidoglycan synthesis. In ovococcus species on the other hand, peptidoglycan is synthesized through a so-called two-state model. Peptidoglycan synthesis in *S. pneumoniae* is believed to occur in a combination of peripheral and septal synthesis in the mid-cell regions of dividing cells (Sham *et al.* 2012; Massidda *et al.* 2013) and is described in

detail in section 1.3.3. The peripheral synthesis occurs longitudinal, while septal synthesis occurs perpendicular of the cell axis (Zapun *et al.* 2008).

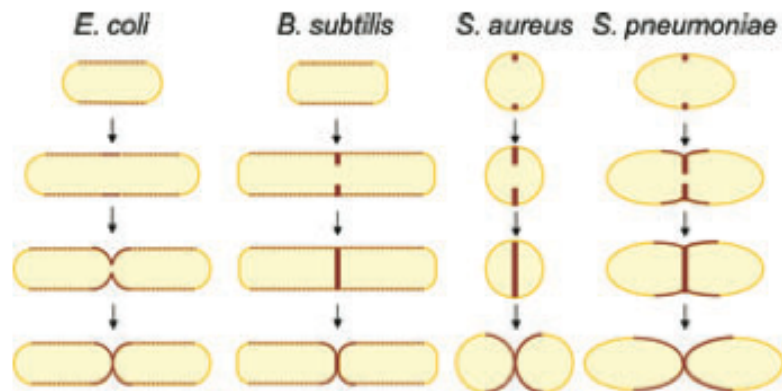


Figure 1.6 Sites of peptidoglycan synthesis during growth and cell division in different bacteria. By insertion of new peptidoglycan into the lateral cell wall, rod shaped bacteria like *E. coli* and *B. subtilis* elongate. In contrast to the rod shaped bacteria, coccal *S. aureus* lacks an elongation phase. The ovococcus *S. pneumoniae* elongates from a growth zone at mid-cell (Egan & Vollmer 2013). Figure from Egan & Vollmer 2013.

1.4 Structure and biosynthesis of the pneumococcal cell wall

Pneumococcal cell wall contains two major polymers in addition to peptidoglycan; choline decorated lip- and wall teichoic acids (LTA and WTA) and the capsular polysaccharides (CPS) (Massidda *et al.* 2013). Pneumococci have a typical Gram-positive cell wall consisting of several layers of glycan chains cross-linked with each other by short peptides. The pentapeptide in pneumococcal peptidoglycan comprises L-Ala-D-iGln-L-Lys-D-Ala-D-Ala and covalently bound to MurNAc. These peptides cross links with nearby peptides (see section 1.3.1). Peptidoglycan is covalently bound with WTA and they are major constituents of the pneumococcal cell wall (Vollmer 2007).

WTA and LTA in *S. pneumoniae* differ from other Gram-positive bacteria in several ways. First, the chemical structure of the repeating units in WTA and LTA are identical. Second, the repeating unit of pneumococcal WTA and LTA are more complex than in other species, and third, both polymers are decorated with choline. Choline is highly unusual in bacteria (Denapaitte *et al.* 2012; Vollmer 2007). As far as we know, the only species where choline is an essential growth factor is in *S. pneumoniae*. Figure 1.7 shows the structure of the repeating unit in WTA and LTA.

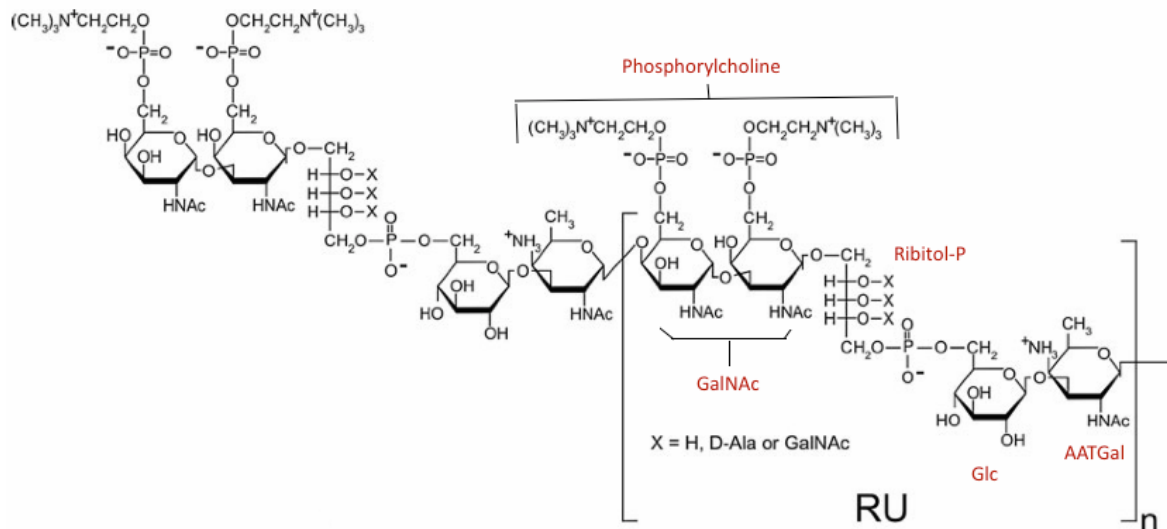


Figure 1.7 Structure of the repeating unit teichoic acid in *S. pneumoniae*. The chemical structure of the repeating units in WTA and LTA are identical. It contains glucose (Glc), a rare amino sugar 2-acetamido-4-amino-2,4,6-trideoxygalactose (AATGal), Ribitol-5-phosphate (Rib-5-P/Rib-P), and two N-acetylgalactosamine (GalNAc) residues, each of which carries a phosphorylcholine (P-Cho) moiety. The figure is modified after Denapaite *et al.* (2012).

1.4.1 Penicillin binding proteins (PBPs)

Penicillin-binding proteins (PBPs) are characterized by their affinity for and binding of penicillin. PBPs are membrane-bound enzymes involved in the final stages of bacterial cell wall synthesis on the periplasmic side of the membrane (Martel *et al.* 2009). Penicillin-binding proteins catalyze a number of reactions involved in the process of synthesizing cross-linked peptidoglycan from lipid II precursors. In pneumococci, PBP1a and PBP2x catalyze the septal peptidoglycan synthesis that occurs at the division site. Peripheral peptidoglycan synthesis is catalyzed by PBP2b and occurs in close proximity to the division site. Other PBPs are also involved in cell wall synthesis (PBP1b and PBP2a) but their exact roles are unknown (Pinho *et al.* 2013). In *S. pneumoniae*, penicillin resistance is a result of the proliferation of mosaic PBP-encoding genes, which can lead to proteins containing several mutations (Chambers 1999; Martel *et al.* 2009; Moriot *et al.* 2003).

PBPs are the primary targets of β -lactam antibiotics by binding irreversibly to the active site of their transpeptidase domain, which disrupts the cell wall biosynthesis. *S. pneumoniae* does not produce β -lactamase. This is why the most relevant mechanism is to alter the target by mutating its PBPs (Chambers 1999; Moriot *et al.* 2003). Penicillin resistance is obtained by expressing mutated PBPs that have low affinity for β -lactam antibiotics.

1.4.2 Peptidoglycan biosynthesis and daughter cell separation in *S. pneumoniae*

Streptococci divide in parallel planes perpendicular to their long axis. In contrast to spherical cocci, peptidoglycan synthesis in ovococci, like *S. pneumoniae*, is believed to occur in a combination of peripheral and septal synthesis in the mid-cell regions of dividing cells (Sham *et al.* 2012; Massidda *et al.* 2013). This so-called two-state model of peptidoglycan synthesis is not strictly synchronized resulting in the characteristic diplococci and/or short chain formations.

Cell division is initiated by an inward growth of the cross wall (localized at the cell equator), marked by an equatorial ring (future division site). Peripheral synthesis is responsible for the longitudinal elongation. Soon after, new peptidoglycan is inserted between the newly generated rings that are formed on each side of the equatorial ring while the initial centripetal growth remains constant. Murein hydrolases complete the cell division by cleaving the peptidoglycan at the septum (septal cross wall) and thus releasing the adjacent daughter cells (Massidda *et al.* 2013; Sham *et al.* 2012; Giefing-Kröll *et al.* 2011; Pinho *et al.* 2013). Peptidoglycan hydrolases are required to cleave various bonds in mature peptidoglycan and thereby allow access points for insertion of newly synthesized glycan strands and the separation of daughter cells. Figure 1.8 shows the two-state model predicted for peptidoglycan biosynthesis in ovococci. Peptidoglycan biosynthesis involves both synthesis and remodeling of peptidoglycan by hydrolase enzymes. In *S. pneumoniae*, there are 11 known or putative murein hydrolases. The single deletion of either *dacA*, *pmp23* or *PcsB* lead to aberrant cell division, while the deletion of *LytB* leads to severe cell chaining. This indicates that these cells have a role of regarding synthesis and/or cleavage of the division septum (Massidda *et al.* 2013). The putative peptidoglycan hydrolase *PcsB* is predicted to perform the operation of splitting the septal cross wall and is explained in detail in section 1.6.

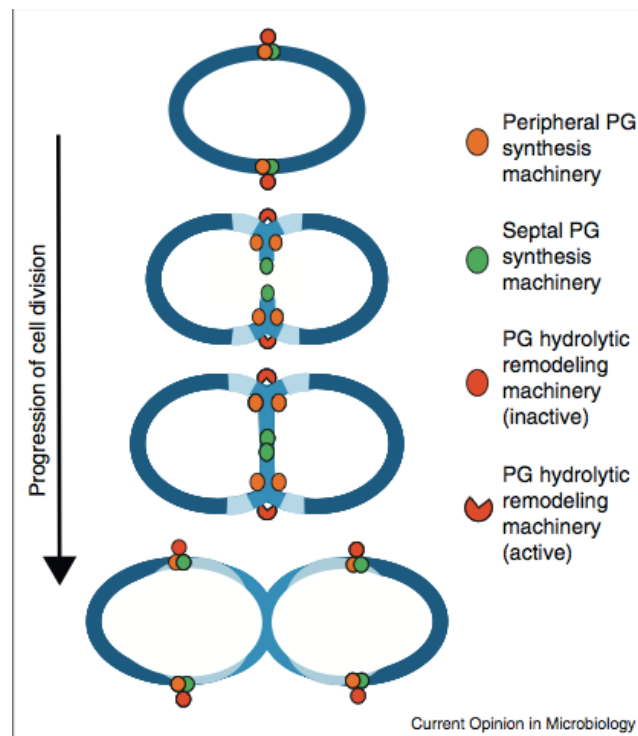


Figure 1.7 Cell division and peptidoglycan (PG) biosynthesis in *S. pneumoniae*. Two machineries are suggested to carry out the septal and peripheral synthesis of peptidoglycan. Both machineries are located at the equators of cells. The orange dots illustrate the peripheral PG synthesis (light blue cell wall), whereas the green dots illustrate the septal PG synthesis. At some point, the septal PG synthesis commences to divide the cell in two. Red dots illustrate PG hydrolases involved in PG remodeling. Figure from Sham *et al.* (2012).

1.5 The peptidoglycan hydrolase PcsB

Peptidoglycan synthesis in *S. pneumoniae* is monitored by a two-component regulatory system called WalKR (VicKR). WalKR controls the expression of a number of peptidoglycan hydrolases. One of these hydrolases is called PcsB (protein required for cell wall separation of group B streptococci). PcsB is highly conserved among group B streptococci and the deletion of the *pcsB* gene results in misplacement of the division septum, reduced growth rate and clumping (Giefing-Kröll *et al.* 2011). Bartual *et al.* (2014) showed that reduced expression of PcsB resulted in reduced growth rate and abnormal cell shape. These studies demonstrate that PcsB is essential for proper cell division and proliferation, but not essential for cell survival in *S. pneumoniae* (Giefing-Kröll *et al.* 2011). However, PcsB has been shown to be essential in pneumococci strains R6 and D39. Therefore, PcsB is regarded as conditionally essential in *S. pneumoniae* (Bartual *et al.* 2014; Massidda *et al.* 2013).

PcsB is 392 amino acids long, localized at the division septa and the cell poles, and is involved in splitting of the cross wall resulting in daughter cell separation during cell division

(Massidda *et al.* 2013; Bartual *et al.* 2014). PcsB consists of four major parts: (i) an N-terminal signal peptide, (ii) a coiled-coil (CC) domain containing putative leucine zipper motifs, (iii) an alanine rich linker region of variable length, and (iv) a C-terminal cysteine, histidine-dependent amidohydrolase/peptidase (CHAP) domain (Bartual *et al.* 2014; Barendt *et al.* 2009).

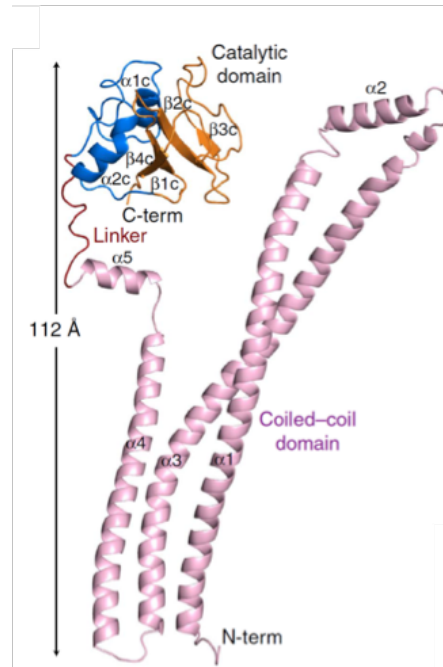


Figure 1.8 Three-dimensional structure of mature PcsB from *S. pneumoniae* R6 (Figure from Bartual *et al.* (2014)).

CHAP domains are known to function as murein hydrolases by cleaving the stem peptides in the peptidoglycan. The CHAP domain of PcsB has been found essential for its functionality. By mutating the conserved cysteine and histidine residues in the active site, these cells acted as $\Delta pcsB$ mutants (Giefing-Kröll *et al.* 2011). Recently, the murein hydrolase activity of the CHAP domain of PcsB was demonstrated for the first time (Bartual *et al.* 2014). The 3D-structure of PcsB showed that its catalytic domain is occluded in the inactive state through homo-dimerisation, preventing the substrate from entering the cavity of the active site. For PcsB to be active, it undergoes a conformational change, which is thought to release the CHAP domain from its locked position in the homo-dimer. This conformational change is mediated via interactions with the membrane-embedded protein FtsX (Bartual *et al.* 2014; Massidda *et al.* 2013; Sham *et al.* 2013). FtsX interacts with the cytoplasmic ATPase FtsE, which provides the energy required by hydrolyzing ATP (Fig. 1.9)

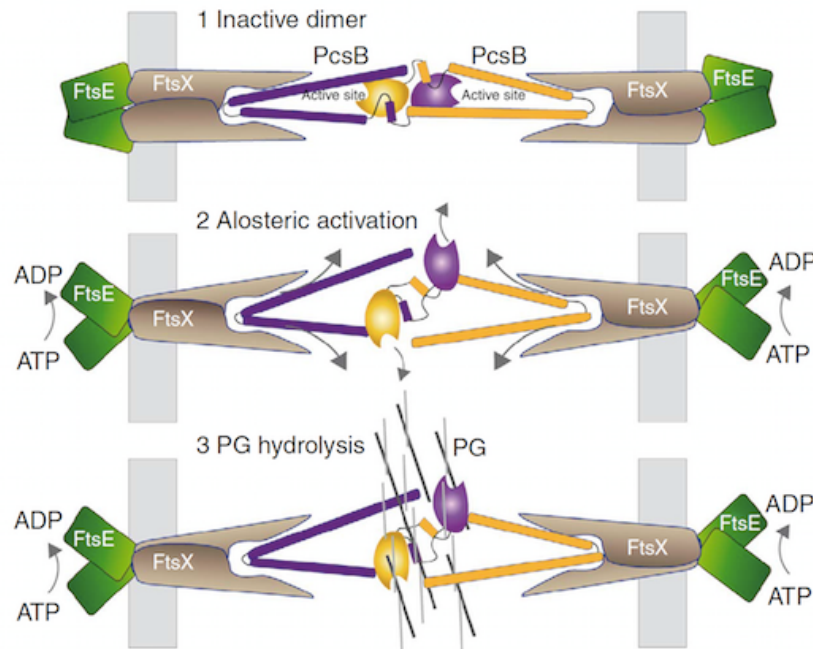


Figure 1.9 Activation and regulation of PcsB. The figure shows the regulation of hydrolytic activity of PcsB. The inactive dimer is located at the septum by FtsX (1). An allosteric change on PcsB is induced by the ATPase activity of FtsE. This happens through FtsX, which produces the release of the CHAP domains (2). The catalytic domains start the peptidoglycan hydrolysis and splitting of the cross wall in the septum (3) (Bartual *et al.* 2014). Figure is taken from Bartual *et al.* (2014).

Recently, PcsB has emerged as a leading candidate for a new-generation pneumococcal vaccine. Current pneumococcal vaccines in use consist of a mixture of 7-23 capsular polysaccharides, depending on the target group and vaccine type. These vaccines are often expensive to produce with limited coverage regarding serotypes. A promising alternative is therefore PcsB, which is surface-exposed and has a highly conserved aa sequence (>99.5% identity) among clinical isolates of *S. pneumoniae* (Giefing *et al.* 2007; Sham *et al.* 2011; Bartual *et al.* 2014).

1.6 Thesis objectives

In order to unravel molecular mechanisms, it is necessary to have the proper molecular tools. The main objective of this study was to develop a tool for detection of native PcsB in *S. pneumoniae*:

- To purify PcsB for immunization and production of PcsB-specific antibodies.
- To test the specificity of antibodies against native PcsB and optimize the conditions for PcsB detection by using Western blotting.
- To investigate the quantity of PcsB present in cells and the amount of PcsB being secreted.
- To determine the stability of PcsB in *S. pneumoniae*.

2. Materials

2.1 Bacterial strains and plasmids

Table 2.1. Bacterial strains and plasmids used in this study

Strains and plasmids	Genotype / relevant features	Antibiotic resistance	Reference / source
<i>S. pneumoniae</i>			
DS125	<i>E. coli</i> BL21, pGS01		Dr. D. Straume Johnsborg <i>et al.</i> (2008)
RH1	R704, but $\Delta comA$, Δebg	Ery ^r , Spc ^r	
SPH131	SPH130, but luc::janus	Kan ^r	Berg <i>et al.</i> (2011)
SPH247	SPH246 but $\Delta native$ PcsB::Janus	Kan ^r	Bartual <i>et al.</i> (2014)
	SPH154, but replacement of Janus by		
SPH234	P _{comX} ::pbp2x-FLAG	Sm ^r	Berg <i>et al.</i> (2014)
SvH1	<i>E. coli</i> BL21, pGS01-ChiC-PcsB		This study
SvH2	SPH247 but janus::PcsB-3xFlag	Strep ^r	This study
SvH3	SvH2, but P _{comX} -PcsB::janus	Kan ^r	This study
<i>E. coli</i>			
BL21	Expression host		Invitrogen
Plasmids			
	pRSET A containing ChiC-fused PcsB		
pGS01	(behind <i>T7/lac</i> promoter)		Stamsås <i>et al.</i> (2012)

2.2 Peptides

Table 2.2: Amino acid sequence of the competence stimulating peptide CSP-1 and ComS*.

Pheromone	Strain	Amino acid sequence (N→C)	Stock solution	Manufacturer
		EMRLSKFFRDFIL		Research
CSP-1	<i>S.pneumoniae</i> R6	QRKK	100 µg/ml	Genetics Inc
ComS*		LPYFAGCL	500 µM	Genosphere Biotech

2.3 Primers

Table 2.3: Overview over primers used in this study, with corresponding oligonucleotide sequences.

Name	Oligonucleotide sequence (5' - 3')	Description	Reference
	TTATTTATCATCATCATCTTTATAATC AATATCATGATTTTATAATCACCATCA TGATCTTTATAATCATCTGCATAAATA		
ds148	TATGTAACAAAAC	Rev PcsB 3xflag	This study
	GATTATAAAGATGATGATGATAAATA		
ds149	ATTACAGAGGGACTCGAATAG	PcsB down flag	This study
	GATTATAAAGATGATGATGATAAATA		
ds150	ATTTCTAATATGTAACCTCTCCCAAT	Fwd khb33 flag component	This study
37	TCAAAGGTGCTTCTGAGAAC	spr2021 pcsB, 1000 bp upstream	Bartual <i>et al.</i> (2014)
38	CTTCTACAACCTCAACGATTTC	spr2021 pcsB, 1000 bp downstream	Bartual <i>et al.</i> (2014)
	AAAAGAAGGAGTATCTACGTAATATG	Fwd start PcsB, overlap	Bartual <i>et al.</i>
216	AAGAAAAAATCTTAGCGTC	upstream PcsB	(2014)
			Bartual <i>et al.</i>
218	ATTACGTAGATACTCCTTCTTTT	Rev PcsB spr2021	(2014)
		cpsO.F, 800 bp	Berg <i>et al.</i>
khb31	ATAACAAATCCAGTAGCTTTGG	upstream	(2011)
		cpsN.R, 800 bp	Berg <i>et al.</i>
khb34	CATCGGAACCTATACTCTTTAG	downstream of insert	(2011)
			PhD-student
		100 bp downstream	G.A.
41	ACGGTAAAACCTGAAAAGAGG	pcsB for sequencing	Stamsås
			PhD-student
		100 bp upstream pcsB	G.A.
42	CGACATATAAATGTAACAAAGG	for sequencing	Stamsås
484			Johnsborg <i>et al.</i>
Janus F	GTTTGATTTTAAATGGATAATGTG		(2008)

2.4 Standards, enzymes and nucleotides

Table 2.4 Overview over standards, enzymes and nucleotides used in this study.

Name	Stock concentration	Supplier
1 kb DNA ladder	500 µg/ml	BioLabs
Prestained Protein Marker, Broad range (10-230 kDa)		New England BioLabs
AcTEV protease	10 U/µl	Invitrogen
DNase 1	1 mg/ml	New England BioLabs
Lysozyme	100 mg/ml	Sigma
Phusion™ High-Fidelity DNA Polymerase	2.0 U/µl	New England BioLabs
Taq DNA Polymerase	5.0 U/ml	New England BioLabs
dNTPs (dATP, dCTP, dGTP, dTTP)	100 mM	Promega

2.5 Antibiotics

Table 2.5: Antibiotics used in this study with corresponding stock solution and concentration used.

Antibiotic	Stocksolution	Concentration used	Supplier
Ampicillin	100 mg/ml	100 µg/ml	Sigma
Streptomycin	100 mg/ml	200 µg/ml	Sigma-Aldrich
Kanamycin	100 mg/ml	400 µg/ml	Sigma-Aldrich

2.6 Kits

Table 2.6 Kits used in this study with area of use.

Name	Area of use	Supplier
NucleoSpin® Extract II	DNA extraction from agarose gel	Macherey-Nagel

2.7 Antibodies and substrates

Table 2.7 Antibodies and substrates used for immunodetection. An overview over primary – and secondary antibodies used in this study.

Name	Source	Concentration / Volume	Supplier
Primary antibody			
Anti-FLAG	Rabbit	1:5000 / 1:200	Sigma Aldrich
Anti-PcsB	Rabbit	1:5000 / 1:10000	ProSci Inc – custom ¹
Secondary antibody			
Anti-rabbit (IgG) AP ²	Goat	1:4000	Sigma
Anti-rabbit (IgG) HRP ³	Goat	1:4000	Sigma
Anti-rabbit Alexa 488	Goat	1:100	Life Technologies
Substrate			
Blue liquid substrate system		3-5 ml	Sigma Aldrich
Pierce ECL Western Blotting substrate		5 ml luminol reagent + 5 ml peroxide solution	Thermo Scientific
Slowfade Gold Antifade		7 µl	Life Technologies

¹Anti-PcsB; custom made antibody delivered by ProSci Inc.

²Conjugated with alkaline phosphatase

³Conjugated with horse raddish peroxidase

2.8 Computer software

Table 2.8 Computer software applied during this study

Software	Application	Available from
	Computation of various physical and chemical parameters	
ProtParam		http://web.expasy.org/protparam/
BLAST	Sequence alignment	http://blast.ncbi.nlm.nih.gov/Blast.cgi
ClustalW	Sequence alignment	https://www.ebi.ac.uk/Tools/msa/clustalw2/
Reverse Complement	Reverse complements DNA-sequences	http://www.bioinformatics.org/sms/rev_comp.html

2.9 Chemicals

Table 2.9 A list of chemicals used throughout the experiments

Name	Chemical formula	Supplier
Acetic acid	CH ₃ COOH	Merck
Acrylamide	C ₃ H ₅ NO	Saveen Werner
Activated charcoal	C	Merck
Agar - agar microbiology		Merck
Agarose		Invitrogen
Albumine/BSA		Sigma Aldrich
APS	(NH ₄) ₂ S ₂ O ₈	Sigma
Bacto-tryptone		BD & Company
Bacto™ Todd Hewitt broth (TH)		BD & Company
Biotin	C ₁₀ H ₁₆ N ₂ O ₃ S	Fluka
Bromphenol blue	C ₁₉ H ₁₀ Br ₄ O ₅ S	Sigma
Calcium Chloride dehydrated	CaCl	Fluka
Calcium panthothenate	C ₁₈ H ₃₂ CaN ₂ O ₁₀	Sigma Aldrich
Choline Chloride	C ₅ H ₁₄ NO*Cl	Sigma
Choline Chloride	C ₅ H ₁₄ NO*Cl	Sigma Aldrich
Coomassie Brilliant blue R-250	C ₄₅ H ₄₄ N ₃ NaO ₇ S ₂ (Sodium salt)	Thermo Scientific
Copper sulphate pentahydrate	CuSO ₄ *5H ₂ O	Sigma
DEAE-cellulose		Sigma
Disodium hydrogen phosphate dihydrate	Na ₂ HPO ₄ *2H ₂ O	Merck
Distilled water	dH ₂ O	-
DTT	C ₄ H ₁₀ O ₂ S ₂	Thermo Scientific
EDTA	C ₁₀ H ₁₆ N ₂ O ₈	VWR
Ethanol	C ₂ H ₆ O	Merck
Ethidium Bromide	C ₂₁ H ₂₀ BrN ₃	Sigma Aldrich
Glucose	C ₆ H ₁₂ O ₆	VWR
Glycerol	C ₃ H ₈ O ₃	Sigma
Glycine	C ₂ H ₅ NO ₂	Merck
Hydrochloric acid	HCl	Riedel-de Haën
Imidazole	C ₃ H ₄ N ₂	Sigma
IPTG	C ₉ H ₁₈ O ₅ S	Promega
Iron sulphate heptahydrate	FeSO ₄ *7H ₂ O	Fluka
L-asparagine monohydrate	C ₄ H ₈ N ₂ O ₃ *H ₂ O	Sigma Aldrich
Magnesium chloride	MnCl ₂	-

Name	Chemical formula	Supplier
Magnesium Chloride hexahydrate	MgCl ₂ *6H ₂ O	Fluka
Manganese(II)-chloride tetrahydrate	MnCl ₂ *4H ₂ O	Riedel-de Haën
Methanol	CH ₂ OH	Merck
Nicotinic acid	C ₆ H ₅ NO ₂	Fluka
PFA	OH(CH ₂ O) _n H (n = 8 - 100)	Sigma Aldrich
Potassium chloride	KCl	Merck
Potassium dihydrogen phosphate	KH ₂ PO ₄	Merck
Pyridoxine hydrochloride		Fluka
Riboflavine	C ₁₇ H ₂ ON ₄ O ₆	Sigma Aldrich
SDS	NaC ₁₂ H ₂₅ SO ₄	Fluka
Skim milk powder		Merck
Sodium chloride	NaCl	Merck
Sodium hydroxide	NaOH	Merck
Sodium pyruvate		Sigma Aldrich
Sucrose	C ₁₂ H ₂₂ O ₁₁	BHD
TEMED	C ₆ H ₁₆ N ₂	Sigma
Thiamine hydrochloride	C ₁₂ H ₁₇ ClN ₄ OS*HCl	Sigma Aldrich
Triton X-100	C ₁₄ H ₂₂ O(C ₂ H ₄ O) _n (n=9-10)	Sigma
Trizma base, minimum 99,9% titration	NH ₂ C(CH ₂ OH) ₃	Sigma
Tween 20 (polyoxyethylene sorbitan monolaurate)	C ₅₈ H ₁₁₄ O ₂₆	BioRad
Yeast extract - granulated		Merck
Zink sulphate heptahydrate	ZnSO ₄ *7H ₂ O	Fluka
β-2-mercaptoethanol	C ₂ H ₆ SO	Sigma Aldrich

2.10 Technical equipment

Table 2.10 A list over equipment used in this study. In addition to the technical equipment listed here, standard laboratory equipment was used.

Equipment	Model	Manufacturer
Anaerobic cultivation bags	AnaeroGen	Oxoid
Autoclave	CV-EL 12L/18L	Certoclav
Centrifuge	5430 R	Eppendorf
Centrifuge	Multifuge 3 S-R	Heraeus
Centrifuge	JA-10	Beckman Coulter
Centrifuge	Avanti J-25	Beckman Coulter

Equipment	Model	Manufacturer
Centrifuge	5424	Eppendorf
Container for anaerobe cultivation		Oxoid
Disposable kyvettes		Brandt
Electrophoresis	Power Pac 200	BioRad
Film	CL-X Posure™ Film, Clear Blue X-Ray Film	Thermo Scientific
Filter (0.2 µm)		Sarstedt
Filter paper	Whatman Gel Blotting Paper	Sigma Aldrich
Freezer	-80°C ULT FREEZER	Thermo Forma
Freezer	-20°C	Bosch
Gel imaging	GelDoc	BioRad
Ice machine		PORKKA
Incubator	Multitron eco / minitron	HT INFORS
Incubator	37°C	Termaks
IE Chromatographer	ÄKTA prime plus	GE
Magnetic stirrer	MR 3001 K	Heidolph
Microscope	LSM700	Zeiss
Microwave	MWO0602	Whirlpool
pH meter	PHM210	MeterLab
Pipette tips		Thermo Scientific
Pipettes	10 µl, 50 µl, 100µl, 1000 µl, 5 ml	VWR
PVDF-membrane	Immun-Blot Tm PVDF Membrane for Protein Blotting (0,2 µm)	BioRad
Quarts cyvette		Hellma
Refrigerator		Bosch
Rocking table		Edmund Bühler
SDS-PAGE	MINI-PROTEAN® Tetra System	BioRad
SDS-PAGE	Power Pac 1000	BioRad
Spectrophotometer	LKB Novaspec 11	Pharmacia Biotech
Spectrophotometer	DV® 800	Beckman Coulter
Sterile benches	AV-100	Telstar
Sterile scalpel		
Syringes		BD Plastipac
Thermocycler	PTC-100	MJ Research Inc.
Thermocycler	2720	Applied biosystems

Equipment	Model	Manufacturer
Vortexer		Janke & Kunkel IKA
Waterbath		Julabo
Waterbath		GFL
Weight	CP 124 S	Sartorius
Western Blot	Trans-Blot SD Semi Dry Electrophoretic transfer Cell	BioRad

2.11 Recipes – growth media, buffers and solutions

2.11.1 Growth media

Luria Bertani (LB) B growth medium	
Bacto-tryptone	10 g
Yeast extract	5.0 g
Sodium chloride (NaCl)	10 g
dH ₂ O	1 L

The solution was autoclaved at 121°C for 15 minutes and stored at 4°C.

Todd-Hewitt Agar (THA)	
30 g/L bacto™ Todd Hewitt Broth	15 g
1.5% (w/v) Agar	7.5 g
Total volume (adjusted with dH ₂ O)	500 ml

The solution was autoclaved at 121°C for 15 minutes. Further, it was casted into plates and stored at 4°C. For TH-agar plates that should contain antibiotics, this was added to cooled (about 60°C) media before casting.

Pre C-Medium	
L-cystein HCl	0.045 g
Sodium Acetate	8.0 g
Bacto™ Casitone	20 g
L-tryptophan	0.024 g
di-potassiumhydrogenposphate (K ₂ HPO ₄)	34 g
Total volume (adjusted with dH ₂ O)	4 L

The solution was autoclaved at 121°C for 15 minutes and stored at room temperature.

C-Medium	To 150 ml pre C-medium, the following was added:
0.4 mM Manganese chloride (MnCl ₂)	150 µl
20% Glucose	1.5 ml
ADAMS III	3.75 ml
3% Glutamine	110 µl
2% Na Pyruvate	2.25 ml
1.5 M Sucrose	95 µl
2 mg/ml Uridine adenosine	1.5 ml
8% Albumin/BSA	1.5 ml
Yeast extract	3.75 ml

Solution is stored at 4°C with a durability of one day.

2.11.2 Solutions for C-medium

Yeast extract	
Yeast extract	40 g
dH ₂ O	360 ml
37 % HCl	6 ml
Activated charcoal	16 g
Total volume (adjusted with dH ₂ O)	400 ml

The yeast extract was dissolved in dH₂O and the pH was adjusted to 3.0 with 37% HCl to precipitate proteins. Furthermore, activated charcoal was added and the solution was stirred with a magnetic stirrer for 10 min followed by incubation at 4°C for two hours. A column filled with glass wool and celite was used for filtration o/n and pH was adjusted to 7.8 with NaOH. The yeast extract was sterile-filtered and stored as 4 ml aliquots at -80°C.

Adams I

0.5 mg/ml Biotin	0.15 ml
Nicotinacid	75 mg
Pyridoxine hydrochloride	87.5 mg
Calcium panthothenate	300 mg
Thiamin hydrochloride	80 mg
Riboflavine	35 mg
Total volume (adjusted with dH ₂ O)	500 ml

pH was adjusted to 7.0 and the solution was stored at 4°C.

Adams II- 10X

Iron sulphate heptahydrate	500 mg
Copper sulphate pentahydrate	500 mg
Zink sulphate heptahydrate	500 mg
Mangan(II)-chloride tetrahydrate	200 mg
Concentrated HCl	10 ml
Total volume (adjusted with dH ₂ O)	100 ml

The solution was sterile-filtered and stored at 4°C.

Adams III

ADAMS I	128 ml
ADAMS II	3.2 ml
Asparagine monohydrate	1.6 g
Choline Chloride	0.160 g
Calcium chloride dehydrated	0.4 g
Magnesium chloride hexahydrate	16 g
Total volume (adjusted with dH ₂ O)	800 ml

The pH was adjusted to 7.6 followed by sterile-filtration and storage at 4°C.

2.11.3 Buffers and solutions for protein purification

1 M Tris-HCl, pH 7.4 (250 ml)

30.3 g Tris Base was dissolved in 200 ml dH₂O. pH was adjusted to pH 7.4 with HCl. .

0.5 M Tris-HCl, pH 6.8 (100 ml)

6.06 g Tris Base was dissolved in 50 ml dH₂O and adjusted with HCl to a pH of 6.8.

10 mM Tris-HCl, pH 7.4, 100 mM NaCl (500 ml)

2.922 g NaCl was added to 5 ml 1 M Tris-HCl, pH 7.4 and diluted with dH₂O to a concentration of 10 mM Tris-HCl and volume of 500 ml.

10 mM Tris-HCl, pH 7.4, 1.5 M NaCl (250 ml)

21.915 g NaCl was added to 2.5 ml 1 M Tris-HCl, pH 7.4 and diluted with dH₂O for right concentration.

10 mM Tris-HCl, pH 7.4, 1.5 M NaCl, 0.14 M Choline (30 ml) (prepare fresh)

0.586 g of Choline Chloride was added to 30 ml 10 mM Tris-HCl, pH 7.4, 1.5 M NaCl.

10 mM Tris-Hcl, pH 7.4, 0.14 M Choline (1 L)

19.55 g Choline chloride was dissolved in 10 ml of 1M Tris-HCl, pH 7.4 and dH₂O was added to a final volume of 1 L. Stored at room temperature.

10 mM Tris-HCl, pH 7.4, 0,5 M NaCl (500 ml)

14.61 g NaCl was added to 5 ml 1 M Tris-HCl, pH 7.4. Final volume was adjusted with dH₂O to 500 ml.

TEV cleavage

100 units (10units/μl) AcTEV protease	10 μl
20 x TEV buffer	25 μl
0,1 M DTT	5 μl
Protein (PcsB)	500 μl

Cleavage at room temperature for 1-3 hr.

2.11.4 Buffers and solutions for agarose gel electrophoresis

6x DNA loading buffer	
10 mM Tris-Hcl, pH 7.4	50 μ l
1 mM EDTA, pH 8.0	10 μ l
40% (w/v) sucrose	2 g
dH ₂ O	4-5 ml
0.01% (w/v) Bromphenol blue	
Total volume	5 ml

50x TAE (Tris-Acetic acid-EDTA)	
Tris Base	242 g
Acetic acid	57.1 ml
0.5 M EDTA, pH 8.0	100 ml
Total volume (adjusted with dH₂O)	1 L

* 1x TAE-buffer was used for electrophoresis.

1 kb DNA ladder	
500 μ g/ml 1 kb DNA ladder (BioLabs)	50 μ l
6x DNA loading buffer	83.3 μ l
Total volume	500 μl

Ethidiumbromide (EtBr)

EtBr was dissolved in dH₂O to a final concentration of 10 mg/ml and stored in an opaque container at room temperature.

2.11.5 Buffers and solutions for SDS-PAGE

10x Tris-Glycine Runningbuffer	
0.25 M Tris Base	30 g
1.92 M Glycine	144 g
1% (w/v) SDS	50 ml
Total volume (adjusted with dH₂O)	1 L

* 1 X Tris-Glycine running buffer was used for SDS-PAGE

2x SDS sample buffer	
0.125 M Tris-HCl, pH 6.8	2.5 ml
4% (w/v) SDS	2.0 ml
0.30 M b-2-mercaptoethanol	0.214 ml
20% (w/v) Glycerol	2.3 ml
0.01% (w/v) Bromphenol blue	
Total volume (adjusted with dH ₂ O)	10 ml

2.11.6 Recipes for separation gel and stacking gel used for SDS-PAGE

Separation gel (for 2 gels)

	8%	10%	12%	15%	18%
ddH ₂ O	5.3 ml	4.78 ml	4.3 ml	3.55 ml	2.8 ml
1.5M Tris-HCl, pH 8.8	2.5 ml	2.5 ml	2.5 ml	2.5 ml	2.5 ml
10% SDS	0.1 ml	0.1 ml	0.1 ml	0.1 ml	0.1 ml
40% acrylamide+0.8%bis-acrylamide	2 ml	2.5 ml	3 ml	3.75 ml	4.5 ml
10% APS	0.1 ml	0.1 ml	0.1 ml	0.1 ml	0.1 ml
TEMED	5 μ l	5 μ l	5 μ l	5 μ l	5 μ l
Total volume	10 ml	10 ml	10 ml	10 ml	10 ml

Grey area needs to be added final because of polymerization

Stacking gel (for 2 gels)

	4%
ddH ₂ O	6.27 ml
0.5M Tris-HCl, pH 6.8	2.5 ml
10% SDS	0.1 ml
40% acrylamide+0.8%bis-acrylamide	1.06 ml
10% APS	0.1 ml
TEMED	0.01 ml
Total volume	5 ml

Grey area needs to be added final because of polymerization

2.11.7 Solutions for Coomassie-staining of gel

Coomassie blue staining solution	
0.2% Coomassie Brilliant Blue	1 ml
50% methanol	250 ml
7.5% acetic acid	37.5 ml
dH ₂ O	211.5 ml
Total volume	500 ml

Destain solution

50% Methanol	250 ml
7,5% acetic acid	37.5 ml
dH ₂ O	212.5 ml
Total volume	500 ml

2.11.8 Solutions for Western Blot**1X Transfer Buffer**

192 mM Glycin	14.4 g
25 mM Tris Base	3.03 g
10% (v/v) Methanol	100 ml
Total volume (adjusted with dH ₂ O)	1 L

Stored at 4°C.

TBS-T

20 mM Tris-HCl, pH 7.4	20 ml
50 mM NaCl	2.922 g
0.05% Tween-20	0.5 ml
Total volume adjusted with dH ₂ O	1 L

Stored at room temperature.

Blocking solution:

5% skim milk powder dissolved in TBS-Tween

2.11.9 Solutions for Immunofluorescence microscopy**4% Paraformaldehyde (PFA)**

Paraformaldehyde was dissolved in PBS pH 7.4 to a final concentration of 4% (w/v) and heated to 60°C until the solution was clear. The fixation solution was stored at 4°C.

1X PBS, pH 7.4

137 mM NaCl	8.0 g
2.7 mM KCl	0.201 g
10 mM Na ₂ HPO ₄ *2H ₂ O	1.7799 g
2 mM KH ₂ PO ₄	0.272 g
Total volume adjusted with dH ₂ O	1.0 L

pH was adjusted to pH 7.4. Short-term storage at room temperature.

To make PBS-T, 200µl Triton X-100 was added to 100 ml PBS (0.2% v/v).

GTE

50 mM Glucose	2,5 ml
1 mM EDTA	50 µl
20 mM Tris-HCl, pH 7.5	0,5 ml
Total volume	25 ml

5% Dry milk (for blocking)

5 g dry milk was added per 100 ml PBS / PBS-T

3. Methods

3.1 Cultivation and storage of bacteria

3.1.1 Cultivation of *Escherichia coli*

E. coli strains were grown in Luria Bertani (LB) medium with shaking at 37°C, or at 28°C during over expression of recombinant proteins. When necessary, ampicillin was added to the growth medium to a final concentration of 100 µg/ml. Strains of *E. coli* were stored as described in section 3.1.4.

3.1.2 Anaerobic cultivation and transformation of *S. pneumoniae*

S. pneumoniae strains were grown in liquid C-medium (Lacks, S.A., Hotchkiss, R.D. 1960) or on Todd Hewitt (TH) agar plates at 37°C. *S. pneumoniae* grows best under anaerobic conditions. Therefore, to optimize for these conditions, liquid C-medium was stored in tubes with caps. Furthermore, when using TH-agar plates, the plates were incubated with AnaeroGen™ bags (Oxoid) in an airtight container. The AnaeroGen™ bag ensures an oxygenlevel of <1% within 30 minutes by absorbing the oxygen and producing carbondioxide instead (Oxoid 2002). When appropriate, kanamycin and streptomycin were added to the growth medium to a final concentration of 400 µg/ml and 200 µg/ml, respectively.

S. pneumoniae was transformed as described by Steinmoen *et al.* 2002 and Knutsen *et al.* 2004. In brief, cells were grown in fresh C-medium to $OD_{550} \approx 0.1$. Natural competence in *S. pneumoniae* was induced by adding 250 ng/ml CSP-1 together with the transforming DNA. The cell cultures were incubated in a water bath at 37°C for 2 hr. Transformants were plated out on TH-agar plates containing relevant antibiotics and ComS* if needed. See table 2.5 for concentration of antibiotics used. The bacterial plates were incubated anaerobically over night at 37°C. The following day, transformants were picked and grown in fresh C-medium containing antibiotics (and 2 µM ComS* if required). When the cells reached exponential phase, freeze stocks were made of the cell cultures. To control if the transformation was successful, PCR screening and/or DNA-sequencing was performed.

3.1.3 Depletion of gene expression in *S. pneumoniae*

Expressing essential genes (genes absolutely necessary to support cellular life) ectopically under the control of a tightly regulated titratable promoter, might be the best approach for functional studies of essential genes. This allows for deletion of the native gene. To gain insight into the genes function, one can manipulate the level of transcription of the ectopically expressed gene (Berg *et al.* 2011).

The gene depletion system ComRS developed by Berg *et al.* (2011) makes it possible to study essential genes in *S. pneumoniae* by deleting the native gene while the level of transcription of the ectopically expressed gene can be manipulated to gain insight into its function (Berg *et al.* 2011). It is based on the *comX*-promotor, the regulator ComR and the inducer peptide ComS* from *S. thermophilus*. The ComRS pathway is unrelated to the ComCDE pathway that regulates competence for natural transformation in *S. pneumoniae*. Hence, application of the ComRS system in *S. pneumoniae* will not interfere with its natural physiology. By varying the concentrations of ComS* in the growth medium, gene expression behind P_{comX} can be manipulated. In this study, the gene depletion system was used to study morphology of *S. pneumoniae* when the level of PcsB is depleted during growth. It was also used to examine the stability of cell-bound PcsB as well as PcsB released into the growth medium.

The bacterial strain SPH247 (see table 2.1) was first grown in C-medium containing 2 μ M ComS* before the culture was washed with C-medium without ComS* to remove extracellular ComS*. Further cultivation of bacteria was done without ComS* present as follows:

1. Cell culture was diluted in fresh C-medium to $OD_{550} \sim 0.05$.
2. Every 30 min, optical density was measured and a 10 ml sample was harvested by centrifugation at 5000x g for 5 min.
3. The supernatant was obtained by sterile filtration and stored at -20°C. Cell pellets were washed with 10 mM Tris-HCl pH 7.4, 100 mM NaCl.
4. Samples were prepared for SDS-PAGE (see section 3.7) and DIC microscopy (section 3.9).

3.1.4 Storage of bacteria

When the bacterial cultures were in exponential growth phase ($OD_{550} \sim 0,3$), freeze stocks and starter cultures were made. The freeze stocks and starter cultures were made by mixing the cell culture with glycerol to a final concentration of 15%. Bacteria in glycerol were stored at -80°C .

3.2 Protein purification of mature PcsB

To characterize the structure and function of a protein, it is a big advantage to have the protein in a purified form. In addition, immunization and antibody production requires large amounts (mg) of pure protein. Protein purification involves a series of processes with the intention to isolate a certain protein from a complex mixture. Due to the variation in size, charge and water solubility amongst proteins, there are several ways of protein purification – occurring in several, complicated steps (Berg *et al.* 2002).

In this study, PcsB was purified by using the tandem-affinity tag called CHiC-tag (Stamsås *et al.* 2013) followed by ion exchange chromatography (Bartual *et al.* 2014). All bacterial strains and plasmids used in this work are listed in table 2.1.

3.2.1 Bacterial strains and growth conditions

1. Cell cultures (50 ml) of *E.coli* BL21 containing the plasmid pGS01 (Stamsås *et al.* 2013) (strain ds125) were grown in LB-media containing $100\mu\text{g/ml}$ ampicillin overnight at 37°C .
2. The following day, the cell culture was diluted to $OD_{600} \approx 0.1$ in fresh LB-meidum (total volume approximately 0.5 L) and further incubated at 37°C for 3-4 hr until $OD_{600} \approx 0.4$.
3. Expression of CHiC-fused PcsB was induced by adding a final concentration of 0.1 mM IPTG to the cell culture followed by incubation at 28°C for approximately 4 hours.
4. After induction, the samples were harvested by centrifugation at $5000\times g$ for 10 min. The cell pellets were resuspended in 15 ml 10 mM Tris-HCl, pH 7.4, containing 100 mM NaCl.
5. The cells were lysed by treating the cells with 1 mg/ml lysozyme at 37°C for 10 min and then stored at -20°C .

3.2.2 DEAE-Cellulose affinity chromatography

The mature PcsB protein was expressed with a CHiC-tag fused to its N-terminus. The CHiC-tag comprises an N-terminal 6xHis-tag followed by a choline binding domain (CBD) and a C-terminal TEV-protease cleavage site (NH₂-ENLYFQG-COOH) allowing its removal from the fusion partner. The CBD domain derives from choline binding protein CbpD of *S. pneumoniae*. Choline binding proteins attach to the pneumococcal cell surface by binding choline residues decorating the teichoic acids in the cell wall. Hence, the CBD have strong affinity for tertiary amines, and will bind strongly to the diethylaminoethanol (DEAE) groups of DEAE-cellulose (Sanz *et al.* 1988). To immobilize and/or purify proteins containing a CBD domain, DEAE-cellulose affinity chromatography was used as described by Sanchez-Puelles *et al.* (1992). DEAE-cellulose is a positively charged resin, and can also be used as an anion-exchange adsorbent. In this study, DEAE-cellulose was used to purify CHiC-PcsB from the soluble protein fraction by affinity chromatography. The CBD domain of the CHiC-tag binds DEAE with high affinity (Stamsås *et al.* 2013).

3.2.2.1 Protocol DEAE-cellulose affinity chromatography

1. The lysed cells containing over-expressed CHiC-PcsB were thawed at 37°C and harvested by centrifugation at 20 000 x g for 20 min. The supernatant was collected.
2. DEAE-cellulose column (approximately “3 ml”) was equilibrated with 10 ml of 10 mM Tris-HCl, pH 7.4, 100 mM NaCl buffer. The buffer was passed through the column by gravity flow or at a maximum flow rate of 1 ml/min.
3. The supernatant was then passed through the DEAE-cellulose column at 1 ml/min for CHiC-PcsB to bind DEAE.
4. The column was washed four times with 10 ml 10 mM Tris-HCl, pH 7.4, 1.5 M NaCl to remove contaminating proteins bound to the column via anionic interactions.
5. CHiC-tagged proteins were eluted by adding 0.14 M choline to the wash buffer.
6. The fusion proteins were collected in 2-3 ml fractions and examined by SDS-PAGE.

The fractions containing the highest amount of CHiC-PcsB were pooled and further purified by affinity chromatography and ion exchange chromatography.

3.2.3 Dialysis and TEV protease digestion

After DEAE-cellulose chromatography dialysis through a semi-permeable membrane was performed to remove salts from the fusion protein, which was eluted in 1.5 M NaCl and 0.14 M choline. Proteins are generally larger than the pores of the membrane and will thus not pass through. The result is a dialysis bag with retained protein inside, while unwanted salts and small molecules have diffused outside the dialysis bag (Berg *et al.* 2002). The purpose of removing the salts from CHiC-PcsB was to give the TEV protease optimal working conditions since high salt concentrations inhibits its activity.

3.2.3.1 Protocol dialysis

1. The dialysis bag was rehydrated in 10 mM Tris-HCl, pH 7.4, 0.14 M Choline buffer.
2. The samples containing protein were injected into the dialysis bag and placed in 1 L 10 mM Tris-HCl, pH 7.4, 0.14 M Choline buffer for 1 h with rotation.
3. The dialyzed fusion protein was transferred to an Amicon centrifugal filter unit (MW cutoff = 10 000 Da) using a syringe.
4. The samples were centrifuged at 5000x g for approximately 10 min to up-concentrate the fusion protein.

After dialysis, the CHiC-tag was separated from PcsB by digestion with AcTEV™ protease (Invitrogen). The protease has a high sequence specificity recognizing the sequence NH₂-ENLYFQG-COOH. The TEV protease cleaves between Q and G leaving a glycine at the N-terminus of the fusion partner. AcTEV™ mixture (section 2.11.3) was blended with 500µl fusion protein and incubated over night. To remove the protease after cleavage, immobilized metal affinity chromatography was performed using the polyhistidine tag.

3.2.4 Immobilized Metal Affinity Chromatography

Immobilized Metal Affinity Chromatography (IMAC) separates proteins on the basis of reversible interaction between a protein (of interest) and a specific metal ligand coupled to a chromatographic matrix. The affinity column will only retain the proteins that bind the ligand; remaining proteins will pass through the column. To recover the target protein, conditions are changed to favor elution of the bound molecules.

After TEV digestion, the His-Tagged TEV protease, the free CHiC-tag and undigested fusion proteins (CHiC-PcsB), which all three contain a His-tag, were separated from PcsB in a single Ni²⁺ affinity chromatography step. This resulted in recombinant PcsB proteins with a purity of more than 85%. To stabilize and to increase the solubility of the CBD domain, choline was included in all buffers (Stamsås *et al.* 2013).

3.2.4.1 Protocol IMAC

1. 1 ml HisTrap column was equilibrated with binding buffer 10 mM Tris-HCl, pH 7.4 (10x column volume).
2. The protein sample after TEV cleavage was applied to the HisTrap column.
3. 10 ml 10 mM Tris-HCl, pH 7.4 passed through the column, and the flow through containing PcsB was collected.
4. For elution of CHiC-tag, TEV protease and uncleaved fusion protein, 10 ml 10 mM Tris-HCl, pH 7.4, 500 mM NaCl, 500 mM Imidazol, 0.14 M Choline was added to the column.
5. The HisTrap column was washed with 5 ml Tris-HCl, pH 7.4 and 5 ml 20% ethanol to remove left-over elutionbuffer before storage.
6. The flow through which contained PcsB in 10 mM Tris-HCl, pH 7.4 was then applied on an anion exchanger. See section below.

3.2.5 Ion Exchange Chromatography

For the final purification step, to achieve >99% pure PcsB, ion exchange chromatography was performed. Ion exchange chromatography separates proteins based on their differences in ionic charge. First, the ion exchanger is equilibrated with a buffer with an appropriate pH. Next, the protein sample is applied and only the desired protein will attach to the column. Using a buffer will wash out unbound substances. Finally, the conditions inside the column are changed, to favor elution of the desired molecule. This is usually achieved by either increasing the ionic strength of the eluting buffer or changing its pH.

3.2.5.1 Protocol Ion Exchange Chromatography

1. 1 ml HiTrap Q HP column was equilibrated with 10 ml 10 mM Tris-HCl, pH 7.4.
2. The flow through retained from IMAC chromatography (containing PcsB) was bound to the anion exchanger.
3. PcsB was eluted gradually by increasing the NaCl concentration from 0-500 mM in a 25 ml gradient at a flow rate of 1 ml/min.
4. The fractions containing >99% pure PcsB were stored in -80°C .

3.3 Polymerase Chain Reaction (PCR)

Polymerase Chain Reaction (PCR) is a method for *in vitro* amplification of DNA sequences. The method was first described by Kjell Kleppe and coworkers in 1971 (Kleppe *et al.* 1971), but it was not until the mid-80s when the use of a thermostable DNA polymerase made it a standard laboratory method (Bartlett and Stirling, 2003, Sambrook & Russel, 2001). A PCR reaction contains a thermostable DNA polymerase, site-specific primers (DNA-oligos), DNA template, DNA polymerase buffer and the four deoxynucleoside triphosphates (dNTPs): dATP, dTTP, dCTP and dGTP.

The basic principles of a PCR involve repeated cycles of heating and cooling where the copy numbers of the target sequence are doubled per cycle. A cycle comprises three different temperatures: (i) $94-96^{\circ}\text{C}$ to denature the double stranded template DNA, (ii) $50-60^{\circ}\text{C}$ to allow the primers to anneal to the template DNA, (iii) and 72°C which is the optimum temperature for the DNA polymerase to synthesize the new DNA strands from the 3'-OH ends of the primers. These three steps are repeated for 25-30 times using a thermocycler. Since the thermostable DNA polymerase tolerates 96°C , it is not necessary to add new enzyme after each cycle. A template sequence will in theory be copied in accordance to the formula 2^n where n is the number of cycles. In this study, two DNA polymerases were used: Phusion® High Fidelity DNA Polymerase and Taq DNA polymerase (NewEnglandBioLabs, 2012). Their enzymatic activities are described below.

3.3.1 Primer Design

To obtain successful PCR reactions, it is essential to design good primers. Primers should be between 18-30 nucleotides with a GC content between 40-60%. Primers of proper length are long enough for adequate specificity as well as being able to provide for efficient annealing.

To elicit strong binding at the start of the elongation site, the presence of G and C bases at the 3' end of the primer is advantageous. To accomplish best results, primers should have melting temperatures in the range of 52-58 °C. Palindrome sequences (equal to its reverse complement) should be avoided because of its ability to form hairpins (Innis & Gelfand, 1991).

3.3.2 Phusion® High-Fidelity DNA Polymerase

For cases when it is important that the DNA sequence is correct after amplification, Phusion® High-Fidelity DNA Polymerase was used. Phusion has high proof reading, 5'→3' polymerase activity and a 3'→5' exonuclease activity. Phusion has a high polymerase rate and therefore reduces the extension time during PCR. It can synthesize up to 1 kb in 15 s using PCR products as templates. Phusion is both faster and has a higher fidelity rate compared to *taq* DNA polymerase (50x greater than *taq*). Because of its versatility and robustness, Phusion High-Fidelity DNA Polymerase can be used for all PCR applications (NewEnglandBioLabs). In this study, Phusion polymerase was used for conventional PCR and for overlap-extension PCR.

3.3.2.1 Protocol for PCR using Phusion® High-Fidelity DNA Polymerase

1. The following reagents were mixed in a PCR-tube (preferably on ice):

Table 3.1 PCR mixture for 50 µl using Phusion® High-Fidelity DNA Polymerase

Reagent	Volume (µl)
10 µM Fwd primer	2.5
10 µM Rev primer	2.5
10-15 ng template	1.0
5X HF buffer	10.0
10 mM dNTPs	1.0
Phusion® HF DNA Polymerase	0.5
dH ₂ O	32.5
Total volume	50

2. The reactions were carried out in a thermocycler (Applied biosystems, MJ research Inc.) using a program suitable for the relevant template, based on the T_m for primers and the length of the fragment that was being amplified.

Table 3.2 PCR program

Step		Temperature	Time
1	Initial denaturing	94 °C	5-10 min
2	Denaturing	94 °C	30 s
3	Annealing	55-65 °C*	15-45 s
4	Extension	72 °C	1-2 min
5		<i>25-30 cycles of step 2-4</i>	
6	Final extension	72 °C	7 min
7	Temporary storage	4 °C	∞

3.3.3 *Taq* DNA Polymerase

Taq DNA Polymerase is a thermostable DNA polymerase. Compared to Phusion, *Taq* is far from as precise during the DNA synthesis (Phusion has approximately 50x higher fidelity) This is because *Taq* DNA Polymerase lacks 3'→5' exonuclease activity. In addition it has lower polymerization rate than Phusion, requiring ~45 s per kb (NewEnglandBioLabs). *Taq* DNA Polymerase was used for PCR screening of mutants and control due to the low costs per unit.

3.3.3.1 Protocol for PCR using *Taq* DNA Polymerase

1. The following reagents were mixed in a PCR-tube (preferably on ice):

Table 3.3 PCR mixture for 20µl using *Taq* DNA Polymerase

Reagent	Volume (µl)
10 µM Fwd Primer	1
10 µM Rev Primer	1
10-15 ng Template	1
10X ThermoPol reaction Buffer	2
10 mM dNTPs	0.5
<i>Taq</i> DNA polymerase	0.5
dH ₂ O	14.0
Total volume	20

2. The reactions were carried out in a thermocycler (Applied biosystems, MJ research Inc.) using a program suitable for the relevant template, based on the T_m for primers and the length of the fragment that is being amplified.

Table 3.4 PCR program

Step		Temperature	Time
1	Initial denaturing	94 C	10 min
2	Denaturing	94 C	30 s
3	Annealing	55-65 C*	15 s
4	Extension	72 C	1-2 min
5		25-30 cycles of step 2-4	
6	Final extension	72 C	7 min
7	Temporary storage	4 C	

3.3.4 PCR-screening

Transformants were examined by performing PCR using either cells directly from the colonies or corresponding PCR product as template. Ideally, primers that only work if the correct construct is present were used. When cells were used as template, a sterile toothpick was used to transfer cells into the PCR mixture (Table 3.3).

3.3.5 Overlap-extension PCR

Overlap-extension PCR is a multistage procedure where two or more DNA-fragments are merged into one new DNA-fragment. This is a useful method when constructing DNA fragments that are not available from existing strains/plasmids. Overlap extension PCR provides a technique of site-directed mutagenesis in which point mutations or insertions/deletions are introduced into a sequence (Higuchi *et al.* 1988; Ho *et al.* 1989). The method can also be used to assemble sequences with different origin (Horton *et al.* 1989). In this study, overlap extension PCR was used to 1) fuse a 3xFlagTag to PcsB and 2) for construction of a janus cassette with PcsB flanking sequences to replace the PcsB protein in *S. pneumoniae* through homologous recombination.

When performing overlap extension PCR, the DNA fragments to be fused are amplified in separate PCRs. The resulting products serve as templates in a subsequent PCR in which they are assembled into a full-length product. To obtain overlapping 3'-ends on the amplified fragments, two primers with complementary 5'-ends and 3'-ends are used in the first PCR reactions. The 5' overlapping tail of the primers can contain a point mutation or an insertion (as shown in Figure 3.1).

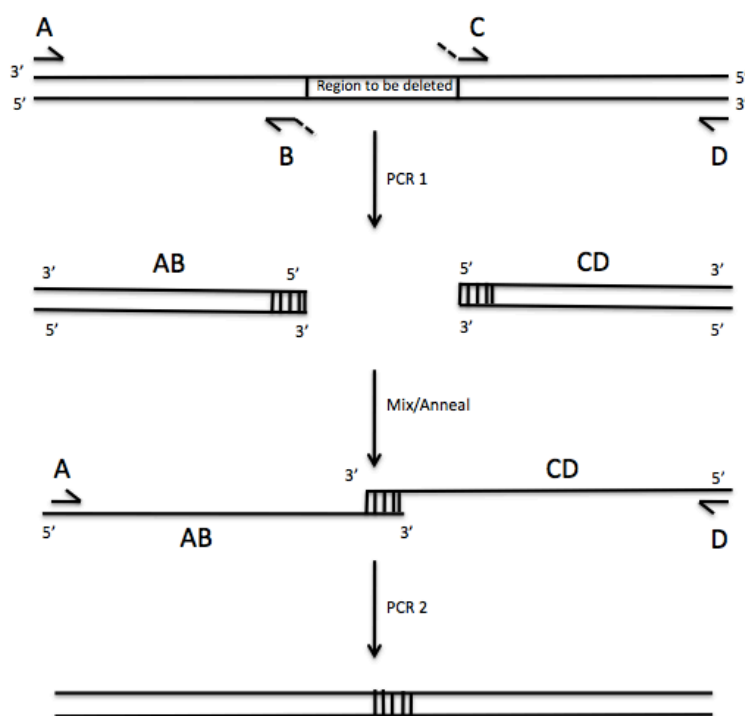


Figure 3.1: Overlap extension PCR. Schematic diagram showing the steps in overlap extension PCR for introduction of mutations at an internal site of a gene. Primers A and D are specific to the 3'-ends of the gene, while the 3'-ends of primers B and C are specific to the complementary to template target sequence on either side of the point at which the mutation/deletion is to be made. The complementary sequence is illustrated by dashes. The end product, a full-length product, is obtained through a subsequent PCR reaction with primers A and D.

3.4 DNA sequencing

DNA sequencing is a method for determining base sequence in DNA. For many years DNA was sequenced using the Maxam-Gilbert (chemical cleavage) or the Sanger method (chain termination). However, it has been a dramatic development in the field of DNA sequencing in recent years, giving rise to high throughput (next-generation sequencing) techniques such as 454 pyrosequencing, Illumina sequencing and Ion Torrent semiconductor sequencing. Although these high-throughput sequencing techniques are getting cheaper to do, the conventional Sanger sequencing technique is still used to a large extent for single reads and verification of DNA constructs for molecular cloning.

Sanger sequencing, also called chain termination sequencing, is based on the use of dideoxynucleotides (ddNTP's) in addition to the normal deoxynucleotides (dNTP's). Dideoxynucleotides contain a hydrogen group on the 3'-carbon instead of the hydroxyl group in deoxynucleotides. The 3'-OH group is required for the formation of a phosphodiester bond

between two nucleotides and when these ddNTPs are incorporated, the strand extension reaction terminates. Due to the ddNTPs, a series of fragments each separated by just one nucleotide are produced (Sanger *et al.* 1977). Sequencing reaction consists of a mixture comprising of DNA polymerase, one primer, dNTPs and ddNTPs. The ddNTPs are fluorescently labeled with different dyes that fluoresce at different wavelengths. This makes it possible to determine the sequence.

In this study, DNA sequencing was used to verify that the 3xFlag-tagged version of PcsB was correct. GATC Biotech performed the DNA-sequencing. A pre-mixture was made (50 ng template, 2.5 pmol primer, 2,5µl dH₂O) of both forward and reverse primer, separately.

3.5 Agarose gel electrophoresis

Agarose gel electrophoresis is a method for separating molecules based on their size to charge ratio. Agarose is a polymer consisting of repeated L- and D-galactose subunits that forms a network of pores in the gel state that allows for separation by size in an electric field (Sambrook & Russel, 2001). Nucleic acids have a constant charge to size ratio and can therefore be separated by size using agarose gel electrophoresis. Based on their net negative charge, DNA/RNA will migrate towards the anode in an electric field. There are several factors that have an effect on the rate of migration of DNA through agarose gels. Amongst others, the molecular size of the DNA, the agarose concentration and the applied voltage used, contribute to separate DNA fragments during electrophoresis (Sambrook & Russel, 2001).

DNA samples were analyzed using a 1% (w/v) agarose gel, buffered with 1x-TAE-buffer as conductor. Agarose suspended in 1xTAE buffer was heated to ~95°C to dissolve the agarose. When the heated agarose-TAE mixture had cooled to ~60°C, ethidium bromide (EtBr) (0.5 µg/ml) was added for visualization of the DNA molecules. Prior to gel loading the samples were mixed with loading buffer, which increases the density and add color (bromophenol blue) to the sample. The increased density ensures that the samples sink into the well of the gel, and the bromophenol blue will migrate close to the migration front. As mentioned before, to visualize DNA in agarose gels, the fluorescent dye EtBr was added to the heated agarose solution before casting the gel. EtBr is an intercalating compound that binds DNA. After electrophoresis the separated DNA molecules can be visualized upon UV-light irradiation since EtBr becomes fluorescent at a wavelength (λ) between 302-366 nm only when bound to

DNA. The lower detection limit for EtBr is in the range 1-5 ng DNA (Sambrook & Russel, 2001). A molecular standard (1 kb ladder from NewEngland BioLabs) with known molecular sizes and concentrations was used to determining the size of the separated DNA fragments and to estimate the amount of DNA in the samples.

3.5.1 Protocol for agarose gel electrophoresis

For 1% gel:

1. 0.5g agarose was added to 50 ml 1x TAE-buffer. The solution was heated in a microwave oven until the agarose was completely dissolved.
2. The solution was cooled to around 60°C by using tap water.
3. EtBr was added to a final concentration of 0.5 µg/ml and mixed by swirling.
4. The agarose solution was poured into the mold and combs of desired sizes were placed inside.
5. When the gel had set, the combs were removed and the gel was placed into the electrophoresis tank with 1x TAE-buffer covering the wells.
6. A volume of 10µl 1 kb ladder (NewEngland BioLabs) was used as standard and appropriate amount of samples (10-30µl) were mixed with 6x DNA loading buffer and added to the remaining wells.
7. Electrophoresis was conducted at 90 V until the samples were adequately separated (15-20 min).
8. The samples were visualized in UV-light using a Gel Doc-1000 (BioRad) and compared to the 1 kb ladder.

3.6 DNA-extraction from agarose gel

DNA was extracted from the agarose gel after gel electrophoresis. This was done to isolate the desired fragment of intact DNA from the agarose gel. DNA bands were cut out of the gel using a sterile scalpel purified through gel-extraction using the NucleoSpin® Gel and PCR Clean-up columns from Macherey-Nagel. DNA was extracted in accordance with the manufacturer's protocol. Briefly, the excised gel piece was solubilized with the NTI buffer, the dissolved gel containing DNA was bound to the NucleoSpin® column followed by a washing step with NT3 to remove salts and other contaminants. Then the silica membrane was dried by centrifugation at 10 000 x g for 1 min. Finally, elution buffer NE was added to release the DNA from the silica membrane. The eluted DNA was stored at -20°C.

3.7 Sodium dodecylsulfate polyacrylamide gelelectrophoresis (SDS-PAGE)

Sodium dodecylsulfate polyacrylamide gelelectrophoresis (SDS-PAGE) is used to separate proteins with relative molecular mass. A polyacrylamide gel is formed when acrylamide monomers are polymerized and cross-linked by methylene-bis-acrylamide. N,N,N',N'-tetramethylethylenediamine (TEMED) accelerates this reaction by catalyzing the formation of free radicals from ammonium persulfate (APS) (Sambrook & Russel, 2001). The concentration of polyacrylamide used to cast the gel combined with the amount of cross-linking, determines the range of separation of SDS-PAGE.

The proteins are linearized before they are loaded onto the gel. This is done by treating the protein sample with SDS and a reducing agent. SDS is an anionic detergent that disrupts nearly all noncovalent interactions in native proteins by binding to the main polypeptide chain. Since SDS is an anion it will give the SDS-protein complex a net negative charge facilitating protein migration towards the positive pole during electrophoresis. The reducing agent β -2-mercaptoethanol is added for breaking covalent disulfide bonds between cysteine residues. In this work the proteins were linearized using a sample buffer containing 4% SDS, 0.3 M β -2-mercaptoethanol, glycerol, Tris-HCl pH 6.8 and bromphenol blue to stain (Laemmli buffer, cf. Laemmli 1970).

SDS-PAGE was carried out using a discontinuous buffer system for increased resolution (Ornstein 1964, Davis 1964). The buffer used to cast the gel differs from the one used in the reservoir by different pH and ionic strength. This is to make sure that all proteins reach the separation gel at the same time and separation based on size is achieved. SDS-PAGE is a relatively sensitive and rapid method with a high degree of resolution. To get a distinct band, visualized by Coomassie blue, only 0.05-0.1 μ g of protein is needed. Usually, a difference in protein mass by 2% or more can be distinguished (Ornstein, 1964). Prestained Protein Marker (New England BioLabs, Invitrogen) was used as internal standard for determination of relative protein sizes.

3.7.1 Protocol for casting SDS-polyacrylamide gels

For recipe on separation gel and stacking gel, see section 2.11.6.

1. Glass plates, combs and spacers were cleaned with water.
2. The glass plates were assembled in the casting frame according to the manufacturer's instructions (Mini-PROTEAN Tetra Cell, BioRad) and checked for leakage by applying water.
3. A separation gel of desired percentage and a 4% stacking gel was prepared by mixing all ingredients except APS and TEMED (This to avoid early polymerization).
4. Immediately before casting, APS and TEMED was added and blended in.
5. A volume of 3,2 ml of separation gel was smoothly poured into the gap between the glass plates.
6. The gel was topped with dH₂O to straighten the level of the gel and left to polymerize for about 20-30 minutes.
7. When the polymerization was complete and the separation gel was solidified, dH₂O was poured off.
8. The stacking gel was poured on top and the combs were inserted into the stacking gel solution.
9. After 20 minutes the gels were assembled into the electrophoresis apparatus (BioRad), and samples were prepared with 2x SDS sample buffer and desired volume (5-15 μ l depending on concentration) was loaded on the gel.
10. Proteins were separated at 1 V/cm² for 10 min followed by 2 V/cm² for approximately 45 min (or until the bromphenol blue reached the bottom of the resolving gel).

3.7.2 Coomassie Blue staining of SDS-polyacrylamide gels

Proteins that were separated by SDS-PAGE were stained with Coomassie blue. Coomassie blue is, since its introduction in 1963, still the most commonly used protein detection method in polyacrylamide electrophoresis gels (Westermeier *et al.* 2005; Sambrook & Russel 2001). Coomassie is a dye that binds unspecifically to proteins on the gel through electrostatic and hydrophobic interactions. The binding of dye is approximately proportional to the amount of protein (Tal *et al.* 1985).

3.7.2.1 Protocol for Coomassie blue staining

1. The gel was submerged in coomassie staining solution, and heated to boiling point in a microwave to speed up and enhance the staining rate.
2. The gel was then placed on a rocking table for about 15 min at room temperature.
3. The staining solution was poured off and the gel was rinsed with dH₂O to remove excess staining solution before destain solution was applied. The gel was incubated in destain solution for at least 1 h (or until sufficient destaining was achieved). To absorb the excess Coomassie dye, a paper towel was placed into the destaining solution.

3.8 Western blot

Western blot is a method used for detection of a protein of interest based on the antibodies's ability to bind specific antigens (proteins). First, the proteins are separated by SDS-PAGE. Then, the proteins are transferred to a polyvinylidene fluoride (PVDF) or nitrocellulose membrane by electroblotting. Electric current is used to transfer proteins from the gel to the PDVF or nitrocellulose membrane. In this study, filter papers soaked in transfer buffer were used as the only buffer reservoir in the apparatus (semi-dry transfer, cf. Kyhse-Andersen 1984). After electrotransfer, areas on the membrane not occupied by proteins are blocked by placing the membrane in a 5% fat free dry milk and TBS-T (Tris-Bufferend Saline and Tween-20) solution. Finally, a two-step immunological detection was achieved by using primary and secondary antibodies.

3.8.1 Electroblotting

By transferring the proteins from within the SDS-PAGE gel and onto a membrane made of nitrocellulose or PVDF, they are made accessible for antibody detection. In semi-dry transfer, only a limited amount of buffer is used. The gel and membrane are sandwiched between stacks of filter paper that are in direct contact with the plate electrodes (Bjerrum and Schafer-Nielsen 1986, Kyhse Andersen 1984). The proteins, which are negatively charged via SDS binding, will migrate towards the anode. By placing the membrane on the anode side of the sandwich the proteins will migrate towards and bind to the membrane during electroblotting. When choosing transfer buffer for electroblotting, physical characteristics of the protein of interest are important to consider (Laurière 1993). In general, transfer buffers must be good conductors, maintain stable pH and both ensure adequate protein transfer and membrane

binding. Membrane of choice depends on amongst others, protein size, transfer conditions and detection method. In this study, PVDF membranes were used as they have a stronger binding capacity (150-160 $\mu\text{g}/\text{cm}^2$) and are more robust than nitrocellulose membranes (BioRad).

3.8.1.1 Protocol for electroblotting

1. Membrane and 3MM Whatman® (Sigma) paper (6 pieces) were cut into equal sizes equivalent to the protein gel (approximately 6x10 cm) for optimal blotting. Gloves were used to avoid protein contamination when handling the membrane.
2. To activate the PVDF-membrane, it was placed in 100% methanol for 30 s.
3. Furthermore, the membrane, 3MM Whatman® papers and the protein gels were soaked in cold transfer buffer.
4. The anode- and cathode plate (bottom and top) on a Trans-Blot SD Semi-Dry Electrophoretic Transfer Cell (BioRad) were washed with dH_2O and air-dried.
5. Three 3MM Whatman® papers were placed on the plate, followed by the membrane, the SDS-gel and three 3MM Whatman® papers on top. Air bubbles were avoided since this prevents protein transfer.
6. The electroblotting was done at $0.2 \text{ V}/\text{cm}^2$ for 1 h.

3.8.2 Membrane blocking

To prevent non-specific binding of primary and secondary antibodies to free sites on the membrane, it was treated with a blocking solution. Two blocking solutions are traditionally used: Bovine serum albumin (BSA) in Tris-Buffered Saline Tween-20 (TBS-T) or fat free dry milk in TBS-T. In this study, fat free dry milk in TBS-T was used as blocking solution. BSA or milk proteins will bind and occupy the free sites on the membrane, hence, the antibodies have no place to attach except on the binding sites of the specific target protein.

3.8.2.1 Protocol for blocking

1. After electroblotting, the membrane was transferred directly to a 5% (w/v) solution of skimmed milk and TBS-T and put on a rocking table at room temperature for 1 h.
2. After blocking, the membrane was washed in TBS-T before immunodetection.

3.8.3 Immunodetection of PcsB

Immunodetection is a method for specific identification of proteins blotted on to a membrane by the use of antibodies. Antibodies are obtained through immunization of laboratory animals such as rabbits, mice or goats with a pure antigen, e.g. a protein. The primary antibody binds specifically to the protein antigen of interest. The secondary antibody, which is produced in a different animal than that of the primary antibody, recognizes and binds to the primary antibody. The secondary antibody is normally conjugated to a label enabling its detection. Between the two antibody incubations and prior to detection, the blot was washed to remove unbound antibody and reduce background signals. See Figure 3.2 for a schematic overview of antibody binding.

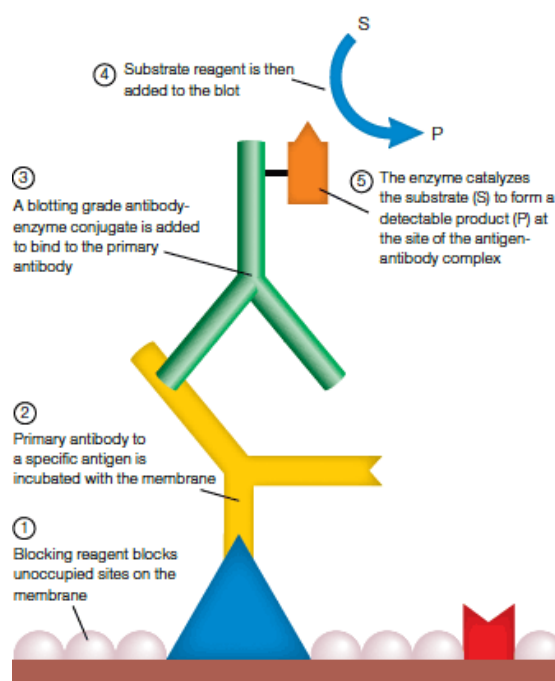


Figure 3.2: Schematic presentation of the different steps involved in immunodetection. (1) Blocking of the membrane. (2) Binding of primary antibody to the protein antigen of interest. (3) Specific enzymatic detection of membrane-bound proteins. Figure from <http://www.bio-rad.com/en-no/applications-technologies/immunodetection>.

3.8.3.1 Protocol for immunodetection

For information about the primary antibody, secondary antibody and substrate used in this study, see Table 2.7.

1. The primary antibody was diluted (1:5000 or 1:10 000) in TBS-T and added to the protein blot, which was placed on a rocking table for 1 h at room temperature.

2. The protein blot was then washed with TBS-T 3x 10 min to remove unbound primary antibody.
3. Secondary antibody diluted 1:4000 in TBS-T was added to the protein blot and placed on a rocking table for 1 h at room temperature.
4. The unbound antibodies were removed by washing the protein blot 4x 10 min with TBS-T.
5. Depending on secondary antibody and development method¹, substrate was added to the protein blot and either left on a rocking table at room temperature until adequate visible bands or developed in dark room by exposure to Thermo Scientific CL-Xposure Film.

¹ Pierce ECL Western Blotting substrate was used for detection of secondary antibody horseradish peroxidase (HRP) enzyme activity.

Working solutions of the Pierce ECL substrate were prepared and carried out according to the manufacturers' instructions. The membranes were exposed to Thermo Scientific CL-Xposure Film and developed.

3.9 Microscopy

3.9.1 Immunofluorescence microscopy of FLAG-tagged PcsB

Immunofluorescence is an antigen-antibody reaction. Antibodies are fluorescently labeled to detect specific target antigens and the complex is visualized using a fluorescence microscope (Odell & Cook, 2013). In this study, immunofluorescence microscopy was used to study the binding pattern and localization of PcsB in pneumococcal cell wall.

Immunofluorescence of PcsB was performed as described by Wayne *et al.* (2010). Briefly, cells were grown to $OD_{550} \approx 0.25$, harvested by centrifugation, and washed with PBS. Cells were fixed in 4% paraformaldehyde (PFA) and fixed cells were resuspended in cold GTE buffer and stored at 4°C for up to 20 hr. Fixed cells were incubated on a microscope glass slide for 5 min to allow the cells to bind the glass surface. The attached cells were permeabilized in PBS-T followed by incubation in MeOH at -20°C for 10 min. Cells were washed with PBS, then blocked with 5% fat free dry milk dissolved in PBS-T for 1 hour. After blocking, anti-FLAG polyclonal antibody was added at a 1:200 dilution, followed by incubation with secondary anti rabbit Alexa488 at a 1:100 dilution. The antibodies were incubated for 1 hour each with 3 washes in PBS in between. Finally, after the cells were air dried, 7 μ l Slowfade Gold Antifade reagent was applied to the cells and coverslips were applied and sealed. Cells were examined using a Zeiss LSM 700 microscope.

3.9.2 Differential interference contrast (DIC)-microscopy

Differential interference contrast (DIC) microscopy is a method based on phase changes of light when it passes through an object or sample. For bacterial cell imaging, the phase differences results in contrast changes, which make the bacterial cells visible through microscope for the human eye (Rosenberger 1977) The human eye will perceive these phase changes as three-dimensional shadow effects and the cells will appear darker than the surroundings (Davidson & Abramowitz 2002). In this study, DIC microscopy was used to examine the impact on the cell morphology when PcsB is depleted.

3.9.2.1 Protocol for DIC

1. Depletion of PcsB was done as described in section 3.1.3.
2. Cell samples of were taken every 30 minutes and fixed by adding 4% paraformaldehyde (PFA); incubated on ice for 15 min followed by incubation at room temperature for 45 min.
3. Fixed cells were studied using Zeiss LSM 700 microscopy with a 63x oil-immersion objective.

4. Results

4.1 Expression and Purification of mature PcsB

In order to immunize animals for production of custom polyclonal antibodies against a protein, it is necessary to obtain the protein antigen in large amounts (mg) and with high purity. Proteins are inherently different from one another and will differ with respect to stability, solubility, host toxicity and yield. Consequently, the protein purification protocol will vary in each case depending on the protein. As described in section 3.2, a series of processes were conducted to obtain PcsB in its purest possible form. PcsB was purified to produce PcsB-specific antibodies, which will be a valuable tool for studying PcsB in *S. pneumoniae*.

In order to purify PcsB, a tandem affinity purification tag called CHiC-tag was used (Stamsås *et al.* 2013). This tag consists of an N-terminal 6x-His tag followed by a choline binding domain and a TEV-proteolytic site at its C-terminus. The plasmid pGS01 (Stamsås *et al.* 2013) containing PcsB fused N-terminally to the CHiC-tag was used in this study to overexpress CHiC-PcsB in *E. coli* BL21. IPTG was added to *E. coli* BL21 containing pGS01 to induce expression of CHiC-PcsB. After expression, CHiC-PcsB (55.4 kDa) was purified from the soluble protein fraction by DEAE-cellulose affinity chromatography (figure 4.1).

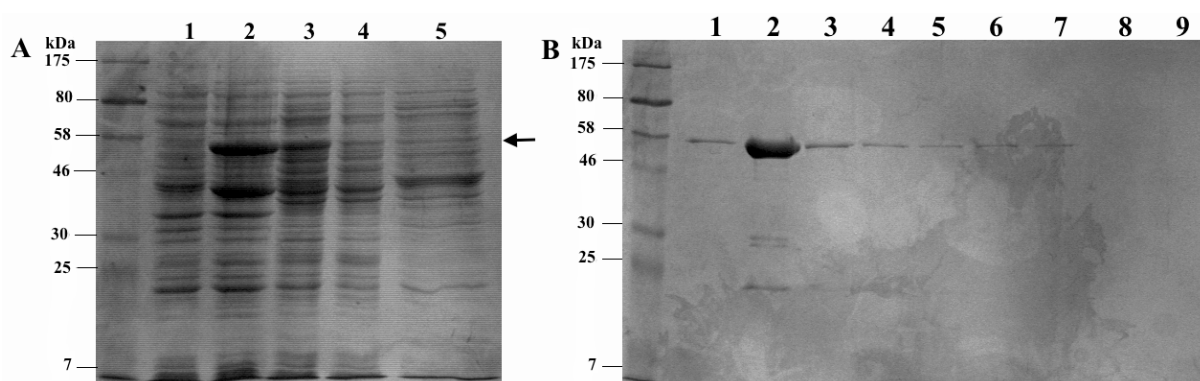


Figure 4.1: Over-expression and purification of CHiC-PcsB. Coomassie blue stained gel displaying (A) cell extracts of *E. coli* before (1) and after (2) IPTG induction, soluble protein fraction before (3) and after (4) DEAE-cellulose affinity chromatography, and a buffer wash of the DEAE-column prior to elution (5). The arrow indicates the position of CHiC-PcsB. (B) Fusion proteins collected at the end of DEAE-cellulose affinity chromatography. Samples 1-7 were pooled for further purification.

DEAE-cellulose chromatography yielded typically 1-2 mg CHiC-PcsB from 0.5 liters of cell culture with a purity of approximately 85% (Figure 4.1B). The purest fractions containing the highest amounts of CHiC-PcsB were pooled and further purified.

4.1.1 Removal of the CHiC-tag

In many cases, the affinity tag can affect the natural function of the target protein. To avoid this it is desirable to remove the tag from its fusion partner. To remove CHiC from CHiC-PcsB, a TEV protease was used. Since the CHiC-PcsB eluate from DEAE-cellulose chromatography contains 1.5 M NaCl, the fusion protein was dialyzed through a semi-permeable membrane to remove salts. This provided better working conditions for the TEV protease to cleave off the CHiC-tag from CHiC-PcsB. TEV protease digestion of CHiC-PcsB resulted in the free CHiC-tag (16.5 kDa), PcsB (38.9 kDa) and undigested fusion protein (55.4 kDa) (figure 4.2). Based on Coomassie blue staining, it was estimated that more than 99% of CHiC-PcsB was cleaved by the TEV protease.

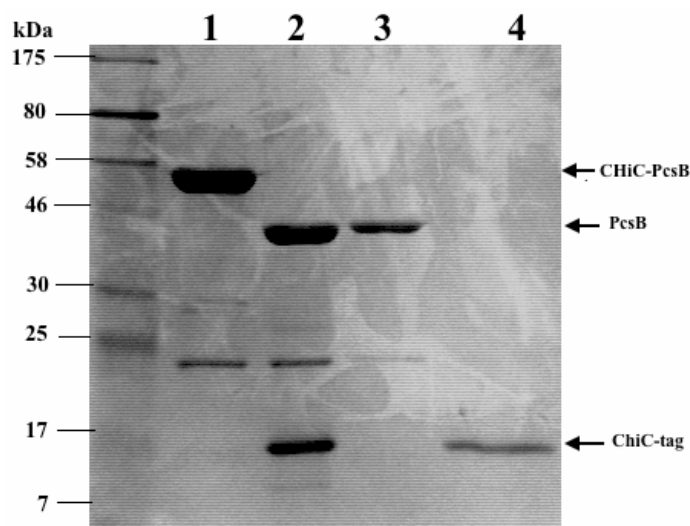


Figure 4.2 Removal of the CHiC-tag from CHiC-PcsB. Coomassie blue stained SDS polyacrylamide gel showing the different steps of TEV digestion of CHiC-PcsB. The gel displays CHiC-PcsB before (1) and after (2) TEV digestion. IMAC flowthrough containing PcsB (3) and imidazole eluent containing the free CHiC-tag, TEV protease and undigested CHiC-PcsB (4).

The free CHiC-tag, the His-tagged TEV protease and undigested fusion protein, all of which contain a His-tag, were separated from PcsB by Ni^{2+} affinity column chromatography (Figure 4.2). The three His-tagged components CHiC-tag, TEV protease and undigested fusion protein were bound to the Ni^{2+} column, while the flow-through contained the recombinant

PcsB protein (purity > 85%) in addition to an unknown contaminating protein of about 20 kDa. The flow-through was collected and PcsB was further purified by ion-exchange chromatography.

4.1.2 Ion exchange chromatography of PcsB

To achieve >99% pure PcsB, ion exchange chromatography was used as the final purification step. PcsB in the flow-through from the Ni²⁺ column was bound to an anion exchanger and eluted by gradually increasing the NaCl concentration from 0 to 500 mM in a 25 ml gradient (see section 3.2.5 for details).

Fractions of 1 ml were collected during protein elution. Absorbance was measured at 280 nm to provide information about eluted proteins and the total protein content. Figure 4.3 shows the results graphically.

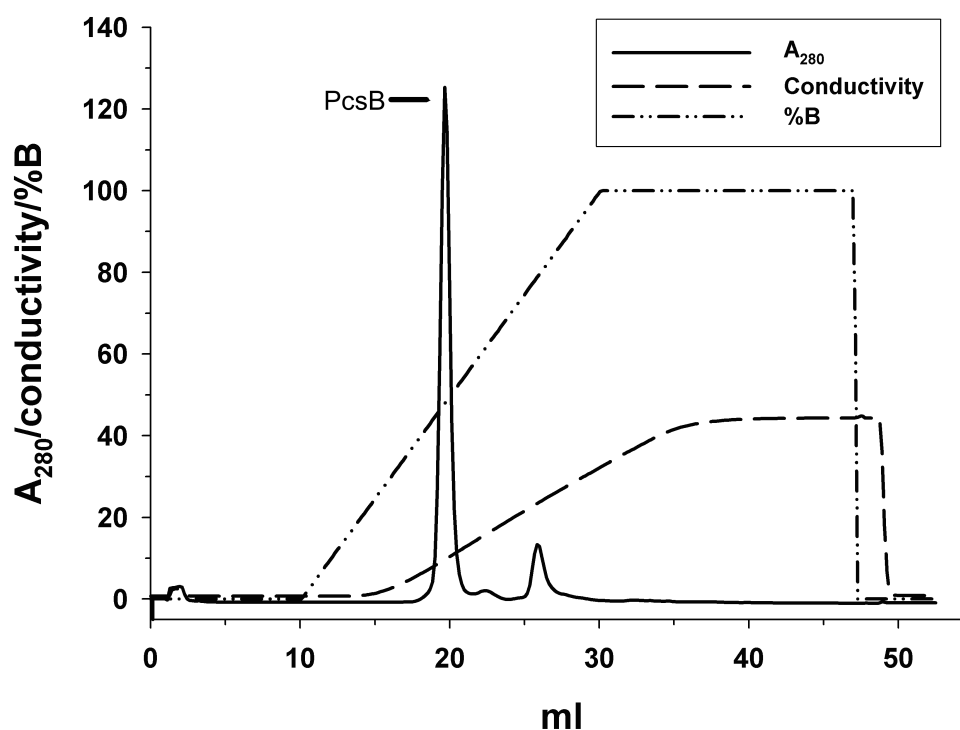


Figure 4.3 Ion exchange chromatography of PcsB. Showing absorbance at 280 nm, conductivity and % gradient of the elution buffer. The two A₂₈₀ peaks represent eluted proteins.

The IEC resulted in two clear peaks eluting after 20 ml and 27 ml. to verify that the high peaks from the IEC graph contained pure PcsB, the fractions covering the peaks were examined by SDS-PAGE (Figure 4.4).

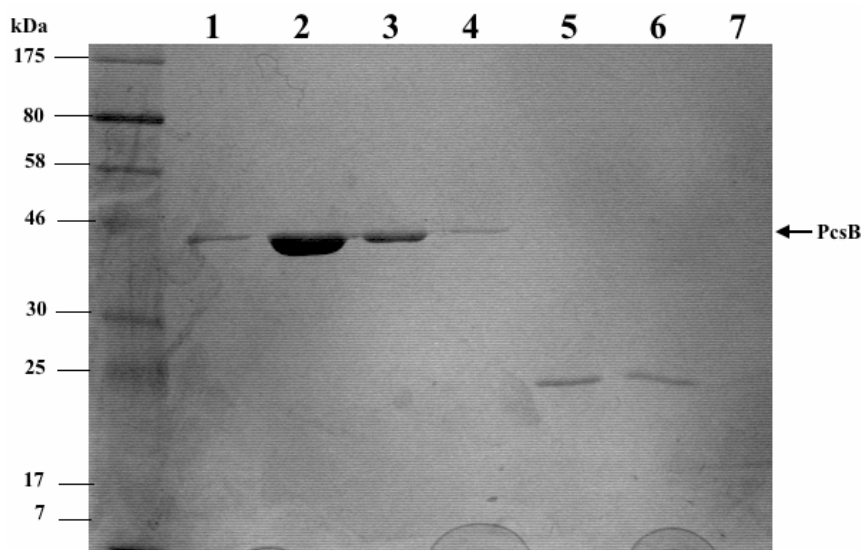


Figure 4.4: Coomassie blue stained 12% SDS-polyacrylamide gel of eluted proteins from ion exchange chromatography. Samples 1-4, representing peak nr. 1 from the IEC purification, contained pure PcsB whereas samples 5 and 6, representing peak nr. 2 contained a contaminant of ~20 kDa.

Examination of the gel showed that the fractions covering peak nr. 1 eluted after 20 ml (see Fig. 4.3) from the IEC contained PcsB, with sample 2 having the highest contents of the protein (Fig. 4.4). Fractions from peak nr. 2 (after 27 ml) contained 20 kDa contaminating protein (Fig. 4.3). By using IEC, this contaminant was removed from PcsB resulting in >99% pure PcsB as judged by the Coomassie blue stained gel.

4.1.3 Calculating the amount of purified PcsB

In many applications regarding protein analysis, it is important to know the amount of protein you are working with. In this study, spectrophotometric measures were made to establish the concentration of PcsB. Studying the results from ion exchange chromatography and the samples displayed in Fig. 4.4, sample 2 appeared to contain the highest amount of PcsB. It was of interest to further calculate the exact concentration of PcsB.

Extinction coefficients for proteins are generally reported with respect to an absorbance measured at 280 nm. Spectrophotometric measures showed that the absorbance of sample 2 was $A_{280} = \underline{1.57}$.

Furthermore, the bioinformatics tool ProtParam was used to gain information about the percent solution extinction coefficient ($\epsilon_{\%}$). The sequence of PcsB (without its signal sequence, see appendix B) was examined using ProtParam: Abs 0.1% = 1.197 mg/ml.

To calculate the concentration of PcsB, the following formula was used (Pierce Biotechnology, 2002):

$$\frac{A}{\epsilon_{\%}} = \frac{1.57}{1.197} = \underline{\underline{1.311 \text{ mg/ml}}}$$

4.2 Immunodetection of recombinant PcsB

The purified PcsB described above was used to immunize rabbits (done by ProSci Inc.) for production of polyclonal antibodies against PcsB. Polyclonal antibodies are glycoproteins derived from multiple B cells (immunoglobulins) and recognize different epitopes on an antigen (Lipman *et al.* 2005). Because of their ability to bind an antigen highly specific and with a high degree of affinity, antibodies are widely used within research.

Because of their ability to detect several epitopes, polyclonal antibodies vary in specificity and may give background signal in some applications. Therefore, it was desirable to find out how specific the antibodies were. To test the specificity of anti-PcsB, a 2-fold dilution series of the purified PcsB (sample 2, Fig. 4.4) was made and prepared for immunoblotting as described in section 3.8. Simultaneously, a control gel was made where the proteins were separated by SDS-PAGE and stained with Coomassie to check the protein loading (data not shown). As displayed in Fig. 4.5A, very strong bands were obtained after immunodetection of PcsB, indicating that very little antibody was needed for detection. However, several unspecific bands were seen for the highest concentrations of PcsB. By doing an expanded 2-fold dilution series of PcsB, much less background was seen (Fig. 4.5B).

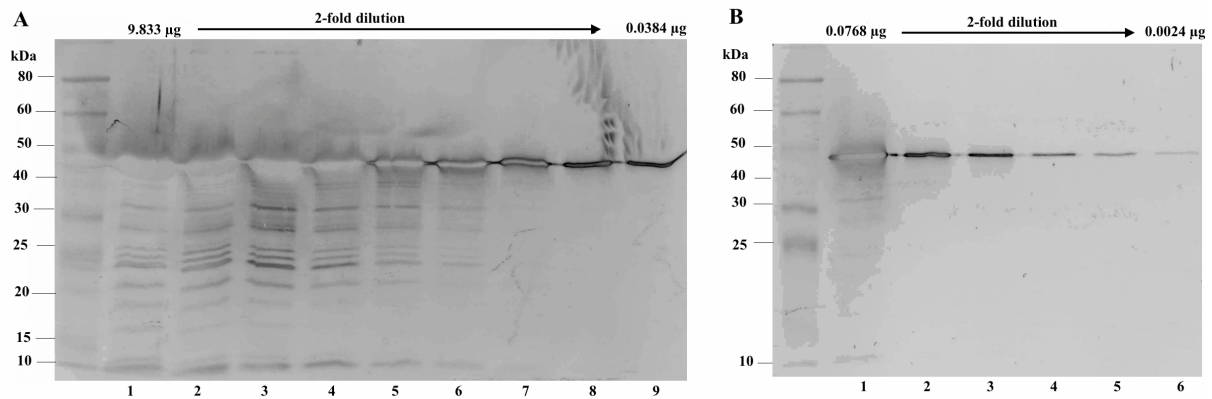


Figure 4.5: Immunodetection of PcsB using anti-PcsB as primary antibody. A 2-fold dilution series of purified PcsB was used as antigen. **(A)** Dilutions 2^0 – 2^{-8} . **(B)** Expanded dilution series of 2^{-7} – 2^{-12} . (The primary antibody was diluted 1: 10 000).

Based on these Western blot results, it was concluded that dilution 2^{-8} (Fig. 4.5B, nr.2) of PcsB gave a strong band with little background signals, and thus this amount of purified PcsB was most suitable as a control sample. This dilution contained 0.0384 µg of PcsB and was used as control throughout the following experiments.

4.3 Immunodetection of native PcsB compared to 3xFlag-tagged PcsB

The anti-PcsB antibodies have high affinity for purified PcsB, but might behave differently when employed for detection of native PcsB in a whole cell extract of *S. pneumoniae*. Therefore, when testing the anti-PcsB antibodies against native PcsB in pneumococcal cell extracts and supernatants we needed a control known to have low background noise. The polyclonal antibody anti-FLAG has been shown to be highly specific and sensitive, and is used to detect Flag-tagged fusion proteins. Anti-FLAG recognizes the FLAG epitope located on FLAG fusion proteins (Sigma Aldrich). Because of the commercial availability of anti-FLAG, it can be used as a control to determine the specificity of other custom made antibodies. In this study, we tagged PcsB C-terminally with a 3xFlag-tag in the native *pcsB* locus of *S. pneumoniae*. This clone was not affected by the Flag-tagging of PcsB and could be used as a control to detect PcsB expressed from its native promoter. Anti-FLAG was used to detect Flag-PcsB and anti-PcsB was used for native PcsB. A comparison between RH1 (wt) immunoblotted with anti-PcsB, and SvH3 (3xFlag-tagged PcsB) immunoblotted with anti-FLAG was made (Fig. 4.6).

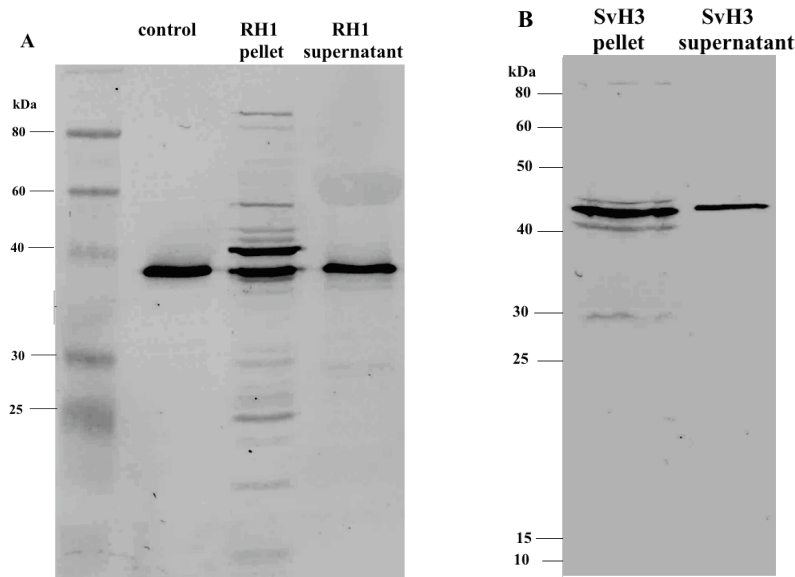


Figure 4.6 Immunodetection of native PcsB compared to 3xFlag-tagged PcsB: (A) purified PcsB control, PcsB detected in RH1 cell pellet and RH1 supernatant using anti-PcsB primary antibody. (B) PcsB detected in SvH3 (3xFlag tagged) cell pellet and supernatant after using anti-FLAG primary antibody. (The primary antibody was diluted 1:5000)

As displayed in the comparison in Figure 4.6, anti-PcsB proved to bind native PcsB quite specific both in RH1 cell extracts and RH1 supernatant. Western blot results show some background signal in RH1 pellet and almost no background in RH1 supernatant. Figure 4B shows SvH3 (3xFlag-tagged PcsB) pellet and supernatant immunoblotted with anti-FLAG and proves to be very specific.

4.4 PcsB is an abundant protein accumulating outside the cells

After the verification of the anti-PcsB specificity, it was desirable to find out how much PcsB is present in cell pellet and how much PcsB is secreted out in the media and supernatant during growth. A growth experiment with *S. pneumoniae* strain RH1 was performed to study the correlation between amounts of PcsB present in cells and in the supernatant at given time points and OD measurements. Cellular amounts of PcsB were determined by growing RH1 exponentially in fresh C-medium at 37°C. Every 30 min (starting at time 0 = OD₅₅₀ ≈ 0.05) 10 ml cell culture samples were taken. By using the spread plate method, a 10-fold dilution series was made and 25 µl cell culture was plated out on TH-agar plates (see table 4.1 for dilution used) for bacterial count. The supernatant was sterile filtered and pellets were washed in 10 mM Tris-HCl pH 7.4 with 100 mM NaCl for further examination with western blot.

Table 4.1 Growth experiment overview. All data collected during the growth experiment. CFU/ml is calculated by using the formula below. Note that 25 μ l of RH1 culture sample was plated out on each petri dish.

Sample	OD ₅₅₀	Dilution	Colonies	CFU/ml	Time (min)
1	0.048	10 ⁻⁴	90	3,60*10 ⁷	0
2	0.088	10 ⁻⁴	188	7,52*10 ⁷	30
3	0.167	10 ⁻⁵	40	1,60*10 ⁸	60
4	0.341	10 ⁻⁵	91	3,64*10 ⁸	90
5	0.613	10 ⁻⁶	13	5,20*10 ⁸	120
6	1.005	10 ⁻⁶	20	8,00*10 ⁸	150
7	0.957	10 ⁻⁷	50	2,00*10 ⁹	180
8	0.945	10 ⁻⁷	10	4,00*10 ⁸	210
9	0.919	10 ⁻⁶	8	3,20*10 ⁸	240
10	0.925	10 ⁻⁶	27	1,08*10 ⁹	270
11	0.940	10 ⁻⁶	16	6,40*10 ⁸	300

Formula for calculating colony-forming units per milliliter:

$$\text{CFU/ml} = \frac{\# \text{ Colonies} \times \text{dilution factor}}{\text{Volume of culture plate}}$$

Based on table 4.1, a graphical representation (Fig. 4.7) was made to see the growth curve and correlation between cell density and numbers of colonies counted. From late lag phase / early exponential growth phase (OD₅₅₀≈0.3) until right before stationary phase, CFU seem to increase at the same rate as increased optical density. The reduced numbers of CFUs in stationary phase is most probably caused by dead cells that have not yet lysed, hence, the OD₅₅₀ remains stable.

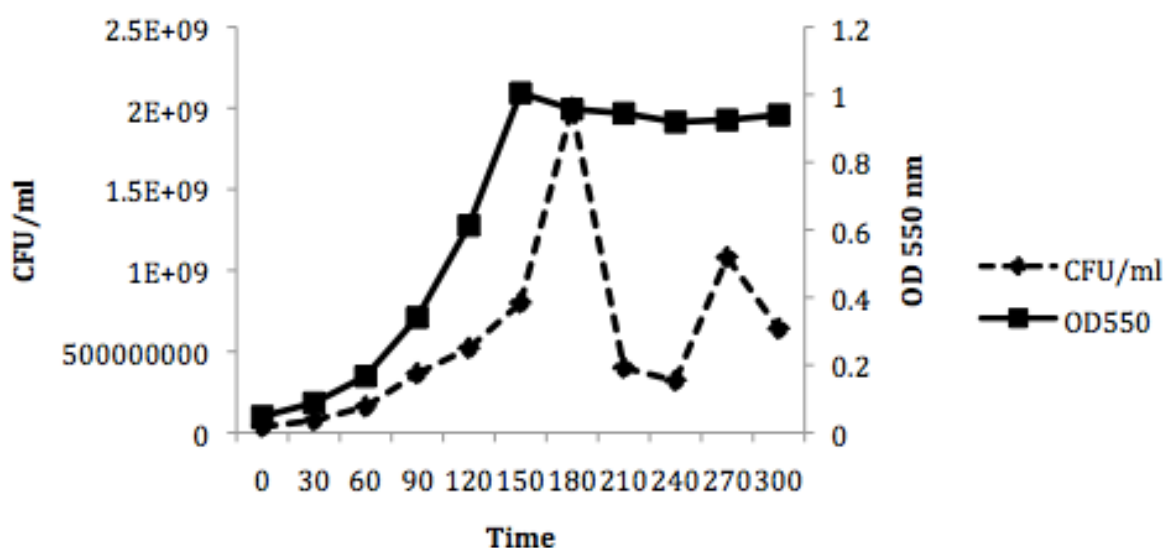


Figure 4.7 PcsB growth curve. Graphical representation of the correlation between CFU/ml over time and optical density development over time. The dots on both graphs indicate the samples taken (table 4.1).

To determine the amount of cell-associated PcsB and secreted PcsB, protein samples from whole cell extracts were examined by western blot using anti-PcsB. To check the protein loading, the proteins were separated by SDS-PAGE and stained with Coomassie blue (data not shown). This was done with the purpose of obtaining a blot with equal amounts of total protein in each well. Figure 4.8 show the result from the immunoblotted cell-associated PcsB and PcsB secreted in the medium. The amount of PcsB present in the cells was relatively stable during the entire growth phase. Secreted PcsB on the other hand, gradually increased from lag phase to growth phase until a small decrease followed by cell death (Fig. 4.8B).

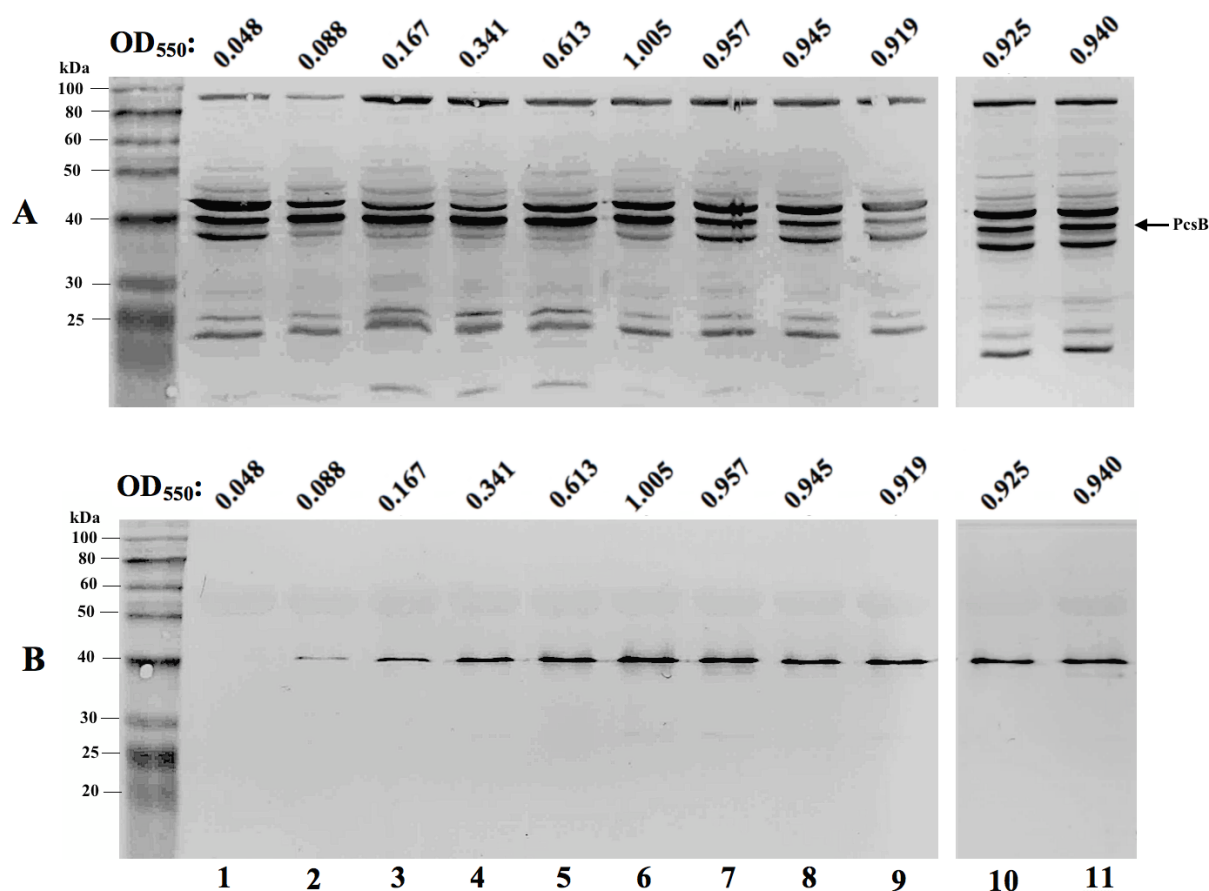


Figure 4.8 Amounts of PcsB in cells during growth. (A) PcsB present in cells during growth. (B) The amount of PcsB present in the cell supernatant during growth. Both (A) and (B) are displayed with OD₅₅₀ measured at times given in Table 4.1 on the figure top.

Based on the growth curve (Fig. 4.7) and the immunoblotted cell pellets and supernatant (Fig. 4.8), PcsB seems to be most abundant when the cells are in the exponential growth phase. Figure 4.8A shows, in addition to processed, an extra band at around 38 kDa that might be a degradation product of PcsB.

4.4.1 PcsB is fairly abundant in *S. pneumoniae*

Quantitation of the amount of cell-associated PcsB, and the amount of secreted PcsB recovered in the medium was performed by immunoblotting, using anti-PcsB antibody, as described in section 3.8. A 2-fold dilution series was made of purified PcsB (Fig.4.5B sample 3; 0.0192 μg) and used as control. For cell-associated PcsB and secreted PcsB found in the growth medium, a 2-fold dilution series of the cell extract and supernatant from samples 4 (Fig. 4.8A and B; $\text{OD}_{550}=0.341$) were made. Quantitation was performed directly from blots by visual inspection and by comparing the dilution series of purified PcsB with known amounts of PcsB with cell-associated PcsB and secreted PcsB, respectively.

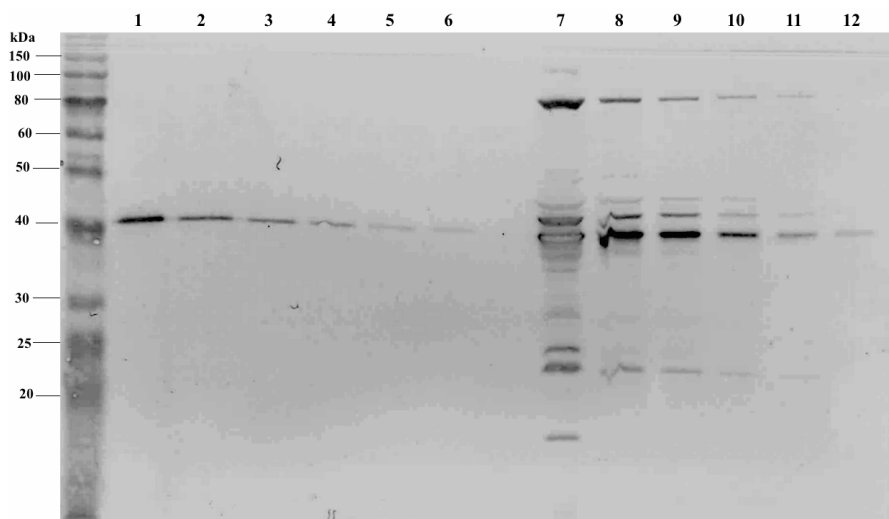


Figure 4.9 Immunodetection and quantification of cell associated PcsB. A 2-fold dilution series of both the purified PcsB control and the cell-associated PcsB (sample 4, Fig.4.8A) was conducted in order to determine the amount of cell-associated PcsB present in a single cell. The control samples 1-6 contain 0.0128, 0.0064, 0.0032, 0.0016, 0.0008, 0.0004 μg PcsB, respectively.

When comparing the signal obtained for purified PcsB control with PcsB found in the cells, it was concluded that control sample 1, containing 0.0128 μg PcsB and sample 10 (Fig. 4.9) were fairly similar. Based on this, it was estimated that approximately 8709 copies of PcsB were present in each *S. pneumoniae* cell at $\text{OD}_{550} = 0.341$ (See appendix C1 for detailed calculations).

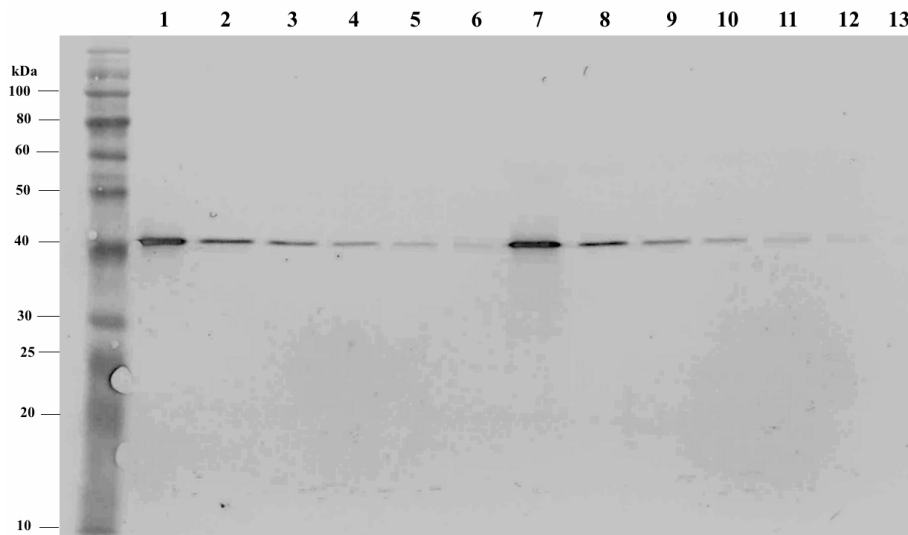


Figure 4.10 Calculating the amount of secreted PcsB in the growth medium. Immunodetection of 2-fold dilution series of a purified PcsB control starting with 0.0128 μg and secreted PcsB in supernatant (sample 4 Fig. 4.8B) for the determination of the number of PcsB molecules present in the growth medium. Samples 1-6 represent purified PcsB control, samples 7-13 represent secreted PcsB. The control samples 1-6 contain 0.0128, 0.0064, 0.0032, 0.0016, 0.0008, 0.0004 μg PcsB, respectively.

Western blot detection of purified PcsB and secreted PcsB in the growth medium (Fig. 4.10) shows that the signal obtained for each 2-fold dilution corresponded well between the controls and the supernatants. Samples 1 and 7 (Fig. 4.10) were chosen for comparison and used for calculating the number of PcsB molecules present in supernatant per cell. It was calculated that 108 939 molecules of PcsB were present in the supernatant per cell at $\text{OD}_{550} = 0.341$ (See appendix C2 for detailed calculations). It must be emphasized that comparisons and calculations should have been done for all samples (at all the given time points) of both the cell-associated PcsB and secreted PcsB (Fig.4.8AB) to get an overview of the development regarding molecules of PcsB present during growth.

4.5 Depletion of PcsB results in reduced growth and morphological abnormalities

An increasing body of evidence indicates that the role of PcsB in *S. pneumoniae* is to cleave peptidoglycan in the septal cross wall to separate the two daughter cells during cell division (Bartual *et al.* 2014). However, the timing of PcsB activity and how it is regulated is not completely understood but several studies have focused on getting more information about its structure and function. Recent studies by Bartual *et al.* (2014) have demonstrated the murein hydrolase activity of the CHAP domain of PcsB and solved the 3D-structure of the full-length

protein. To determine if the amounts of cell-associated PcsB and secreted PcsB was maintained or degraded during growth, PcsB was depleted in *S. pneumoniae*. Depletion of PcsB was done using the ComRS gene depletion system developed by Berg *et al.* (2011). Depletion based on the ComRS system also makes it possible to determine the degree of depletion that is required for growth effects and morphological changes. The bacterial pneumococcal strain SPH247 was grown and depleted as described in section 3.1.3.

Table 4.2 Depletion of PcsB. Samples were taken every 30 min for which optical density was measured.

Sample	Optical density	Time (min)
1	0.064	0
2	0.107	30
3	0.193	60
4	0.376	90
5	0.581	120
6	0.706	150
7	0.755	180
8	0.780	210
9	0.813	240
10	0.809	270
11	0.778	300

Based on table 4.2, a graphical representation (Fig. 4.11) was made to better display the growth curve of depleted PcsB. At the end of the exponential growth phase, the cells grew slower (optical density rate decreases drastically) until they stopped growing just before stationary phase. Samples 6-11 (Table 4.2) were taken after the cell growth had stagnated. In figure 4.11 they are called A-F, respectively, and correspond to further studies done by immunoblotting (Fig. 4.12).

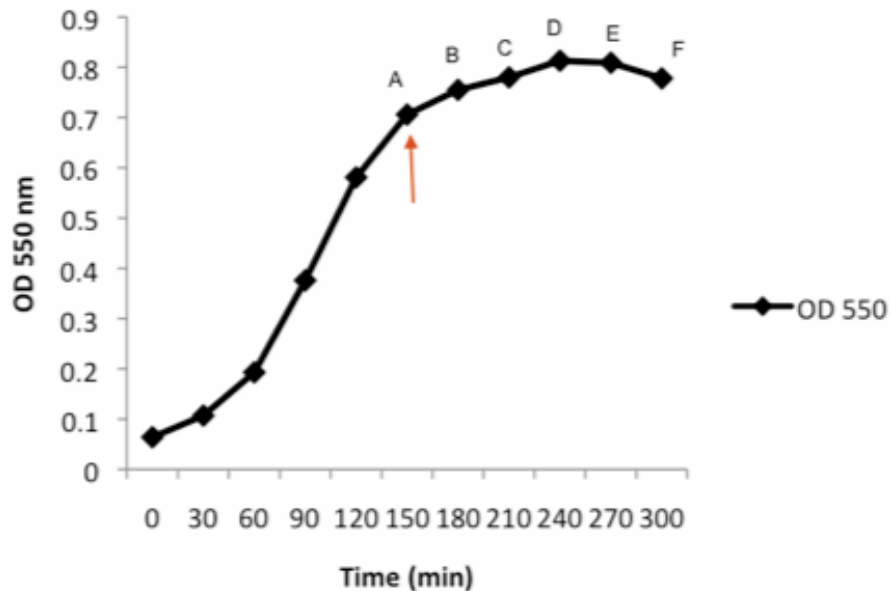


Figure 4.11: Growth curve of strain SPH247 depleted for PcsB. Depletion of PcsB in *S. pneumoniae* RH1 results in reduced growth and premature autolysis. Samples were taken for DIC-microscopy and western blot. Red arrow indicates the point where PcsB depletion affects the growth rate. Samples were taken at point A-F for microscopic study. A, B, C, D, E, F indicate the same samples as shown in microscopy images below.

The presence of PcsB was examined in all points in Fig. 4.11 by western blotting. This was done to study the stability of cell-associated PcsB and secreted PcsB in the growth medium. As shown in figure 4.12A, the amount of cell-associated PcsB appears to decrease from start of depletion; that is soon after ComS* was removed from the growth medium. Secreted PcsB in medium (Fig. 4.12B) on the other hand, appears to be quite stable and almost unaffected by the absence of ComS* in growth medium. During the growth experiment of PcsB (Section 4.4), an extra band was discovered on the blots (Fig. 4.8), thought to be a degradation product of PcsB. Therefore, it was interesting to see if this band was present during PcsB depletion as well or if it decreases in concert with PcsB. As shown in figure 4.12A, several bands with lower size than PcsB decrease in intensity similarly as full-length PcsB during gene depletion suggesting that these are degradation products of full-length PcsB.

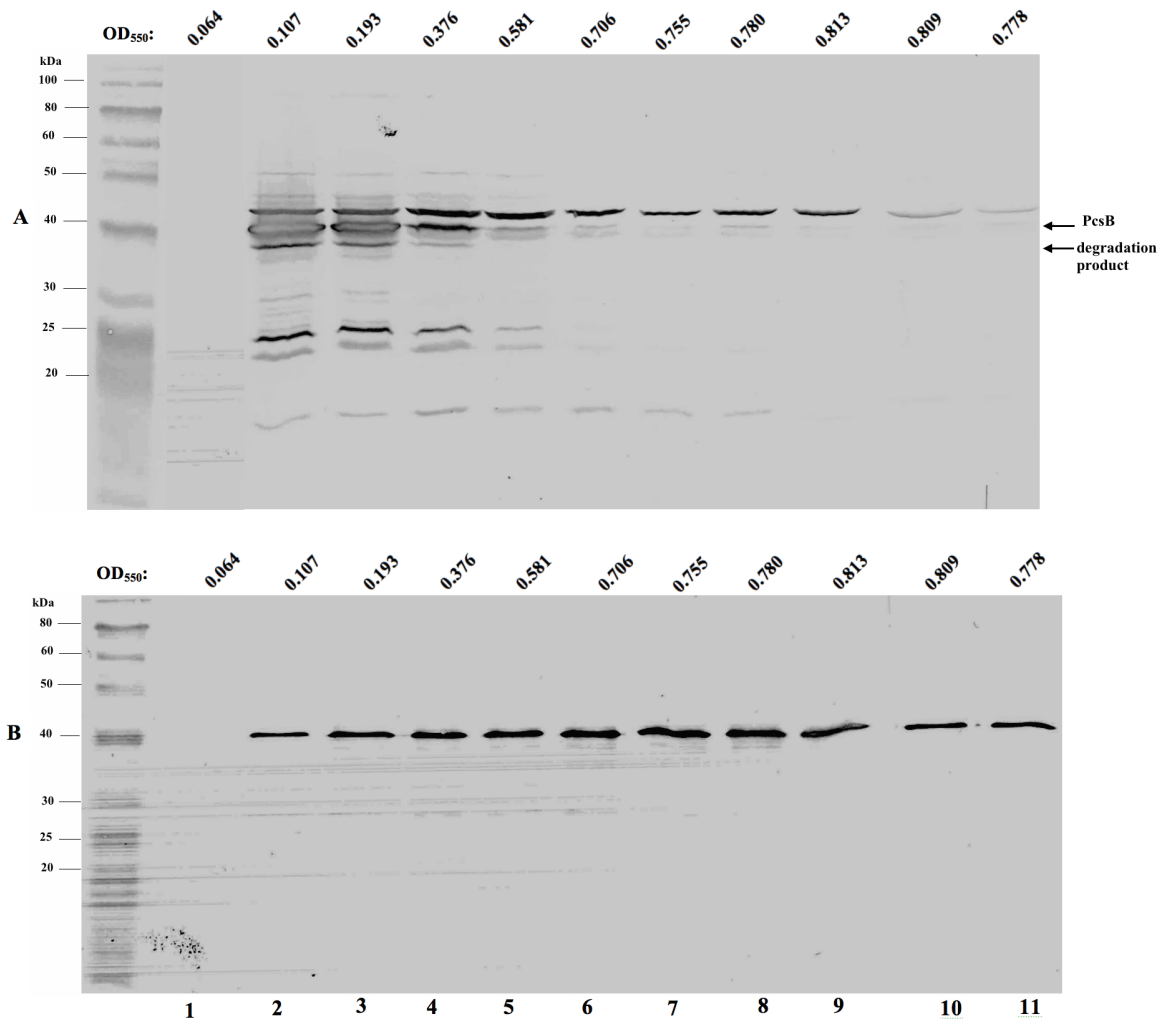


Figure 4.12 Depletion of PcsB. (A) Amount of PcsB present in cell pellet during depletion. (B) Amount of PcsB present in supernatant during depletion. Both (A) and (B) are displayed with OD measured at times given in table 4.2. Note that sample 1 (OD₅₅₀= 0.064) does not show any bands on western blot because there was no cell pellet retrieved through centrifugation.

4.5.1 Low levels of PcsB results in morphological abnormalities

As described in the introduction, PcsB has been shown to be essential in some group B streptococci (*S. pneumoniae* strain R6 and D39), and conditionally essential in other *S. mutans* (Bartual *et al.* 2014; Massidda *et al.* 2013; Mattos-Graner *et al.* 2006). The underexpression of *pcsB* in R6 and D39 and deletion of PcsB in *S. mutans* has shown to cause distorted and morphologically abnormal cells demonstrating PcsB's importance in cell division. Here *pcsB* was depleted in the R6 strain to determine the correlation between PcsB expression and growth defects and morphological changes. DIC microscopy was used to examine the impact on the cell morphology when PcsB was depleted.

The growth curve for depleted PcsB in strain SPH247 ($\Delta PcsB_{wt}::janus$, P_{comX} -PcsB) (Fig. 4.11) was followed when samples were made for microscopy study. When the growth rate of GS9 was negatively affected by PcsB depletion (after approximately 150 min), samples were taken every 30 min and fixed as described in section 3.9.2.

Strain RH1 (wt) was used as control strain. The morphology of RH1 (Fig. 4.13) shows normal, ovoide diplococci. There was a strong correlation between the amount of PcsB expressed and defects in cell morphology. The depletion of PcsB in SPH247 resulted in the formation of longer chains of irregular shaped cells. Figure 4.14 shows the development of the depleted cells

The cells collected at $OD_{550} = 0.706$ (Fig. 4.14A) seem to have less irregularities regarding growth morphology compared to cells collected at $OD_{550} = 0.809$ (Fig 4.14E) and $OD_{550} = 0.778$ (Fig. 4.14F). These cells were fixed after the growth leveled off due to low PcsB expression, right before cell death.

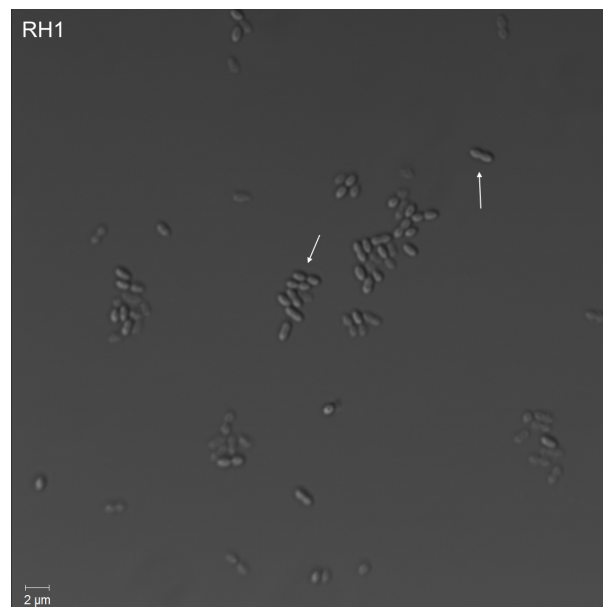


Figure 4.13: RH1 control strain. The arrows show good examples of diplococci morphology typical in *S. pneumoniae*

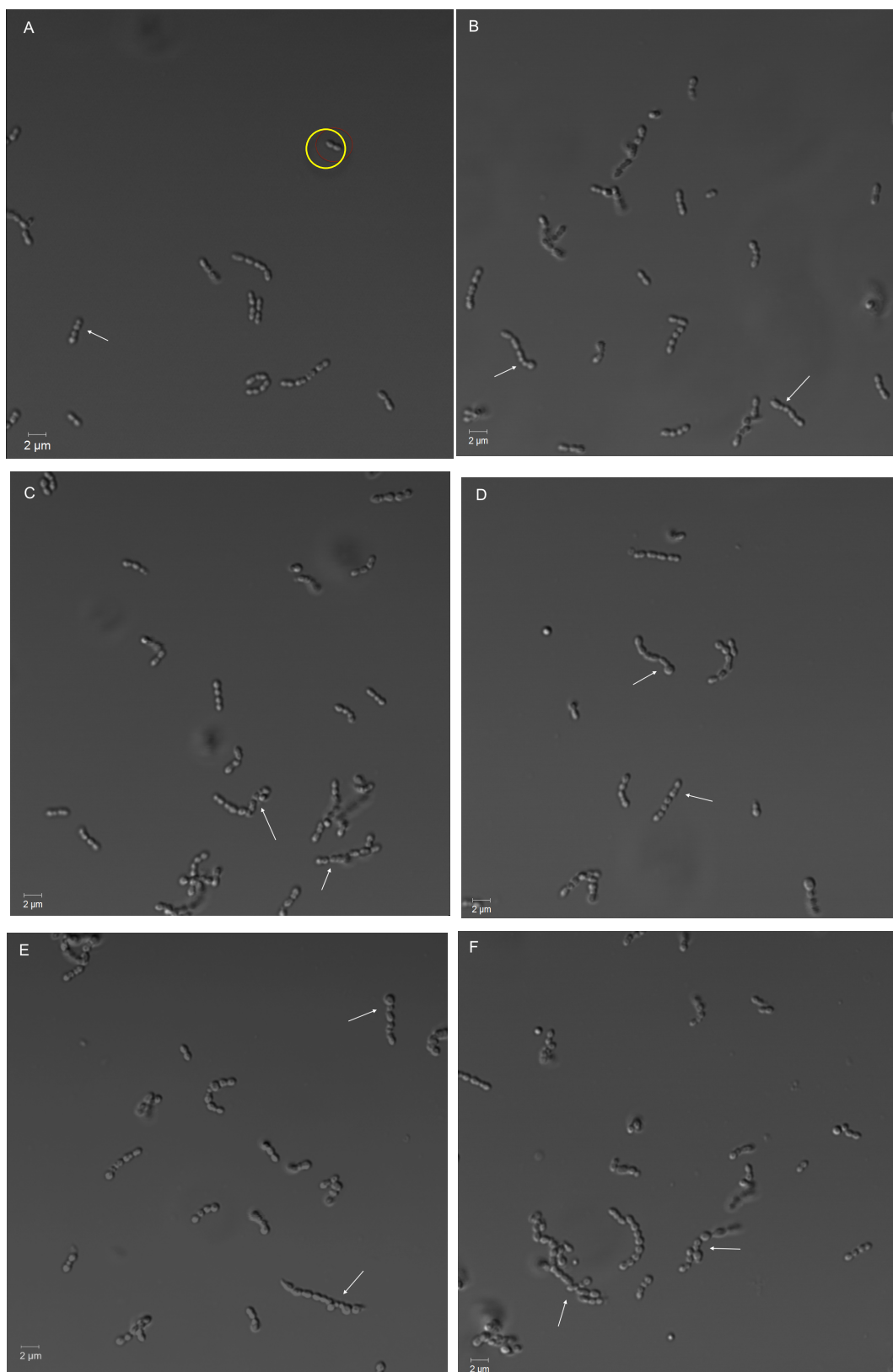


Figure 4.14: Shows the development of morphological defects correlated to PcsB depleted in SPH247. Arrows indicate typical growth defects that are formed. Cells at $OD_{550} = 0.706$ still shows signs of normal morphology (yellow circle).

An attempt was made to study the binding pattern and localization of native PcsB in *S. pneumoniae* (*S. pneumoniae* strains RH1 and SvH3) using immunofluorescence microscopy and the anti-PcsB as primary antibody. The experiment was carried out as explained in section 3.9.1, however the fluorescence signals obtained were too weak for determining PcsB localization in these cells.

5. Discussion

5.1 Anti-PcsB shows satisfactory specificity

PcsB has been suggested to have a critical role in daughter cell separation during cell division in *S. pneumoniae* and has been found to be essential in the R6 and D39 pneumococcal strains and conditionally essential in several group B streptococci (Barendt *et al.* 2009; Barendt *et al.* 2014; Massidda *et al.* 2013). To get deeper insight into how PcsB work in pneumococcal cell division, it was of interest to get hold of antibodies against PcsB as a tool to study native PcsB in *S. pneumoniae*. the first step to succeed in this was to purify mature PcsB to >99% purity. Protein purification involves several complex processes with the intention to achieve a final, isolated, protein product of a purity >99%. The purified PcsB was used to immunize rabbits for production of polyclonal antibodies against PcsB.

Because of polyclonal antibodies' ability to recognize different epitopes on antigens (Lipman *et al.* 2005), it is important to determine the specificity and sensitivity of the antibodies before it can be used as a molecular tool. Immunoblotting was performed to study the specificity of anti-PcsB. As shown in Figure 4.5, very strong bands were obtained even at highest dilutions of the antibody (1:10 000); indicating that anti-PcsB is very sensitive and very little antibody is needed for detection. However, for the smallest amounts of PcsB the signal was somewhat higher when using a 1:5000 dilution of the antibody. Hence, for detection of small amounts of PcsB the antibody should be diluted at a lower scale. In addition to the desired band, representing PcsB, a lot of background signal was detected for the samples containing the highest amount of PcsB. This suggests that a fraction of the polyclonal PcsB-antibodies bound unspecifically to other proteins present in purified PcsB sample, or that the secondary anti-rabbit antibody bound unspecifically to other proteins. To ascertain whether it was the primary- or secondary antibody that was unspecific, a control test was done where the primary antibody was excluded. This resulted in no visible bands at all (data not shown), showing that it was the primary PcsB-antibodies that were unspecific. However, it proved possible to dilute the protein even more (Fig 4.5B) to remove some of the background signal. The reason for the relatively high background noise in the samples containing high amounts of pure PcsB is most likely caused by contaminating proteins derived from *E. coli* after PcsB purification. These contaminants have been in the pure PcsB sample used for immunization, thus, the rabbits have also produced antibodies against these *E. coli* contaminants. The amount of these proteins is low since they cannot be detected by Coomassie blue staining

(Fig. 4.4). When detecting native PcsB in pneumococcal cell extracts this background noise is almost gone because there are no proteins from *E. coli* in those samples. The anti-PcsB antibodies are therefore suitable for detection of native PcsB.

Furthermore, anti-PcsB was compared to anti-FLAG to confirm its specificity. The polyclonal antibody anti-FLAG has been shown to be highly specific and sensitive, and recognizes the FLAG epitope located on FLAG fusion proteins (Sigma Aldrich). The comparison was made between RH1 (wild type expressing native pcsB) immunodetected with anti-PcsB primary antibody, and SvH3 (expressing 3xFlag-tagged PcsB) immunodetected with anti-FLAG primary antibody (Fig. 4.6). Results displayed in Fig. 4.6A show that anti-PcsB were very specific for PcsB. Not surprisingly, some background signal was detected in cell-associated PcsB. This is probably due to some unspecific binding of the antibodies to other pneumococcal proteins found in the cell lysate. In the supernatant on the other hand, little background was detected implying satisfactory level of specificity. 3xFlag-PcsB is located slightly higher (around approximately 44 kDa) than RH1 (38.9 kDa)(Fig.4.6) on the membrane. This was expected since SvH3 contains an additional 3xFlag tag tail. Another interesting observation was that unprocessed PcsB was not detected in the cell lysate. This suggests that PcsB is translocated across the cell membrane simultaneously or immediately after translation.

5.2 PcsB accumulates outside the cells

To study the correlation between amounts of PcsB present in cells and in the supernatant, a growth experiment was conducted with *S. pneumoniae* strain RH1. Judging from Table 4.1 and corresponding graph (Fig. 4.7), it seems that after 150 min, cell density remains somewhat uniform while CFU reduces drastically. As mentioned before, this is most likely caused by dead cells that have not yet lysed. In addition, some uncertainty must be taken into account regarding the calculations of CFU/ml. As seen in table 4.1, some of the TH-agar plates contained very few colonies. This is probably because the dilution factor used was too high.

The amount of cell-associated PcsB and secreted PcsB, protein samples from whole cell extracts and the supernatants were examined by Western blot using anti-PcsB. Whole cell extracts were washed in 10 mM Tris-Hcl pH 7.4 with 10 mM NaCl and the supernatants were

sterile filtered before analysis. When interpreting the immunoblots of secreted and cell-associated PcsB (Fig. 4.8), the level of cell-associated PcsB appears to be relatively stable during the entire growth phase while the concentration of secreted PcsB increases during growth. Since the whole cell extracts contain all the proteins expressed in *S. pneumoniae*, some background noise in Fig. 4.8A was expected. In addition to full-length PcsB, other proteins of lower size were detected. An extra band at around 38 kDa is thought to be a degradation product of PcsB (see section 5.3). It appears during the lag phase but weakens during exponential growth phase before it stabilizes again. The level of secreted PcsB in the growth medium increased from lag phase throughout exponential growth phase and seemed to stabilize during the stationary phase.

The amount of cell-associated PcsB and the amount of secreted PcsB recovered in the growth medium was calculated by visually inspecting immunoblots and by comparing with the dilution series of purified PcsB (with known PcsB concentration). Based on the results, the numbers of PcsB copies in *S. pneumoniae* cells measured at $OD_{550} = 0.341$ were estimated to 8709, implying that PcsB is relatively abundant in *S. pneumoniae*. Despite the relative abundance of cell-associated PcsB, it is probable to assume that approximately at least an equal amount of PcsB is secreted into the growth medium. Calculations showed that PcsB seemed to be much more abundant in supernatant per cell with approximately 108939 molecules (also measured at $OD_{550} = 0.341$). This might be explained by the mechanism of how PcsB is thought to work. Bartual *et al* (2014) proposed a model in which PcsB located in the septum is released to the surroundings once it has cleaved a small part of the cross wall. The released PcsB is shown to be inactive due to structural constraints. New PcsB molecules must then be recruited to the septum cross wall from inside the cells when the previous copy of PcsB has done its job and are released. This goes on as the cross wall is cleaved towards its centre and the daughter cells are separated. Such a mechanism requires a lot of PcsB, and the enzyme will accumulate in the surroundings as the cross wall is split down the middle, which is what we see in the supernatant of growing cells. The advantage with this mechanism is that it serves as a brilliant control mechanism of PcsB. PcsB can only cleave peptidoglycan in the cross wall, and are inactive when released to the extracellular space. As mentioned in the results, calculations should have been done for every OD_{550} measured to create a fully-fledged overview of the development of PcsB accumulation. Secreted PcsB will most likely accumulate significantly during the exponential growth phase. It seems like PcsB accumulates

without being recycled, indicating that the cells invest a lot of energy in PcsB production without being able to reuse the enzyme or its amino acids.

5.3 Depletion of PcsB

Previous studies have shown that *pcsB* is essential in serotype 2 strains in *S. pneumoniae*, based on the fact that PcsB under-expression directly causes cell defects (Barendt *et al.* 2009). In this study, PcsB was depleted using the ComRS system (Berg *et al.* 2011) to determine the degree of depletion that is necessary for visible growth and morphological defects. In addition, PcsB was depleted to determine whether the amounts of cell-associated PcsB and secreted PcsB in growth medium remained stable or showed some kind of degradation over time.

Compared to the growth curve of RH1 cells in Fig. 4.7, a slight decrease in growth rate and early cell lysis in PcsB-depleted SPH247 is shown. *S. pneumoniae* SPH247 had first been grown with ComS*, then washed and grown in the absence of ComS*. The removal of ComS* from the growth medium results in gradual depletion of PcsB expression which is likely the cause for the inhibition of growth observed after 150 minutes. An advantage of this delayed growth rate would be that the cells have time to develop phenotypic changes before they stop growing (Berg *et al.* 2011). Interestingly, the absence of PcsB resulted in apparent differences in protein abundance between cell-associated PcsB and secreted PcsB in medium. As the level of cell-associated PcsB seemed to go down over time, secreted PcsB in medium proved to remain stable and somewhat unaffected by the depletion (Fig.4.12). Also in depleted cells, a degradation product of PcsB was seen on the immunoblots of the cell pellets. The reason why the amount of cell-associated PcsB declined might be that it is still transported to the periplasm in the septum even though its expression is turned off. Another explanation could be that it is degraded inside the cells when the cells stop growing as there is no use for cross wall splitting in non-growing cells. Moreover, it is evident that *S. pneumoniae* cannot utilize or reuse the PcsB that is released from the cells. A lot of PcsB was found extracellularly in severely PcsB-depleted cells, but they still stopped growing.

5.4 Depletion of PcsB influences cell shape and chain formation

The growth curve for depleted PcsB in strain SPH247 (Fig. 4.11) was followed, and samples were collected for microscopic studies when PcsB depletion had a negative effect on the growth rate. Figure 4.14 shows the microscopic images taken from the PcsB-depleted cells. The cells collected at $OD_{550} = 0.706$ (Fig. 4.14A) display almost no irregularities regarding cell shape. Here, the typical diplococci formation is still intact. As expected, there is a correlation between PcsB levels in the cells and the severity of growth defects. Reduced amounts of PcsB immediately resulted in growth defects. When the cell growth leveled out as a consequence of PcsB depletion (Fig. 4.11), the abnormalities start evolving. The under-expression of PcsB in *S. pneumoniae* SPH247 reach a critical level after approximately 180 min and will not recover from these morphological changes. Cells collected at $OD_{550} = 0.809$ and $OD_{550} = 0.778$ (Fig. 4.14 E and F, respectively) display severe growth defects such as clumping, long chains, irregular cell shapes and cell division defects. These morphological changes indicate that PcsB-depleted cells have lost their ability to divide properly.

The depletion of PcsB in bacterial strain SPH247 resulted in misplaced division septa, irregular shaped cells and the formation of longer chains. This corresponds to previous studies showing the same morphological changes for PcsB-underexpressed R6 strains (Ng *et al.* 2004; Barendt *et al.* 2009). It is clear that the role of PcsB in cross wall splitting is critical for the pneumococcus regarding cell division and daughter cell separation. Although, based on these results, one cannot conclude that PcsB is solely responsible for growth and morphological defects. Both the peripheral and septal peptidoglycan synthesis contain several components that might affect growth and morphology. It is possible that these components may be affected indirectly by the depletion of PcsB.

5.4.1 Immunofluorescence microscopy

As mentioned in section 4.4.1, an attempt was made to fluorescently stain and visualize both native and FLAG-tagged PcsB in *S. pneumoniae* RH1 and SvH3 through immunofluorescence microscopy. The purpose was to study the binding pattern and the localization of PcsB in pneumococcal cell walls using the new anti-PcsB antibodies. Previous studies have shown that PcsB is localized in the division septa and/or poles and that the protein is involved in cell separation (Sham *et al.* 2011). The experiment was carried out as

explained in section 3.9.1 although for some reason, it appeared to be difficult to detect any form of binding pattern. Since this method is proven to be successful (cf. Wayne *et al.* 2010), other reasons for the failed attempts were investigated. To see whether the secondary antibody conjugated with a fluorophore was functional or not, an additional test was done using bacterial strain SPH234 expressing Flag-tagged Pbp2x. Recent work done by Dr. Kari Helene Berg showed that Flag-Pbp2x could be detected using this technique (Berg *et al.* 2014). Results indicated that the secondary antibody was nonfunctional. However, further experiments using new secondary antibody and different dilutions of the antibodies still showed no signs of binding pattern. PscB proved to be rather difficult to detect using immunofluorescence microscopy. It could be that the epitopes of PcsB were destroyed during fixation of the cells so that it was unrecognizable to the antibodies or that the antibodies somehow were unable to get access to PcsB. Additional studies are required to solve this problem.

6. Concluding remarks and future work

S. pneumoniae is a serious human pathogen that causes invasive diseases such as meningitis, septicaemia and pneumonia worldwide (Hoskins *et al.* 2001; Sham *et al.* 2012). Horizontal gene transfer among streptococci leads to capsular switching and increased penicillin resistance in *S. pneumoniae* (Giefing *et al.* 2008; Sham *et al.* 2012). This complicates the treatment of pneumococcal diseases and reports a challenge in vaccine development. All vaccines currently in use target the pneumococcal polysaccharide capsule. A promising candidate to develop new generation vaccines is the peptidoglycan (PG) hydrolase PcsB (Sham *et al.* 2012). PcsB is very well conserved (>99% identity) among clinical isolates of *S. pneumoniae* and is surface-exposed. It is also reported to induce a strong immune response in pneumococcal hosts (Massidda *et al.* 2013; Bartual *et al.* 2014). Immunization with PcsB may provide protection against lethal pneumococcal challenges (Mills *et al.* 2007).

Because of their ability to bind an antigen highly specific and with a high degree of affinity, antibodies are widely used within research. In this study, mature PcsB was purified to produce PcsB-specific antibodies, which will be a valuable tool for studying PcsB in *S. pneumoniae*. The sensitivity and specificity of the antibody anti-PcsB have been determined and proved to be satisfactory through several tests using Western blot. The amount of cell-associated PcsB and secreted PcsB in medium was also established through growth studies of *S. pneumoniae* strain RH1. This revealed that PcsB is a relative abundant protein in *S. pneumoniae*. Recent studies indicate that PcsB is involved in the cleavage of PG in the septal cross wall to separate the two daughter cells during cell division (Bartual *et al.* 2014). To determine whether the amounts of cell-associated PcsB and secreted PcsB was maintained or degraded, and to study morphological changes, PcsB was depleted in *S. pneumoniae*. The under-expression of PcsB caused growth arrest and distorted and morphologically abnormal cells demonstrating PcsB's importance in cell division. Moreover, the level of cell-associated PcsB is quickly reduced as expression of PcsB is turned off, while the amount of PcsB outside the cells remained unaffected by PcsB-depletion.

Further research on PcsB by using anti-PcsB will continue in the Molecular Microbiology Group at NMBU. The PcsB-specific antibody is intended to be used for determination of the exact localization of PcsB in septum by immuno-gold labeling. Sham *et al.* (2011) showed that PcsB interacts with the membrane protein FtsX_{spn} complex in cell membranes. The PcsB-

specific antibody could also be used for protein complex immunoprecipitation (“pull down”) of PcsB to see if PcsB interacts with other proteins in addition to FtsX. Another area of application of the antibody could be in an ongoing study at the laboratory of the Molecular Microbiology Group regarding Pbp2b involved in peripheral peptidoglycan synthesis. A mutant that expresses low levels of Pbp2b is unable to split the cross wall. The antibody can be used to examine the expression of PcsB in this mutant, and whether PcsB is miss-located or if it is released from the cells or not. Changes in any of these compared to wild type cells might give important clues to how PcsB is regulated.

7. References

- Austrian, R.** (1981). Pneumococcus: the first one hundred years. *Reviews of Infectious Diseases*, **3**(2):183-189.
- Avery, O.T., MacLeod, C.M., McCarty, M.** (1944). Studies of the chemical nature of the substance inducing transformation of pneumococcal types: induction of Transformation by a Deoxyribonucleic Acid Fraction Isolated from Pneumococcus Type III. *The Journal of experimental Medicine*, **79**(2): 137-158.
- Barendt, S.M., land, A.D., Sham, L-T., Ng, W-L., Tsui, H-C.T., Arnold, R.J., Winkler, M.E.** (2009). Influences of Capsule on Cell Shape and Chain Formation of Wild-Type and *PcsB* Mutants of Serotype 2 *Streptococcus pneumoniae*. *Journal of Bacteriology*, 3024-3040
- Bartlett, J.M.S., Stirling, D.** (2003). A Short History of the Polymerase Chain Reaction. *Methods in Molecular Biology*. **226**:3-6
- Bartual, S.G., Straume, D., Stamsås, G.A., Alfonso, C., Martinez-Ripoll, M., Håvarstein, L.S., Hermoso, J.A.** (2014). Structural basis of PcsB-mediated cell separation in *Streptococcus pneumoniae*. *Nature Communications*, **5**:3842, DOI: 10.1038/ncomms4842
- Berg, J.M., Tymoczko, J.L., Stryer, L.** (2002). Biochemistry 5th edition. New York: *W H Freeman*
- Berg, K.H., Biørnstad, T.J., Straume, D., Håvarstein, L.S.** (2011). Peptide-Regulated Gene Depletion System Developed for Use in *Streptococcus pneumoniae*. *Journal of Bacteriology*, **193**(19):5207-5215
- Berg, K.H., Biørnstad, T.J., Johnsborg, O., Håvarstein, L.S.** (2012). Properties and Biological Role of Streptococcal Fratricins. *Applied and Environmental Microbiology*, **78**(10):3515-3522.
- Berg, K.H., Straume, D., Håvarstein, L.S.** (2014). The function of the transmembrane and cytoplasmic domains of pneumococcal Pbp2x and Pbp2b extends beyond that of simple anchoring devices. *Microbiology*, (doi:10.1099/mic.0.078535-0)
- BioRad** (2014) Protein Blotting Guide. BioRad Laboratories Inc. Available: http://www.bio-rad.com/webroot/web/pdf/lsr/literature/Bulletin_2895.pdf
- Bjerrum, O.J. & Schafer-Nielsen, S.** (1986). Buffer systems and transfer parameters for semi-dry electroblotting with a horizontal apparatus. I: Dunn, M.J. (red) *Analytical Electrophoresis*. Weinheim: VCH Publishers, 315-327.

- Bogaert, D., de Groot, R., Hermans, P.W.M.** (2004a). *Streptococcus pneumoniae* colonization: the key to pneumococcal disease. *The Lancet Infectious Diseases*, 4:144-154.
- Bogaert, D., Hermans, P.W.M., Adrian, P.V., Rümke, H.C., de Groot, R.** (2004b). Pneumococcal vaccines: an update on current strategies. *Vaccine*, 22:2209-2220.
- Cabeen, M.T., Jacobs-Wagner, C.** (2005). Bacterial Cell Shape. *Nature reviews Microbiology*, 3:601-610.
- Chambers, H.F.** (1999). Penicillin-Binding Protein – mediated resistance in pneumococci and staphylococci. *The Journal of Infectious Diseases*, 179(Suppl 2):S353-9
- Chandler, M.S., Morrison, D.A.** (1988). Identification of Two Proteins Encoded by *com*, a Competence Control Locus of *Streptococcus pneumoniae*. *Journal of Bacteriology*, 3136-3141
- Claverys, J-P., Martin, B., Polard, P.** (2009). The genetic transformation machinery: composition, localization, and mechanism. *FEMS Microbiological reviews*, 33:643-656.
- Davidson, M.W., Abramowitz, M.** (2002). Optical Microscopy. *Encyclopedia of Imaging Science and Technology*.
- Davis, B.J.** (1964). Disc Electrophoresis II. Method and application to human serum proteins. *Annals of the New York Academy of Sciences*, 121:404-427.
- Denapaite, D., Brükner, R., Hakenbeck, R., Vollmer, W.** (2012). Biosynthesis of Teichoic Acids in *Streptococcus pneumoniae* and Closely Related Species: Lessons from Genomes. *Microbial Drug Resistance*, 18(3):344-358
- Egan, A.J.F., Vollmer, W.** (2013). The physiology of bacterial cell division. *Annals of the New York Academy of Sciences*, 8-28
- Fontaine L., Goffin P., Dubout H., Delplace B., Baulard A., Lecat-Guikket N., Chambellon E., Gardan R., Hols P.** (2013). Mechanism of competence activation by the ComRS signalling system in streptococci. *Molecular microbiology*, 87(6):1113-1132
- Garrity, G.M., Bell, J.A., Lilburn, T.G.** (2004). Taxonomic outline of the Prokaryotes, *Bergey's Manual® of Systematic Bacteriology*, Second Edition. *New York: Springer, for Bergey's Manual® Trust*.
- Giefing, C., Meinke, A.L., Hanner, M., Henics, T., Minh, D.B., Gelbmann, D., Lundberg, U., Senn, B.M., Schunn, M., Habel, A., Henriques-Normark, B., Örtqvist, Å., Kalin, M., von Gabain, A., Nagy, E.** (2007). Discovery of a novel class of highly

- conserved vaccine antigens using genomic scale antigenic fingerprinting of pneumococcus with human antibodies. *The Journal of Experimental Medicine*, **205**(1):117-131.
- Giefing-Kröll, C., Jelencsics, K.E., Reipert, S., Nagy, E.** (2011). Absence of pneumococcal PcsB is associated with overexpression of LysM domain-containing proteins. *Microbiology*, **157**:1897-1909
- Griffith, F.** (1928). The Significance of Pneumococcal types. *The Journal of Hygiene*, **27**:113-159.
- Hardie, J.M., Whiley, R.A.** (1997). Classification and overview of the genera Streptococcus and Enterococcus. *Journal of Applied Microbiology Symposium Supplement*, **83**:1S-11S.
- Higuchi, R., Krummel, B., Saiki, R.K.** (1988). A general method of *in vitro* preparation and specific mutagenesis of DNA fragments: study of protein and DNA interactions. *Nucleic Acids Research*, **16**(15):7351-7367
- Hiller, N.L., Janto, B., Hogg, J.S., Boissy, R., Yu, S., Powell, E., Keefe, R., Ehrlich, N.E., Shen, K., Hayes, J., Barbadora, K., Klimke, W., Dernovoy, D., Tatusova, T., Parkhill, J., Bentley, S.D., Post, J.C., Ehrlich, G.D., Hu, F.Z.** (2007). Comparative Genomic Analyses of Seventeen *Streptococcus pneumoniae* Strains: Insight into the Pneumococcal Supragenome. *Journal of Bacteriology*, **189**(22):8186-8195.
- Ho, S.N., Hunt, H.D., Horton, R.M., Pullen, J.K., Pease, L.R.** (1989). Site-directed mutagenesis by overlap extension using the polymerase chain reaction. *Gene*, **77**:51-59
- Horton, R.M., Hunt, H.D., Ho, S.N., Pullen, J.K., Pease, L.R.** (1989). Engineering hybrid genes without the use of restriction enzymes: gene splicing by overlap extension. *Gene*, **88**:61-68
- Hoskins, JA., Alborn Jr, W.E., Arnold, J., Blaszcak, L.C., Burgett, S., DeHoff, B.S., Estrem, S.T., Fritz, L., Fu, D-J., Fuller, W., Geringer, C., Gilmour, R., Glass, J.S., Khoja, H., Kraft, A.R., Lagace, R.E., LeBlanc, D.J., Lee, L.N., Lefkowitz, E.J., Lu, J., Matsushima, P., McAhren, S.M., McHenney, M., McLeaster, K., Mundy, C.W., Nicas, T.I., Norris, F.H., O’Gara, M.J., Peery, R.B., Robertson, G.T., Rockey, P., Sun, P-M., Winkler, M.E., Yang Y., Young-Bellido, M., Zhao, G., Zook, C.A., Baltz, R.H., Jaskunas, R., Rosteck Jr., P.R., Skatrud, P.L., Glass, J.I.** (2001). Genome of the Bacterium *Streptococcus pneumoniae* Strain R6. *Journal of Bacteriology*, **183**(19):5707-5717

- Hui, F.M., Morrison, D.A.** (1991). Genetic transformation in *Streptococcus pneumoniae*: nucleotide sequence analysis shows comA, a gene required for competence induction, to be a member of the bacterial ATP-dependent transport protein family. *Journal of Bacteriology*, **173**(1):372-381
- Håvarstein, L.S., Coomaraswamy, G., Morrison, D.A.** (1995). An unmodified heptadecapeptide pheromone induces competence for genetic transformation in *Streptococcus pneumoniae*. *Proceedings of the National Academy of Sciences of the USA*, **92**(24):11140-11144.
- Håvarstein L.S., Hakenbeck R., Gaustad P.** (1997). Natural competence in the genus *Streptococcus*: Evidence that Streptococci can change phenotype by interspecies recombinational exchanges. *Journal of bacteriology*, **179**(21):6589-6594.
- Håvarstein, L.S., Martin, B., Johnsborg, O., Granadel, C., Claverys, J-P.** (2006). New insight into the pneumococcal fratricide: relationship to clumping and identification of a novel immunity factor. *Molecular Microbiology*, **59**(4): 1297-1307.
- Håvarstein, L.S.** (2010). Increasing competence in the genus *Streptococcus*. *Molecular Microbiology*, **78**:541-544
- Innis, M.A., Gelfand, D.H.** (1991). Optimization of PCRs. PCR Protocols: A Guide to Methods and Applications. *Academic press inc.* 3-12.
- Jedrzejewski, M.J.** (2001). Pneumococcal Virulence Factors: Structure and Function. *Microbiology and Molecular Biology Reviews*, **65**(2):187-207.
- Johnsborg O., Eldholm V., Håvarstein L.S.** (2007). Natural genetic transformation: prevalence, mechanisms and function. *Research in microbiology*, **158**:767-778
- Johnsborg O., Eldholm, V., Bjørnstad, M.L., Håvarstein, L.S.** (2008). A predatory mechanism dramatically increases the efficiency of lateral gene transfer in *Streptococcus pneumoniae*. *Molecular microbiology*. **69**:245-253
- Johnsborg, O., Håvarstein, L.S.** (2009). Regulation of natural genetic transformation and acquisition of transforming DNA in *Streptococcus pneumoniae*. *FEMS Microbiological reviews*, **33**:627-642
- Kadioglu, A., Weiser, J.N., Paton, J.C., Andrew, P.W.** (2008). The role of *Streptococcus pneumoniae* virulence factors in host respiratory colonization and disease. *Nature reviews Microbiology*, **6**:288-301.
- Kawamura, Y., Hou, X-G., Sultana, F., Miura, H., Ezaki, T.** (1995). Determination of 16S rRNA Sequences of *Streptococcus mitis* and *Streptococcus gordonii* and Phylogenetic

- Relationships among Members of the Genus Streptococcus. *International Journal of Systematic Bacteriology*, 406-408.
- Kibbe, W.A.** (2007). OligoCalc: an online oligonucleotide properties calculator. *Nucleic Acids Research*. 35:W43-W46.
- Kilian, M.** (1998). Streptococcus and Lactobacillus. I: Balows, A. & Duerden, B.I. (red.) b. 2 *Topley and Wilson's Microbiology and Microbiological Infections*, 633-667.
- Kilian, M., Poulsen, K., Blomqvist, T., Håvarstein, L.S., Bek-Thomsen, M., Tettelin, H., Sørensen, U.B.S.** (2008). Evolution of *Streptococcus pneumoniae* and Its Close Commensal Relatives. *PLoS ONE*, 3(7):e2683.
- Kleppe, K., Ohtsuka, E., Kleppe, R., Molineux, I., Khorana, H.G.** (1971). Studies on polynucleotides. XCVI. Repair replication of short synthetic DNA's as catalyzed by DNA polymerases. *Journal of Molecular Biology*, 56(2): 341-361
- Knutsen, E., Ween, O., Håvarstein, L.S.** (2004). Two Separate Quorum-Sensing Systems Upregulate Transcription of the Same ABC Transporter in *Streptococcus pneumoniae*. *Journal of Bacteriology*. 186(10):3078-3085.
- Kyhse-Andersen, J.** (1984). Electroblotting of multiple gels: a simple apparatus without buffer tank for rapid transfer of proteins from polyacrylamide to nitrocellulose. *Journal of Biochemical and Biophysical Methods*, 10: 203-209
- Lacks, S.A. & Hotchkiss, R.D.** (1960). A study of the genetic material determining enzyme activity in pneumococcus. *Biochimica et Biophysica Acta*, 39:508-517.
- Laemmli, U.K.** (1970). Cleavage of Structural Proteins during the Assembly of the Head of Bacteriophage T4. *Nature*, 227:680-685
- Laurière, M.** (1993). A Semidry Electroblotting System Efficiently Transfers Both High- and Low-Molecular-Weight Proteins Separated by SDS-PAGE. *Analytical Biochemistry*, 212(1): 206-211.
- Lee, M.S., Morrison, D.A.** (1999). Identification of a New Regulator in *Streptococcus pneumoniae* Linking Quorum Sensing to Competence for Genetic Transformation. *Journal of Bacteriology*, 181(16):50044-5016
- Lipman, N.S, Jackson, L.R., Trudel, L.J., Weis-Garcia, F.** (2005). Monoclonal versus polyclonal antibodies: Distinguishing characteristics, applications and information resources. *ILAR journal*, 46(3): 258-268
- Lorenz M.G., Wackernagel W.** (1994). Bacterial gene transfer by natural genetic transformation in the environment, *Microbiological reviews*, Vol.58(3):563-602

- Macherey-Nagel.** (2012). PCR clean-up Gel extraction, User manual NucleoSpin® Gel and PCR clean up. Available at www.mn-net.com
- Martel, C.C., Gonzalez, C.D., Martins, A.D.S., Kotnik, M., Dessen, A.,** 2009. PBP active site flexibility as the key mechanism for α -lactam resistance in pneumococci. *Journal of Molecular Biology*, **387**:899-909
- Martin, B., Granadel, C., Campo, N., Hénard, V., Prudhomme, M., Claverys, J-P.** (2010). Expression and maintenance of ComD-ComE, the two-component signal-transduction system that controls competence of *Streptococcus pneumoniae*. *Molecular Microbiology*, **75**(6): 1513-1528
- Martin, B., Soulet, A-L., Mirouze, N., Prudhomme, M., Mortier-Barrière, I., Granadel, C., Noiro-Gros, M-F., Noiro, P., Polard, P., Claverys, J-P.** (2013). ComE/ComE~P interplay dictates activation or extinction status of pneumococcal X-state (competence). *Molecular Microbiology*, **87**(2): 394-411
- Massidda, O., Nováková, L., Vollmer, W.** (2013). From models to pathogens: how much have we learned about *Streptococcus pneumoniae* cell division? *Environmental microbiology*, **15**(12):3133-3157
- Mattos-Graner, R.O., Porter, K.A., Smith, D.J., Hosogi, Y., Duncan, M.J.** (2006). Functional analysis of Glucan binding Protein B from *S. mutans*. *Journal of Bacteriology*, **188**(11): 3813-3825
- Mirouze, N., Bergé, M.A., Soulet, A-L., Mortier-Barrière, I., Quentin, Y., Fichant, G., Granadel, C., Noiro-Gros, M-F., Noiro, P., Polard, P., Martin, B., Claverys, J-P.** (2013). Direct involvement of DprA, the transformation-dedicated RecA loader, in the shut-off of pneumococcal competence. *PNAS*, 1-10.
- Moriot, C., Zapun, A., Dideberg, O., Vernet, T.** (2003). Growth and division of *Streptococcus pneumoniae*: localization of the high molecular weight penicillin-binding proteins during the cell cycle. *Molecular biology*, **50**(3):845-855
- Ng, W-L., Kazmierczak, K.M., Winkler, M.E.** (2004). Defective cell wall synthesis in *Streptococcus pneumoniae* R6 depleted for the essential PcsB putative murein hydrolase or the VicR (YycF) response regulator. *Molecular microbiology*, **53**(4): 1161-1175
- Ochman, H., Lawrence, J.G., Groisman, E.A.** (2000). Lateral gene transfer and the nature of bacterial innovation. *Nature*, **405**:299-304.
- Odell, I.D, Cook, D.** (2013). Immunofluorescence Techniques. *Journal of Investigative Dermatology*. **133**:1-4.

- Ornstein, L.** (1964). Disc Electrophoresis I. Background and theory. *Annals of the New York Academy of Sciences*, **121**:321-349.
- Pakula, R., Walczak, W.** (1963). On the Nature of Competence of Transformable Streptococci. *Journal of genetic Microbiology*, **31**: 125-133
- Pierce Biotechnology.** (2002).
<http://classes.soe.ucsc.edu/bme220l/Spring11/Reading/Extinction-coefficients.pdf>
- Pinho, M.G., Kjos, M., Veening, J-W.** (2013). How to get (a)round: mechanisms controlling growth and division of coccoid bacteria. *Nature reviews microbiology* , **11**:601-614
- Rosenberger, H.E.** (1977). Differential Interference Contrast Microscopy. *Interpretive Techniques for Microstructural Analysis*, 79-104.
- Sambrook, J. & Russel, D.W.** (2001). Molecular Cloning. A Laboratory Manual. 3rd edition. *New York: Cold Spring Harbour Laboratory Press.*
- Sanchez-Pulles, J.M., Sanz, J.M., Garcia, J.L., Garcia, E.** (1992). Immobilization and single-step purification of fusion proteins using DEAE-cellulose. *Eur.J.Biochem*, **203**:153-159.
- Sanger, F., Nicklen, S., Coulsen, A.R.** (1977). DNA sequencing with chain-terminating inhibitors. *Proceedings of the National Academy of Sciences of the USA*. **74(12)**:5463-5467
- Sanz , J.M., Lopez, R., Garcia, J.L.** (1988). Structural requirements of choline derivatives for ‘conversion’ of pneumococcal amidase. A new single-step procedure for purification of this autolysin. *FEBS Lett.* **232(2)**:308-312.
- Scheffers, D-J., Pinho, M.G.** (2005). Bacterial Cell Wall Synthesis: New Insight from Localization Studies. *Microbiology and Molecular Biology Reviews*, **69(4)**:585-607
- Schleifer, K.H., Ludwig, W.** (1995). Phylogenetic relationships of lactic acid bacteria. *The Genera of Lactic Acid Bacteria*. Volume **2**:7-18.
- Sham, L-T., Barendt, S.M., Kopecky, K.E., Winkler, M.E.** (2011). Essential PcsB putative peptidoglycan hydrolase interacts with the essential FtsX_{Spn} cell division protein in *Streptococcus pneumoniae*, *PNAS*, **108(45)**: E1061-E1069
- Sham, L-T., Tsui, H-C.T., Land, A.D., Barendt, S.M., Winkler, M.E.** (2012). Recent advances in pneumococcal peptidoglycan biosynthesis suggest new vaccine and antimicrobial targets. *Current Opinion in Microbiology*, **15**:194-203.
- Sham, L-T., Jensen, K.R., Bruce, K.E., Winkler, M.E.** (2013). Involvement of FtsE ATPase and FtsX Extracellular Loops 1 and 2 in FtsEX-PcsB Complex Function in Cell Division of *Streptococcus pneumoniae*. *mBio*, **4(4)**: 1-9

- Sigma Aldrich** www.sigmaaldrich.com/catalog/product/sigma/f7425?lang=en®ion=NO
- Song, J-H., Ko, K.S., Lee, J-Y., Baek, J.Y., Oh, W.S., Yoon, H.S., Jeong, J-Y., Chun, J.** (2005). Identification of Essential Genes in *Streptococcus pneumoniae* by Allelic Replacement Mutagenesis. *Molecules and cells*, **19**(3):365-374
- Stamsås, G.A., Håvarstein, L.S., Straume, D.** (2013). ChiC, a new tandem affinity tag for the protein purification toolbox. *Journal of Microbiological Methods*, **92**:59-63.
- Steinmoen, H., Knutsen, E., Håvarstein, L.S.** (2002). Proceedings of the National Academy of Sciences. **99**:7681-7686.
- Tal, M., Silberstein, A., Nusser, E.** (1985). Why does Coomassie Brilliant Blue R Interact Differently with Different Proteins? A Partial Answer. *The journal of biological chemistry*, **260**(18):9976-9980
- Tomasz, A., Hotchkiss, R.D.** (1964). Regulation of the transformability of pneumococcal cultures by macromolecular cell products. *Microbiology*, **51**:480-487
- Tomasz, A.** (1966). Model for the Mechanism Controlling the Expression of Competent State in Pneumococcus Cultures. *Journal of Bacteriology*, **91**(3):1050-1061
- Vollmer, W.** (2007). Structure and Biosynthesis of the Pneumococcal Cell Wall. I: Hakenbeck, R. & Chhantwal, G.S. (red.) *Molecular Biology of Streptococci*, Norfolk: Horizon Bioscience, 83-117.
- Vollmer, W., Joris, B., Charlier, P., Foster, S.** (2008a). Bacterial peptidoglycan (murein) hydrolases. *FEMS Microbiology reviews*, **32**: 259-286
- Vollmer, W., Blanot, D., de Pedro, M.A.** (2008b). Peptidoglycan structure and architecture. *FEMS Microbiology reviews*, **32**:149-167
- Wayne, K.J., Sham, L-T., Tsui, H-C.T., Gutu, A.D., Barendt, S.M., Keen, S.K., Winkler, M.E.** (2010). Localization and Cellular amounts of the WalRKJ (VicRKX) Two-Component Regulatory System Proteins in Serotype 2 *Streptococcus pneumoniae*. *Journal of Bacteriology*, **192**(17):4388-4394
- Westermeier, R., Marouga, R.** (2005). Protein Detection Methods in Proteomics Research. *Bioscience Reports*, **25**:19-32
- World Health Organization (WHO).** (2012). Pneumococcal vaccines – WHO position paper. *Weekly Epidemiological Record*, **87**(14):129-144.
- World Health Organization (WHO).** (2013). Pneumonia – fact sheet. *Media center WHO*.
- Zapun, A., Vernet, T., Pinho, M.G.** (2008). The different shapes of cocci. *FEMS Microbiology reviews*, **32**(2): 345-360

Appendix A

Standards

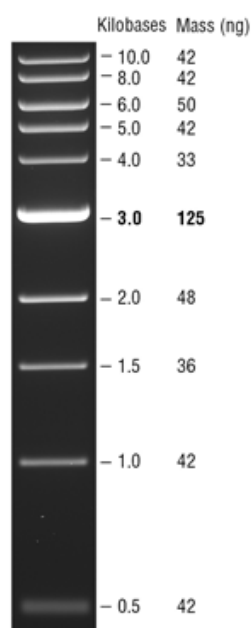


Figure A.1 1 Kb DNA-ladder visualized by EtBr, is useful to estimate sizes of dsDNA fragments ranging from 500 bp – 10 kB. Mass values: 0.5 µg/lane. (Figure taken from <https://www.neb.com/products/n3232-1-kb-dna-ladder>)

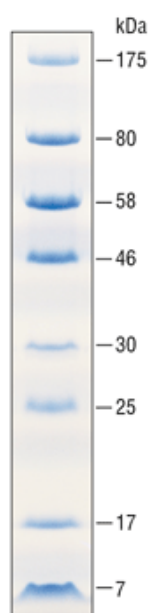


Figure A.2. Prestained Broad Range Marker is a mixture of purified proteins that are covalently bound to a blue dye. When separated on SDS-PAGE, the gel results in 8 bands with specific molecular weight (kDa). (Figure taken from <https://www.neb.com/products/p7708-prestained-protein-marker-broad-range-7-175-kda>).

Appendix B

pcsB sequence:

TATGGAATTATTATTGGCTATGACAAGGAAAATGACGTTCTTAAAAATTAGCCAATTAATAAGTAAT
 AGCGATATTAGTGCGGGAGATAAAGGTGACTACTGGTGGATTAGGAAACTTTAACGTTGCTGATATT
 CCTGTTGGTGAAGTGGTTGCCACAACGCATAGTACAGACTATTTGACACGAGAAGTAACTGTTAAA
 TTGAGTGCAGATACTCATAATGTAGATGTGATAGAATTAGTGGGGAATTCATAATGAGACAGTTGA
 AGCGAGTTGGAGTATTTTTATTGCTTCCTTTCTTTGTTCTAATTGACGCCCATATTAGCCAGCTTCTG
 GGCTCATTTTTCCCCATGTACATTTGGCTAGTCATTTTCTTTTTCTATTTCTCTTATTTGAGACGAT
 AGAAGTATCAGAGTATCTCTACCTAGTCTATTGTTTTGTTATAGGCTTGGTTTATGATGTTTACTTTT
 TCCATCTAATAGGGATTACAACCTCTTATTTATCTTATTGGGAGCCTTCCTTCATAAATTGAATAG
 TGTATTTTTGTTGAATCGTTGGACAAGAATGCTAGCTATGATTGTGCTGACATTCCTGTTGAAATG
 GGTAGTTATCTTTTGGCTTTTATGGTAGGGTTGACAGTAGATAGCATGTCGATTTTTATAGTCTATA
 GCTTGGTACCGACGATGATTTTAAATTTTTATGGATTACTGTTTTTCAATTTATTTTTGAAAAATAT
 TATCTATAAGAACGACATATAAATGTAACAAAGGCGTAATATTTATTAGGCCTTTTTTTGGTATACT
 AGTATTGTCTTTAAAAGAAGGAGTATCTACGTAATATGAAGAAAAAATCTTAGCGTCACTTTTAT
 TAAGTACAGTAATGGTTTCTCAAGTAGCTGTTTTAACAACTGCGCATGCAGAAACGACTGATGACA
 AAATTGCTGCTCAAGATAATAAAATTAGTAACTTAACAGCACAAACAAGAAGCCCAAAAACAA
 GTTGACCAAATTCAGGAGCAAGTATCAGCTATTCAGCTGAGCAGTCTAACTTGCAAGCTGAAAA
 GATAGATTACAAGCAGAATCTAAGAACTCGAGGGTGAGATTACAGAACTTTCTAAAAACATTGTT
 TCTCGTAACCAATCGTTGGAAAAACAAGCTCGTAGTGCTCAAACAAATGGAGCCGTAAGTACTGAT
 ATCAATACCATTGTAAACTCAAAATCAATTACAGAAGCTATTTACGTGTTGCTGCAATGAGTGAA
 ATCGTATCTGCAAACAACAAAATGTTAGAACAACAAAAGGCAGATAAAAAAGCTATTTCTGAAAA
 ACAAGTAGCAAATAATGATGCTATCAATACTGTAATTGCTAATCAACAAAAATTGGCTGATGATGC
 TCAAGCATTGACTACGAAACAGGCAGAACTAAAAGCTGCTGAATTAAGTCTTGCTGCTGAGAAAG
 CGACAGCTGAAGGGGAAAAAGCAAGTCTATTAGAGCAAAAAGCAGCAGCTGAGGCAGAGGCTCG
 TGCAGCTGCGGTAGCAGAAGCAGCTTATAAAGAAAAACGAGCTAGCCAACAACAATCAGTACTTG
 CTTACAGCAAACACTAACTTAACAGCTCAAGTGCAAGCAGTATCTGAATCTGCAGCAGCACCTGTCC
 GTGCAAAAAGTTCGTCCAACATACAGTACAAACGCTTCAAGTTATCCAATTGGAGAATGTACATGGG
 GAGTAAAAACATTGGCACCTTGGGCTGGAGACTACTGGGGTAAATGGAGCACAGTGGGCTACAAGT
 GCAGCAGCAGCAGGTTCCGTACAGGTTCAACACCTCAAGTTGGAGCAATTGCATGTTGGAATGAT
 GGTGGATATGGTCACGTAGCGGTTGTTACAGCTGTTGAATCAACAACACGTATCCAAGTATCAGAA
 TCAAATTATGCAGGTAATCGTACAATTGGAAATCACCGTGGATGGTTCAATCCAACAACAACCTTCT
 GAAGGTTTTGTTACATATATTTATGCAGATTAAATTTACAGAGGGACTCGAATAGAGCCCTCTTTCA
 GTTTTACCGTGACAATCCCTATTAATAAATTATATCAAAATAGCTTGAAAATATTGGAAAAGTATG
 GTAAAATGAAAATTGTCTGTGAACGATAATACTCATTCTTGATGAATTGTGAAGCAGTTGCCCTT
 GGGTCGTTTTGCGAGTTGAAGTCAAGAAGAGGAAAAAACAAGGAGAAATACTCATGGCAGT
 AATTTCAATGAAACAACCTTCTTGAGGCTGGTGTACACTTTGGTCACCAAACCTCGTCGCTGGAATCCT
 AAGATGGCTAAGTACATCTTTACTGAACGTAACGGAATCCACGTTATCGACTTGCAACAACTGTA
 AAATACGCTGACCAAGCATAACGACTTCATGCGTGATGCAGCAGCTAACGATGCAGTTGTATTGTT
 GTTGGTACTAAGAAACAAGCAGCTGATGCAGTTGCTGAAGAAGCAGTACGTTCAAGTCAATACTTC
 ATCAACCACCGTTGGTTGGGTGGAACCTTACAACTGGGGAACAATCCAAAACGATATCGCTCGT
 TTGAAAGAAATTAACGATGGAAGAAGATGGAACCTTCGAAGTTCTTCCTAAGAAAGAAGTTGC
 ACTTCTTAACAACAACGTCGCGCTTTGAAAAATTCTTGGGTGGTATCGAAGATATGCCTCGTAT
 CCCAGATGTGATGTACGTAGTTGACCCACATAAAGAGCAAATCGCTGTTAAGAAGCTAAAAAAT
 TGGGAATCCCAGTTGTAGCGATGGTTGACACCAATACTGATCCAGATGATATCGATGTAATCATCC
 CAGCTAACGATGACGCTATCCGTGCTGTTAAATTGATCACAGCTAAATTGGCTGACGCTATTATCG
 AAGGACGTC AAGGTGAGGATGCAGTAGCAGTTGAAGCAGAATTTGCAGCTTCAGAACTCAAGCA
 GATTCAATTGAAGAAATCGTTGAAGTTGTAGAAGGTGACAACAAATAGTAATTACCTAGGAGGGC
 GGGGCTTAGCCCGGCTCTCCTA

The PcsB-coding sequence is shown in yellow.

3xFlag:

Base sequence:

GATTATAAAGATCATGATGGTGATTATAAAGATCATGATATTGATTATAAAGATG
ATGATGATAAA

Amino acid sequence:

DYKDHDGDYKDHDIDYKDDDDK

>Pre-PcsB:

MKKKILASLL LSTVMVSQVA VLTTAHAETT DDKIAAQDNK ISNLTAQQQE AQKQVDQIQE
QVSAIQAEQS NLQAENDRLQ AESKKLEGEI TELSKNIVSR NQSLEKQARS AQTNGAVTSY
INTIVNSKSI TEAISRVAAM SEIVSANNKM LEQQKADKKA ISEKQVANND AINTVIANQQ
KLADDAQALT TKQAEKAAE LSLAAEKATA EGEKASLLEQ KAAAEAEARA
AAVAEAAAYKE
KRASQQQSVL ASANTNLTAQ VQAVSESAAA PVRKVRPTY STNASSYPG ECTWGVKTLA
PWAGDYWGNG AQWATSAAAA GFRTGSTPQV GAIACWNDGG YGHVAVVTAV
ESTTRIQVSE
SNYAGNRTIG NHRGWFNPTT TSEGFVYIY AD

PcsB sequence without signal sequence:

ETDDDKIAAQDNKISNLTAQQQEAQKQVDQIQE
QVSAIQAEQSNLQAENDRLQAESKKLEGEITELSKNIVSRNQSLEKQARSAQTNGAVTSY
INTIVNSKSITEAISRVAAMSEIVSANNKMLEQQKADKKAISEKQVANND AINTVIANQQ
KLADDAQALTTKQAEKAAELSLAAEKATAEGEKASLLEQKAAAEAEARAAA VAEAAAYKE
KRASQQQSVLASANTNLTAQVQAVSESAAAPVRKVRPTYSTNASSYPGECTWGVKTLA
PWAGDYWGNGAQWATSAAAA GFRTGSTPQV GAIACWNDGGYGHVAVVTAVESTTRIQVS
E
SNYAGNRTIGNHRGWFNPTTTSEGFVYIYAD

Appendix C1

Calculations on amounts of cell-associated PcsB and secreted PcsB

Amount of cell-associated PcsB:

CFU/ml: $3.64 \cdot 10^8$

0.0128 μg PcsB concentration

0.3125 μl loaded onto gel

molecular weight PcsB: 38,869.7 g/mol

.....

$3.64 \cdot 10^8$ cells/ml * 10 = $3.64 \cdot 10^9$ cells in pellet.

$3.64 \cdot 10^9$ / 50 μl = $7.28 \cdot 10^7$ cells/ μl

$7.28 \cdot 10^7$ * 0.3125 μl = $2.275 \cdot 10^7$ cells in well nr.10

0.0128 μg / $2.275 \cdot 10^7$ cells = $5.62 \cdot 10^{-10}$ $\mu\text{g}/\text{cell}$

$5.62 \cdot 10^{-10}$ $\mu\text{g}/\text{cell}$ / 10^6 = $5.26 \cdot 10^{-16}$ g/cell

$5.26 \cdot 10^{-16}$ g/cell / 38 860.7 g/mol = $1.45 \cdot 10^{-20}$

$1.45 \cdot 10^{-20}$ * $6.022 \cdot 10^{23}$ = 8709

Appendix C2

Amount of secreted PcsB:

CFU/ml: 3.64×10^8

0.0128 μg PcsB concentration

0.3125 μl loaded onto gel

molecular weight PcsB: 38,869.7 g/mol

.....

3.64×10^8 cells/ml / 1000 = 1.82×10^6 cells in supernatant.

$0.0128 \mu\text{g} / 1.82 \times 10^6 = 7.03 \times 10^{-9} \mu\text{g/cell}$

$7.03 \times 10^{-9} \mu\text{g/cell} / 10^6 = 7.03 \times 10^{-15} \text{g/cell}$

$7.03 \times 10^{-15} \text{g/cell} / 38\,860.7 \text{g/mol} = 1.81 \times 10^{-19}$

$1.81 \times 10^{-19} * 6.022 \times 10^{23} = \underline{108\,939}$



Norwegian University
of Life Sciences

Postboks 5003
NO-1432 Ås, Norway
+47 67 23 00 00
www.nmbu.no